

DEVELOPMENT OF NITRILE BUTADIENE RUBBER-
BASED COATING MATERIAL USING WASTE TIRE
POWDER FOR GASKET APPLICATION

CHAI KAH SIONG

MASTER OF ENGINEERING SCIENCE

FACULTY OF ENGINEERING AND GREEN
TECHNOLOGY

UNIVERSITI TUNKU ABDUL RAHMAN

November 2022

**DEVELOPMENT OF NITRILE BUTADIENE RUBBER-BASED
COATING MATERIAL USING WASTE TIRE POWDER FOR
GASKET APPLICATION**

By

CHAI KAH SIONG

A dissertation submitted to the Faculty of Petrochemical Engineering,

University Tunku Abdul Rahman,

in partial fulfilment of the requirements for the degree of

Master of Engineering Science in

November 2022

ABSTRACT

DEVELOPMENT OF NITRILE BUTADIENE RUBBER-BASED COATING MATERIAL USING WASTE TIRE POWDER FOR GASKET APPLICATION

The study of replacement of carbon black with waste tire powder in a formulation to avoid usage of carcinogenic and high agglomerate filler and waste tire powder is a initiate of cost saving and environment friendly. Thus, a new gasket coating materials has been developed using nitrile butadiene rubber (NBR) as the matrix and waste tire powder (WTP) as the filler to replace commercially used carbon black through solution mixing method. The formulation optimization was done by manipulating the loading of WTP, dioctyl phthalate (DOP) used as plasticizers, and sulphur as the curing agent. Different loading of compounding and manipulation has been study in this experiment such as 80phr and 90phr for WTP, 10phr and 15phr for DOP, and 1phr and 2phr for sulphur. Upon compounding, the processing parameters such as foaming and curing time and temperatures were optimized. The coating solutions with different compounding formulation undergoes foaming at different temperature of 70°C and 80°C for 20 mins, followed by curing at 130°C for 30 mins and 40 mins. Characterisation and mechanicals testing were conducted to study the processability, mechanical properties, thermal stability, oil absorption, solvent fraction, and the hardness of the coating materials to determine the suitability of WTP as the filler for NBR. The experimental result show that formulation D10-

W90-S2 (A) is the most optimum and suitable for gasket making. The formulation with higher filler and sulphur loading can form a barrier and entanglement to minimize the oil absorption intake and gel fraction. The formulation D10-W90-S2 (A) has 16.01% of mass increase which comply with the oil absorption tolerance and 14.02% of mass changes in solvent fraction. Furthermore, the thermal aging test shows that D10-W90-S2 (A) is most stable formulation as it has the lowest variance before and after thermal aging test. The gasket is heated under 150⁰C for thermal aging test and follow up with oil absorption test for further justification. The result shows that formulation D10-W90-S2 (A) has comparative mass changes under aged and unaged gasket. The aged gasket has mass increase of 16.52% while unaged gasket has 16.01%. Besides, the three least formulations from oil absorption were selected and repeated with rolling process. The comparison of rolling and casting shown that casting specimens has better mechanical properties as compared to rolling. The occurrence of shear strain during rolling process results in the destruction of the foam structure and reduction in mechanical properties. D10-W90-S2 (A) has the least oil absorption of 17.13% as compared to D10-W90-S1 (C), and D15-W80-S2 (C) which had 26.32% and 22.33% respectively. However, gasket produced through casting method has lower oil absorption as compared to those produced through rolling method. Thus, casting method is more preferable as compare to rolling method.

ACKNOWLEDGEMENTS

First and foremost, I would like to appreciate everyone for their kindness, support, and advice for me to complete my master dissertation. I would like to thank University Tunku Abdul Rahman for providing the financial scheme with research grant number (UTAR-IPSR-RS-002 vote number 6220/0C44) while I am taking my master's degree. Besides, I would like to appreciate my supervisor Dr. Mathialagan Muniyadi for his guidance and wisdom to solve the challenges together. Secondly, I would like to appreciate my co-supervisor and Dr Yamuna a/p Munusamy for her advice and technical skill in my projects.

Furthermore, never forget the helpful lab officers who are helpful in preparing and ordering the research materials, and their helps in mechanical testing equipment. There are Mr. Yong Tzyy Jeng, Ms. Lim Cheng Yen, and Puan Ropidah. Lastly, I would like to express my gratitude towards my family and friends who are giving their support throughout my research programme.

APPROVAL SHEET

This dissertation entitled “**DEVELOPMENT OF NITRILE BUTADIENE RUBBER-BASED COATING MATERIAL USING WASTE TIRE POWDER FOR GASKET APPLICATION**” was prepared by CHAI KAH SIONG and submitted as partial fulfilment of the requirements for the degree of Master of Engineering Science in at University Tunku Abdul Rahman.

Approved by:



(Dr. Mathialagan a/l Muniyadi)

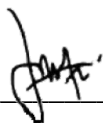
Date: 06th November 2022

Supervisor (Assistant Professor)

Department of Petrochemical Engineering

Faculty of Engineering and Green Technology

University Tunku Abdul Rahman



(Dr Yamuna a/p Munusamy)

Date: 06th November 2022

Co-supervisor (Associate Professor)

Department of Petrochemical Engineering

Faculty of Engineering and Green Technology

University Tunku Abdul Rahman

FACULTY OF ENGINEERING AND GREEN TECHNOLOGY
UNIVERSITY TUNKU ABDUL RAHMAN

Date: 06th November 2022

SUBMISSION OF DISSERTATION

It is hereby certified that **CHAI KAH SIONG** with ID No **20AGM05905** has completed this dissertation entitled “DEVELOPMENT OF NITRILE BUTADIENE RUBBER-BASED COATING MATERIAL USING WASTE TIRE POWDER FOR GASKET APPLICATION” under the supervision of Dr. Mathialagan a/l Muniyadi from the Department of Petrochemical Engineering, Faculty of Engineering and Green Technology, and Dr Yamuna a/p Munusamy from the Department of Petrochemical Engineering, Faculty of Engineering and Green Technology.

I understand that the University will upload softcopy of my thesis in pdf format into UTAR Institutional Repository, which may be made accessible to UTAR community and public.

Yours truly,

Chai Kah Siong

(CHAI KAH SIONG)

DECLARATION

I, CHAI KAH SIONG hereby declare that the thesis based on my original work except for quotations and citations which have been duly acknowledged. I also declare that it has not been previously or concurrently submitted for any other degree at UTAR or other institutions.

Chai Kah Siong

(CHAI KAH SIONG)

Date: 06th November 2022

TABLE OF CONTENTS

	Page
ABSTRACT	i
ACKNOWLEDGEMENTS	iii
APPROVAL SHEET	iv
SUBMISSION SHEET	v
DECLARATION SHEET	vi
TABLE OF CONTENTS	vii
LIST OF TABLES	xi
LIST OF FIGURES	xiii
LIST OF ABBREVIATIONS	xvii

CHAPTER

1.0 INTRODUCTION	1
1.1 Introduction	1
1.2 Problem Statement	5
1.3 Objective of the research	6
1.4 Scope of study	7
2.0 LITERATURE REVIEW	10
2.1 Introduction to Nitrile Butadiene Rubber (NBR)	10
2.1.1 Properties of NBR	12
2.1.2 Comparison of Nitrile Butadiene Rubber (NBR) and Natural Rubber (NR)	14

2.2	Gasket	16
	2.2.1 Gasket material selection	19
	2.2.2 Gasket manufacturing process	24
2.3	Waste tire recycling and application	27
	2.3.1 An existing method in rubber recycling	27
	2.3.2 Composition of tire	31
2.4	Carbon black	33
2.5	Carbon Black/ Nitrile Butadiene Rubber Composite	36
2.6	Waste tire powder / rubber composite	44
2.7	Foaming and curing parameters	50
2.8	Introduction to rolling method in gasket coating	53
2.9	Principle of rolling process and deflect.	56
3.0	METHODOLOGY AND MATERIAL	58
3.1	Compounding materials	60
3.2	Preliminary experiments	61
	3.2.1 Identify total contain of WTP loading in formulation.	61
	3.2.2 Optimum weight of NBR/WTP blend in petri dish.	62
3.3	NBR solution compounding steps	64
	3.3.1 Dissolution of NBR	64
	3.3.2 NBR solution compounding	64
3.4	Experimental design for optimization of NBR/WTP	66
	3.4.1 Phase 1: Optimization of foaming and curing parameters.	66

3.4.2	Phase 2: Optimization of filler, plasticizer, and cross-linking agent.	67
3.4.3	Phase 3: Optimization of coating methods	69
3.5	Characterization and Mechanical Testing	70
3.5.1	Particle Size Analysis (PSA)	70
3.5.2	Scanning electron microscopy (SEM)	70
3.5.3	Thermal gravimetric analysis (TGA)	71
3.5.4	Oil Absorption Test	71
3.5.5	Gel fraction / solvent extraction test	72
3.5.6	Thermal aging test	73
3.5.7	Peeling test	73
4.0	RESULT AND DISCUSSION	74
4.1	Characterization of Waste Tire Powder (WTP)	74
4.1.1	Particle size analysis (PSA)	74
4.1.2	Thermal Gravimetric Analysis (TGA)	79
4.1.3	SEM of CB and WTP	81
4.2	Characterization of NBR/ WTP for Phase 1 and 2	84
4.2.1	Compound weight for curing and foaming of NBR/ WTP.	84
4.2.2	Surface texture observation	87
4.2.3	Oil absorption test	92
4.2.4	Gel Fraction / Solvent Absorption Test	97
4.2.5	Thermal aging test	101

4.2.6	Thermogravimetric analysis of NBR/WTP	104
4.2.7	Scanning electron microscope (SEM)	108
4.2.8	Hardness test (Shore A)	115
4.2.9	Formulation selection	118
4.3	Characterization of NBR/ WTP for Phase 3 Optimization - Rolling Method.	122
4.4	Characterization of NBR/WTP formulation by using rolling method.	125
4.4.1	Oil absorption test.	125
4.4.2	Gel fraction / solvent extraction test	129
4.4.3	Peeling test	133
4.4.4	Scanning electron microscope (SEM)	135
5.0	CONCLUSION AND RECOMMENDATION	138
5.1	Conclusion	138
5.2	Recommendation	142
6.0	REFERENCES	145
7.0	LIST OF PUBLICATION	151

LIST OF TABLES

Table		Page
2.1	NBR classification by using ACN content	12
2.2	Physical and Chemical properties of NBR	13
2.3	Comparison of all three grinding methods	29
2.4	Material composition of car and truck tire	32
2.5	Tensile modules of 100% elongation of SBR/ various pre-treated tire rubber	47
2.6	Tensile modules of 100% elongation of SBR/ various pre-treated tire rubber	48
3.1	Functions of compounding ingredients and distributor	60
3.2	Compounding Formulation for NBR / WTP compounds	65
3.3	Phase 1 manipulation factors	67
3.4	Phase 1 Treatment conditions	67
3.5	Phase 2 manipulation factors	68
3.6	Phase 2 Treatment Condition	68
4.1	PSA Data of WTP	78
4.2	Characteristic of thin and thick gasket	85
4.3	Acceptable surface texture among all compounding with different treatments.	89
4.4	Mass and thickness changes in NBR/WTP for each formulation.	97
4.5	Mass changes for NBR/WTP under solvent for a different formulation.	100

4.6	Comparison of aged and unaged NBR/WTP with different formulations.	104
4.7	TGA for various NBR/ WTP formulations, CB and WTP.	107
4.8	Formulations of NBR/WTP for SEM.	109
4.9	Comparison of hardness value with sulphur, DOP, and WTP content.	117
4.10	Formulation selection from various experimental testing	121
4.11	Formulation comparison D15-W90-S1 (A) and D15-W90-S1 (B)	121
4.12	Gasket thickness with the different numbers of a stack of rulers.	123
4.13	Formulation comparison of mass and thickness changes for rolling and casting.	127
4.14	Formulation comparison for mass changes for rolling and casting.	132
4.15	UTS (MPa) and hand peeling justification for three formulations in casting and rolling.	135
4.16	Rheometer parameters reading method.	150

LIST OF FIGURES

Figure		Page
2.1	Structure of monomer butadiene and acrylonitrile.	10
2.2	NBR Manufacturing process.	11
2.3	Relationship of Acrylonitrile content to NBR properties.	13
2.4	Natural and synthetic rubber consumption statistic in worldwide from year 1990 to 2020.	16
2.5	Global market for gaskets and seals	19
2.6	Semi-metallic gasket (a) Cross section of metal reinforced with non-metal gasket, (b) Corrugated gaskets, (c) Jacketed gaskets, (d) Kammprofile gasket, (e) Spiral wound gasket, and (f) Envelope gasket.	23
2.7	Metallic gasket (a) Flat gasket, (b) Grooved metal gasket, (c) round cross-section solid metal gasket, and (d) corrugated metal gasket.	24
2.8	Process line of gasket calendaring and stamping.	25
2.9	Static curing machine.	26
2.10	Gasket is under silk-screen printing.	27
2.11	Pyrolysis Plan.	33
2.12	Composition breakdown after pyrolysis.	32
2.13	Carbon black structural size	34
2.14	Global market demand of carbon black until the year 2018.	35
2.15	Carbon black application in various products.	36
2.16	Effect of CB loading on Cure Time.	39
2.17	Effect of CB loading on minimum torque.	40
2.18	Effect of CB loading on Tensile Strength.	40

2.19	Effect of CB loading on composite swelling.	41
2.20	Effect of CB loading on Elongation at break.	41
2.21	Effect of CB loading on Tensile Modulus.	42
2.22	Effect of CB loading on the hardness.	42
2.23	Effect of CB loading on Compression set.	43
2.24	Effect of CB on tear resistance.	43
2.25	Effect of CB on resilience (%).	43
2.26	Mooney viscosity of NR with WTP and CB.	48
2.27	Swelling ratio on different loading of raw and devulcanized GTR.	49
2.28	Tearing strength of SBR reinforce with different type of DWR under different gamma radiation dose	49
2.29	Tensile strength of different loading of irradiated SBR with TMTD waste tire powder.	50
2.30	Torque vs time at 140 ⁰ C	52
2.31	Rubber vulcanization curve rate	52
2.32	Calendaring rolling process of the rubber	55
2.33	Roll coating set up	55
3.1	Compounding flow chart of NBR/WTP.	59
3.2	Gasket compounding with different WTP loading. (a) 15phr, (b) 30phr, (c) 35phr, (d) 40phr, (c) 50phr, (f) 60phr, (g) 70phr, and (h) 80phr	62
3.3	NBR/ WTP Gasket sheet with different weights (a) 5g, (b) 10g, and (c) 15g	63
3.4	Compounding blending by using IKA RW 20 Digital	65
3.5	Gasket rolling method	69
3.6	Casting gasket	69
4.1	Concept of aggregate, agglomerate, and primary	75

4.2	Solid flow time lap during hopper filling process.	76
4.3	Particle size graph of waste tire powder	78
4.4	Particle size graph of carbon black	78
4.5	Mass loss of CB and WTP under Thermal Gravimetric Analysis	80
4.6	SEM image of CB particle under (a) 500X, (b) 1000X magnification.	83
4.7	SEM image of WTP under (a) 500X, (b) 1000X magnification.	83
4.8	NBR/ WTP gasket samples with (a) 5g, (b) 10g and (c) 15g.	87
4.9	Physical appearance for acceptable formulation and treatment:	90
4.10	The formulation with void surfaces.	91
4.11	Schematic diagram of swelling and collapse of rubber.	108
4.12	Cell density increase with filler (silica) content	113
4.13	Comparison of surface morphology of foaming temperature (a) 70°C, and (b) 80°C under 200X magnification.	113
4.14	Gasket formulation with 90phr of WTP (a) D10-W90-S1 (b) D10-W90-S2 (c) D15-W90-S1 (d) D15-W90-S2 under 200X magnification.	114
4.15	Gasket formulation with 80phr of WTP (a) D10-W80-S2 (b) D15-W80-S2 under 200X magnification.	114
4.16	Gasket formulation with higher sulphur (2phr) (a) D10-W90-S2 (b) D15-W90-S2 under 500X magnification.	114
4.17	Gasket formulation with lesser sulphur (1phr) (a) D10-W90-S1 (b) D15-W90-S1 under 500X magnification.	115
4.24	Hardness values graph for NBR/WTP at different formulations.	118
4.25	Torque over curing time	120
4.26	Gasket calendaring modelling in the lab-scale	123
4.27	Gaskets surface upon completion after curing and foaming.	124

4.28	Comparison of mass changes in percentage for rolling and casting methods	128
4.29	Comparison of thickness changes in percentage for rolling and casting methods.	128
4.30	Numerical stimulation stress distribution on the width cross-section.	131
4.31	Comparison of mass percentage changes in the rolled and cast gasket.	133
4.32	The cross-section SEM for rolling and casting gasket under 500X magnification.	137
5.1	Mooney viscosity graph by using large motor	143
5.2	ODR cure graph	143

LIST OF SYMBOLS AND ABBREVIATIONS

Symbols/Abbreviations

ACN	Acrylonitrile
ASTM	American Society for Testing and Materials
ADCA	Azodicarbonamide
BD	Butadiene
CB	Carbon black
C-S	Carbon-sulphur
EECO	Canola oil
cm	Centimetre
CAGR	Compound Annual Growth Rate
CNC	Computer Numerical Control
t_{35}	Cure time
$(t_{35} - t_5)$	Cure index
$^{\circ}\text{C}$	Degree Celsius
DCP	Dicumyl peroxide
DOP	Diethyl Phthalate
DD	Diphenyl disulphide
-S-S-	Disulphide
DWR	Devulcanized waste rubber
EPDM	Ethylene-Propylene-Diene
W3	Final weight of dried samples with wire mesh
g	Gram

GTR	Grinded tire rubber
H ₂ S	Hydrogen sulphite
W1	Initial weight of sample
Kg	Kilo gram
kV	Kilo Volt
MSDS	Material Safety Data Sheet
MEK	Methyl Ethyl Ketone
m ² g ⁻¹	Meter square per gram
MPa	Mega pascal
μm	Micrometre
mm	Millimetre
-S-	Mono-sulphide
NR	Natural Rubber
NBR	Nitrile butadiene rubber
N/A	Not applicable
ODR	Oscillating Disc Rheometer
PSA	Particle Size Analysis
phr	Part per hundred rubbers
%	Percentage
PTFE	Polytetrafluoroethylene
-S _x	Polysulphide
PTFE	Polytetrafluoroethylene
SSA	Specific surface area
SBR	Styrene Butadiene Rubber
SEM	Scanning Electron Microscope

t ₅	Scorch time
EESO	Soybean oil
S-S	sulphur- sulphur
TMTD	Tetramethyl Thiuram Disulphide
TGA	Thermogravimetric analysis
TDAE	Treated distillate aromatic extracts
R-SH	Thiols
UTS	Ultimate tensile strength
WTP	Waste tire powder
wt%	Weight percentage
W2	Weight of wire mesh
ZDEC	Zinc diethyldithiocarbamate
ZMBT	Zinc-2-mercaptobenzothiazole
ZnO	Zinc Oxide
MBTS	2-mercapto benzothiazole disulphide

CHAPTER 1

INTRODUCTION

1.1 Introduction

A gasket is a form of seal that is placed in between two or more mating surfaces. There are different types of gaskets used in the oil and gas industry and other heavy-duty industries such as envelope gasket, flat gasket, non- asbestos sheet material gasket, ring type joint, kammprofile gasket, spiral wound gasket, and corrugated metal gasket (Hamilton, 2021). In general, gasket materials should have properties of low density, high tensile strength, and good flexibility. Other than that, the gasket should have excellent in chemical resistance, internal pressure resistance, and high durability. Lastly, excellent adhesion properties, abrasion, and good counter-vibration impact are necessary for gaskets (Chambers, 2021).

Nitrile butadiene rubber (NBR) which is also known as acrylonitrile butadiene copolymer takes up 18% to 50% portion in nitrile-based seal and gives the physical properties of gasket. Furthermore, acrylonitrile content provides better resistance toward oil and fuel and better elasticity. Other than that, NBR is chosen as it has good in tensile strength, low compression set, elongation properties, and heat resistance. Thus, it can use in an environment with acids, petroleum, mineral, and others ('Rubber gasket', 2017).

In addition, a vulcanization agent is used in this gasket-making process. During the curing process, the mixture added with sulphur or peroxide is heated and crosslinking bond is formed in between polymer chains. This chain or chemical bond can turn the mixture into an elastic form even after deformation. Besides vulcanization agents, rubber mixture can be added with other additives such as filler, plasticizer, anti-degradants, and other additives. Filler can provide rubber strength and resistance toward abrasion and reduce the final cost. The function of plasticizer is used to soften and ease the processing. Anti-degradant is considered as it can prevent the rubber from ozone degradation. Other additives such as foaming agents, dyes, abrasives, flame retardants can give the gasket desired texture, strength, and other specifications (Neris, 2018).

Furthermore, alternate composing materials especially reuse waste materials are part of our goals to reduce the undecomposed wastes and minimizing processing cost at the same time. The research done by Munikanan et al in year 2018 shows that Malaysia produces 30,000 tons of waste every day and only 5% of the daily waste is reused. The part of non-degradable wastes includes metal, plastics, hardware parts and scrapped tires. The tires production has been increase annually with increase of vehicles number on the road (Munikanan *et al.*, 2018). In addition, more specific tires discard in Malaysia is reported that average of 758 tonnes of used or wear tires are generate daily reported from year 2010 to 2015. Among all the scraped tires, there are 170 tonnes of tires are being recycled and treated. (Abidin *et al.*, 2021).

The ways of waste management are done through landfilling, stockpiling, open burning, and other short-term solutions which is illegal and will cause harm to the environment and humans. Pyrolysis is one of the ways to convert waste tires into new resources. The process is undergoing the thermal decomposition of scrap tires without the presence of oxygen. The waste tire is combusted under 450-500°C to break into different parts such as tire-derived fuel, char, and synthetic gas. Pyrolysis is not an effective method to recycle tires due to large energy consumption to produce little energy from the waste, and decomposed gases such as carbon dioxide and monoxide without proper capturing may cause harm to environment. Thus, the most applicable way to recycle waste tires is to turn the tire into particles through mechanical shredding and used as filler with other materials such as thermoplastic, thermoset, and concrete as reinforcement (Zafar, 2019).

Besides, making use of new coating materials in automotive industries are drastically happening in recent years. CB is familiar as a filler to produce latex-based coating materials for car gasket application. The research shows that carbon black filler gives a great impact on the mechanical properties and is better in resistivity to the natural rubber. Reinforce rubber has better tear resistance and high oil resistance for gasket application. The study indicates that the tear resistance increase with the filler loading increase (Azura and Leow, 2019). However, implementing carbon black as filler results in higher costing in gasket materials and latex-based gasket will experience heat aging at the operation temperature of vehicles. Hence, it is essential to develop a new coating material

with better performance and low cost at the same time and yet it can establish by using waste materials or recycled materials such as polymer and rubbers.

Furthermore, gasket or seal is relatively importance in our study as guideline and parameter for gasket material study application. Gasket demand is granular increase in trend as it is used in many different industries. The forecast of 3.6% of annual growth from year 2020 to year 2028. Gaskets are found in sector of aircraft manufacturing, chemical processing, medical equipment, electrical components such as switches, transformer etc.

This research is focusing to develop a new thin and smooth gasket coating material by using nitrile butadiene rubber (NBR) solution and waste tire powder (WTP) with superior shock resistance, abrasion resistance, and thermal stability for automobile application, especially in gaskets. WTP consists of a mixture of polyisoprene, polybutadiene, and styrene-butadiene which inherently possess excellent shock, abrasion, and thermal resistance due to its crosslink three-dimensional network (Asaro *et al.*, 2018). The right formulation of WTP and nitrile butadiene rubber (NBR) solution will be established through the solution mixing method (which is suitable for different grades of rubber) and applied to the surface of coating papers as a thin and smooth coating. In previous research, which is done by Ramadas, N. in the year 2020, carbon black was mixed with NBR latex through the latex compounding method. However, due to the poor miscibility of carbon black, the latex compounding destabilizes quickly, and it is hard to produce a thin and smooth coating material. Besides, the latex compounds can only be kept for a short period before it coagulates and therefore

latex compounding method is not feasible to produce the rubber gasket materials. In other research, however, it was stated that solution mixing of rubber and fillers can produce a smooth coating material due to better stability of the rubber solution and high content of filler can be added to reduce the compounding cost without jeopardizing the compound stability and processing feasibility (Wong, 2013).

1.2 Problem statement

This research was carried out to develop a new coating material for gasket applications utilizes NBR rubber as matrix and WTP as the fillers. Due to high cost of carbon black, a study that has been carried out to reduce the usage of carbon black in the development of coating materials. Thus, alternative filler shall be introduced to substitute percentage of carbon black in the compound. Besides, due to its carcinogenic properties, utilization of carbon black could be harmful to human during the production period due to its carcinogenic characteristics. The consequences of carbon black will cause skin and eyes irritation and cause cancer in long term. Furthermore, carbon black may cause agglomeration in fine particles which contribute to uneven distribution of filler among the matrix (Carbon Black MSDS, 2019).

Meanwhile, increasing amount of waste tire by years cause more serious problem to environment upon improper waste management via landfilling, stockpiling and open burning. In general tires are made of rubbers and carbon

black as fillers. 47% composition of tire consist of rubber and 22% contribute by carbon black, 17% of metal, 6% textile and the rest will contribute by additive (Gómez-Hernández, Panecatl-Bernal and Méndez-Rojas, 2019). Thus, replacement of carbon black by WTP in gasket application may reduce the cost of the materials and retain the desired properties. Thus, research to develop a new value-added material using recycled and used materials such as waste tire powder for gasket application could be beneficial to reduce impact to environment. Nearly 1 billion of waste tires are being disposed yearly and add to estimated 4 billion waste tires already existing in the landfills and stockpiles. One should put attention on this because more than 50 % of tires are discarded without any treatment and estimation of 1.2 billion of waste tire increment yearly by the year 2030 (Gómez-Hernández, Panecatl-Bernal and Méndez-Rojas, 2019).

1.3 Objectives of the research

1. To optimize the curing and foaming parameters of the coating material.
2. To formulate the optimum compounding formulation recipe for coating for gasket material.
3. To develop the suitable coating techniques for the new coating material on the gasket paper.

1.4 Scope of study

In this research, waste tire powder (WTP) is studied as an objective to replace carbon black (CB) in gasket production due to cost, hazardous, and processing factors. Generally, CB is costlier than WTP. The price of CB is RM 2.72/ kg while the price for WTP is RM 1.40/ kg. Besides, WTP contain 22% of carbon which is suitable for our application (Gómez-Hernández, PanecatI-Bernal and Méndez-Rojas, 2019). Furthermore, the second reason for the replacement of CB is due to the carcinogenic characteristics of CB which is affecting human health, particularly during the processing and storage of CB. Other than that, fine particles of CB will cause agglomeration during the compounding process which will decrease the mechanical properties of the gasket. Moreover, NBR latex compounding with CB will destabilized quickly and will agglomerate before the coating process is carried out due to the acidic nature of CB.

The experiment is carried out in three stages. In Stage 1, the curing and foaming parameters such as the temperature and time for curing and foaming was optimized by using suggested formulation given by Wong, 2013. The surface finish of the coating materials on the coating paper was evaluated and the resistance towards oil and solvent method was used to optimize the curing and foaming parameters.

In Stage 2, the composition of the main compounding ingredients that can influence the properties of the gaskets such as sulphur (crosslinking agent), WTP (Filler), and DOP (plasticizer), will be optimized to develop a product that fulfils the American Society for Testing and Materials (ASTM) standards for automobile applications. The oil and solvent-resistance of the coating materials produced were studied to optimize the composition of the compounding ingredients. Test such as aging test under ambient and processing conditions was carried out according to ASTM D7912. Other testing such as scanning electron microscope (SEM) analysis will be carried out to evaluate the morphological properties of the coating materials. Other than that, oil absorption test, solvent fraction, Thermogravimetric analysis (TGA), hardness tests are used to evaluate the properties of the composite. The physical appearance based on the smooth texture of the coating developed and the dispersion of WTP in NBR was also observed.

In Stage 3, different techniques to apply the new coating material such as casting, and rolling were evaluated to compare the efficiency of surface coating on coating paper using different techniques. This is very crucial because emulsion has low particle stability and is sensitive to the force applied; inappropriate force will cause uneven coating and destruction of foam structure of the coating material. Thus, the right method of coating is important to establish a thin, continuous, and smooth coating to produce a fine finish surface of the coating. Visual inspection of the surface finish will be observed through an optical microscope, as well as the binding quality of the coating materials will be determined through peeling off and sealing tests (ASTM F0607 – 03R08).

Other necessary testing such as the oil absorption test, SEM and gel fraction was carried out on the final coating specimen.

Besides, increasing amount of waste tire by years invites more serious problem to environment. In general tires are made of rubbers and carbon black as fillers. 47% composition of tire consist of rubber and 22% contributed by carbon black, 17% of metal, 6% textile and the rest by the additives (Gómez-Hernández, PanecatI-Bernal and Méndez-Rojas, 2019). Thus, replacement of carbon black by WTP in gasket application may reduce the cost of the materials and retain the desired properties. Thus, research to develop a new value-added material using recycled and used materials such as waste tire powder for gasket application could be beneficial to reduce impact to environment. Nearly 1 billion of waste tires are being disposed yearly and add to estimated 4 billion waste tires already existing in the landfills and stockpiles. One should put attention on this because more than 50% of tires are discarded without any treatment and estimation of 1.2 billion of waste tire increment yearly by the year 2030 (Gómez-Hernández, PanecatI-Bernal and Méndez-Rojas, 2019). As mentioned in the introduction, new methods of recycling waste tire powder such as cryogenic grinding can produce micronized particles which resembles carbon black and could be beneficial to replace carbon black in coating material development.

CHAPTER 2

LITERATURE REVIEW

2.1 Introduction to Nitrile Butadiene Rubber (NBR)

Nitrile butadiene rubber (NBR) is made up of individual copolymers of acrylonitrile and butadiene. NBR is well known for its oil resistance properties which are resistant to oil, non-polar solvents, fats, and other fuel. In addition, the property of oil resistance is increased when the portion of acrylonitrile is higher. The combination of butadiene and acrylonitrile undergo co-polymerization emulsion reaction to form NBR under 5-30°C where oxidation and reduction initiation and follow by chain transfer and end with polymerization stopper. Figure 2.1 show the different structure of monomer butadiene and monomer of acrylonitrile (Dinsmore, 2007).

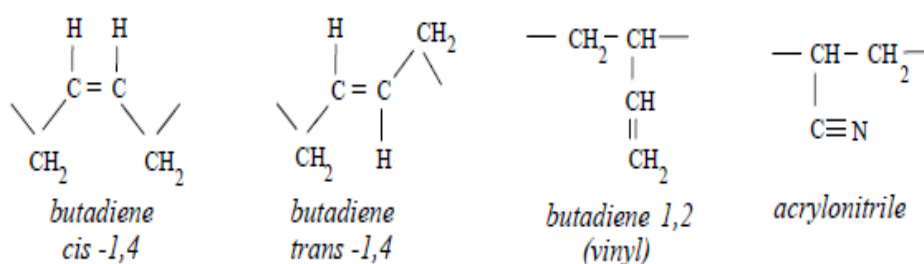


Figure 2.1: Structure of monomer butadiene and acrylonitrile (Dinsmore, 2007).

The process of emulsion polymerization of NBR begins with an added emulsifier, both monomers, water, radical generating activator, and some other additive into polymerization vessels. Polymer latex from emulsion is then further coagulated, dried, and compressed into bales to form a rubber crumb. Figure 2.2 shows the NBR manufacturing process. NBR manufacturer offers more than 100 grades of variation and acrylonitrile (ACN) and butadiene (BD) ratios that are varied for specific oil and fuel resistance design and low-temperature application. Furthermore, hydrogenated NBR elastomer is offered in the market to reduce the chemical reactivity of the NBR and it can increase the thermal resistance properties of the rubber (Rubber, Finished and Articles, 2005).

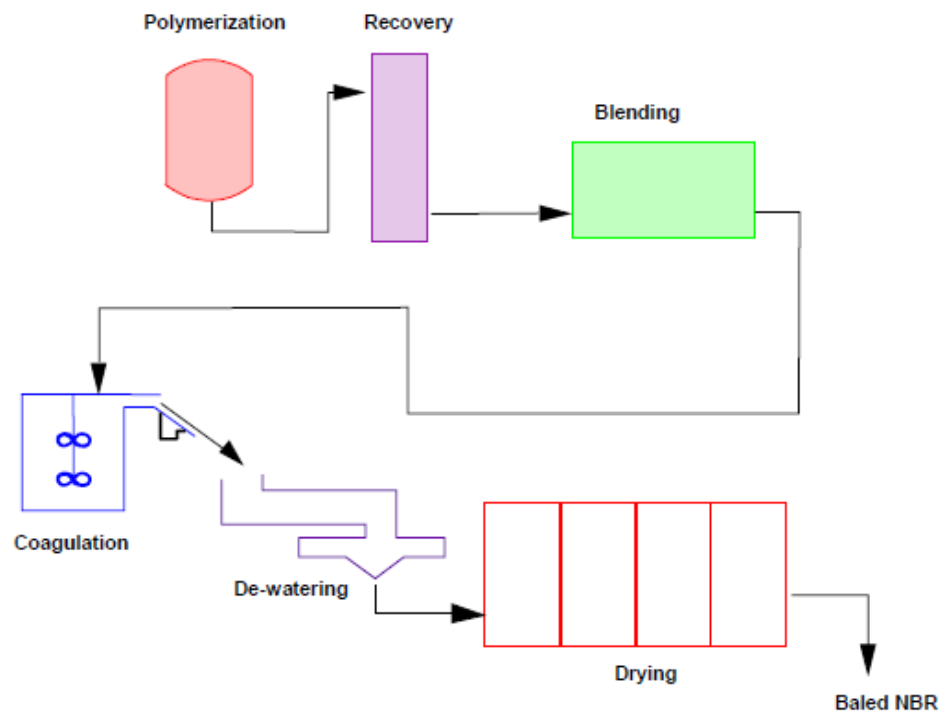


Figure 2.2: NBR Manufacturing process (Rubber, Finished and Articles, 2005)

2.1.1 Properties of NBR

Properties of NBR is highly related to monomer ACN content in the polymer. The higher the monomer ACN portion, the higher the resistance toward hydrocarbons while the lower the ACN portion, the better the flexibility at low temperature. Table 2. 1 shows the classification of NBR with different ACN percentage content (Polymer Properties Data, 2021).

Table 2.1 NBR classification by using ACN content

NBR classification	Acrylonitrile Percentage Content
High Nitrile	>45%
Medium Nitrile	30 % - 45 %
Low Nitrile	< 30 %

Besides oil resistance, ACN content can provide better abrasion resistance and higher glass transition temperature, better processability, sulfur cure rate, and better polar polymers compatibility. Furthermore, tensile strength, heat aging, and gas impermeability are improving as well. However, there are decreases in compression set, resilience, hysteresis, and low-temperature flexibility. Figure 2.3 shows the relationship between acrylonitrile content and NBR properties (Rubber, Finished and Articles, 2005). Table 2.2 shows the properties of NBR physically or chemically with the data retreated from the material safety data sheet of NBR. (*Material Safety Data Sheet (MSDS) Nitrile Rubber Sheet, 2007*)

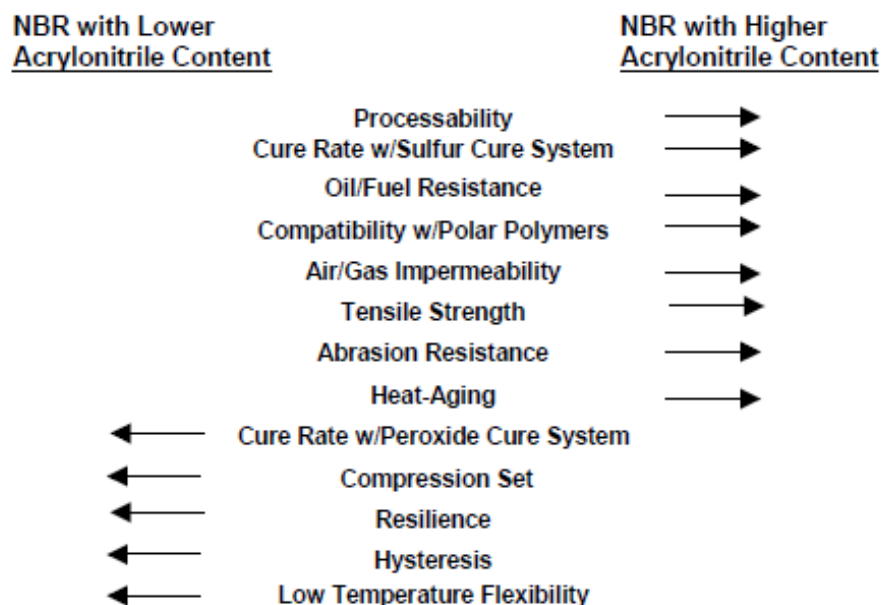


Figure 2.3 Relationship of Acrylonitrile content to NBR properties (Rubber, Finished and Articles, 2005)

Table 2.2 Physical and Chemical properties of NBR

Physical and Chemical Properties	Details
Appearance:	Flexible rubber sheet
Odor:	Slight typical rubber product odor
Specific Gravity:	1.2-1.5
Boiling Point:	N/A
Melting Point:	N/A
Decomposition temperature:	>250°C
Vapor Pressure:	N/A
Percent Volatile:	N/A
Water solubility:	Insoluble
Flash Point:	>300°C

Fire Hazard:	Stable under normal situations, and flammable under high temperature
Physical contact:	May cause skin irritation
Inhalation:	There is some symptom like headache, nausea, and irritation.
Stability:	NBR is not reactive with non-polar chemicals and hydrocarbon.

2.1.2 Comparison of Nitrile Butadiene Rubber (NBR) and Natural Rubber (NR)

NBR and NR are both different polymers that are widely used in many industries and daily utensils. However, both rubbers have their own physical and chemical properties. The nitrile rubber comprises of functional group $-CN$ group and given $R-C\equiv N$ as molecular structure. Furthermore, the nitrogen atom of NBR is highly electronegative due to differences of electronegativity of carbon and nitrogen. Besides, NR is milky white colloidal dispersion polymer particles. It can mainly be found in some plant's cells. (Madhusa, 2017)

Besides, NR polymer is obtained through biosynthesis from the plant called "*Hevea brasiliensis*". The colloidal dispersion of NR comprises of few hundred nanometers diameter polymeric particles and water. The weight fraction of dispersion is generally comprising of 50% of water. In contrast, NBR is produced through man-made synthesis under control conditions. NR is well

known for its strong tensile strength and greater structural regulation for a faster vulcanization rate. Furthermore, NR has other advantages such as good performance with low hysteresis loss, ease in processing and manufacturing, good low-temperature properties, high tear, and abrasion resistance. Besides, it can bond with metal parts to increase the implementation of NR in the industry. In addition, NR has low heat buildup and a low level of damping. (Yashoda, 2016) Advantage of natural rubber better in tensile strength, and tear resistance with low odor added by Tran. B in the year 2021. Apart from that, the disadvantages of NR are poor resistance to ozone and oxygen. NR is also low in resistance to hydrocarbon solvents and oils. To date, NR is taking 30-40% of the total rubber market share. The application of NR can be found in a rubber gasket, hoses and tubes, shock mounts, drive coupling, tires, gloves, etc. (Yashoda, 2016).

Synthetic rubber or NBR product are derived from crude oil side products. Emulsion or solution polymerization is the path to synthesis rubber and NBR can be fabricated to suit many applications such as good chemical and solvent resistance and high tolerance toward weather and temperature (Yashoda, 2016). Furthermore, the properties of synthetic rubber can be included with electrical resistance, ozone resistance, and others. Despite on differences between natural rubber and synthesis rubber, both rubbers are in high demand manufacturing due to different application properties. Figure 2.4 shows total consumption of natural and synthetic rubber worldwide from year 1990 to 2020. The statistic shows that demand of 12.7 million metric tons of natural rubber, and 14.2 million metric tons of synthetic rubber is needed globally. The research also says that China is

the main consumer for natural rubber with 5.5 million tons in year 2019 and India as the second major rubber consumption in the same year (Tiseo, 2021).

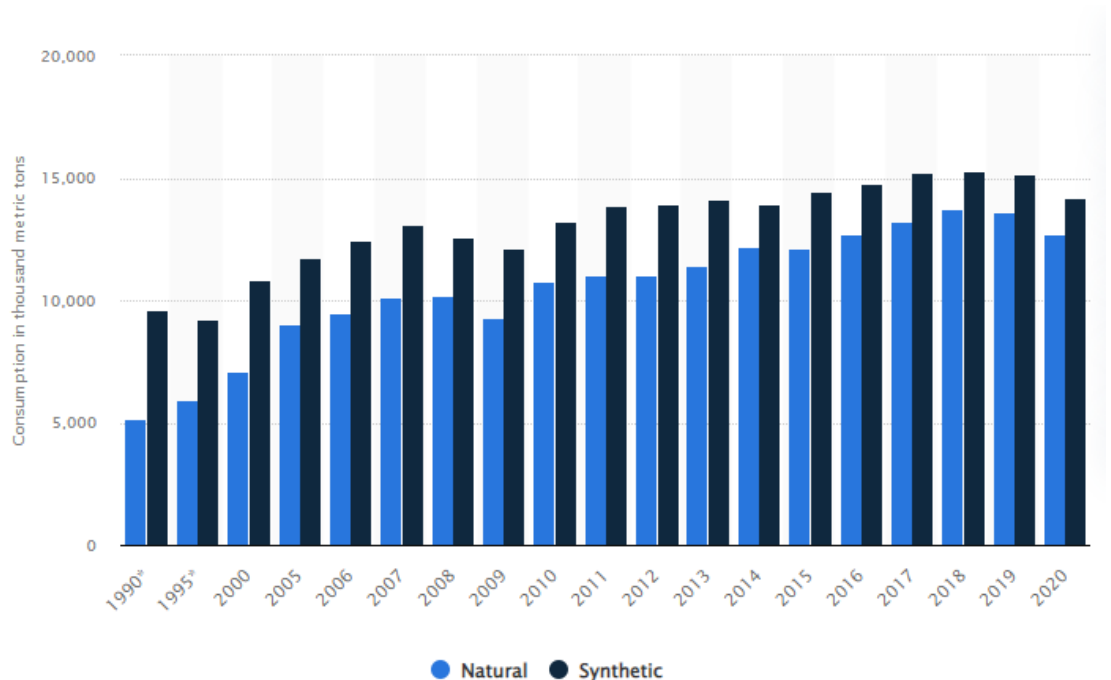


Figure 2.4: Natural and synthetic rubber consumption statistic in worldwide from year 1990 to 2020 (Tiseo, 2021).

2.2 Gasket

The gasket materials also known as sealant functions as a seal and fill up the space between two joint surfaces to avoid leakage from the joint and can fit irregularities of the surfaces. Meanwhile, the gasket is able resilient and cancel the vibration during operating conditions. Thus, the gasket is designed with material that can deform and fully tightly fill the space so that it can prevent ingress or leaking of fluids or gases. However, there are some criteria and

guidelines for gasket selection to suit various applications. The most important aspects that must be considered are application under fluid type, temperature, and pressure. After that, the dimension such as thickness, diameter and shape of the gasket is considered according to the surface of the flanges. Next, optimum gasket material should be selected from accountability of tolerant leakage volume, workability, maximum force can apply, and most important is cost of the gasket. Lastly, application of gasket type is considered as classification of gasket is limited to certain usage only. The examples of gasket types are foamed carbon gasket, (polytetrafluoroethylene) PTFE gasket, non-asbestos joint sheet, metal flat gasket, serrated gasket, ring joint gasket and others. (Asuka Matsushita, 2018)

Research and study on gasket manufacturing and application are very important and relevant to our lives since the application of gasket has an increasing trend. According to Grand View Research in 2021, the report shows that global gaskets and seals market size has valued at USD 56.14 billion in the year 2020 and estimates continue annual growth rate of 3.6% in the market from the year 2020 to 2028. The demand growth of gasket is due to the high supply to aircraft manufacturing, chemical processing, medical equipment. Figure 2.5 shows the increasing demand for gaskets and seals from the year 2018 to 2028. Furthermore, increases in oil and gas exploration and chemical process industry denote that application of gasket is increase. In the year 2020, the gaskets segment was valued at USD 22.1 billion. In addition, automotive dominated overall gasket, and seal use with 33.3% in the year 2020. This is because gasket has a wide range of applications in automotive such as engine block, body parts,

electronic, etc. Apart from that, seals and gaskets are requiring in applications in electrical, electronic components such as switches, transformers, telecommunication devices, LCD, and others. Thus, seals and gaskets need will increase with appliances such as smartphones, watches, electronic devices, and TVs which will drive the use of seals (Gaskets and Seals Market Size, 2021).

The report also shows that the European market has a CAGR of 3.0% from 2018 to 2020 of gaskets and seals that were driven in growth due to expansion in the aerospace and defence sector. Furthermore, some are growing in investment and manufacturing output happens in the Asia Pacific especially in China and Japan. Furthermore, an increase in the number of motor vehicles sale in this region requires more gaskets and seals. In addition, U.S chemical manufacturers are demanding a large volume of gaskets as they are the primary chemical industry in piping installation and production of equipment and components (Gaskets and Seals Market Size, 2021).

Besides, Business wire also reported in the Year 2020 that global gasket demand has increased continuously with a CAGR of 5.43% with USD 15.18 Billion in between the forecast period of 2020 to 2026. Concurrent with growing demand from oil and gas in Gulf countries and reinforce law of leakage regulation to avoid environment pollution has triggered the market demand of gasket. North America become a primary gasket market consumer, and wind power development in the Asia Pacific triggers the demand for gaskets in this region. Furthermore, China needs more gaskets for the high demand for fuel in their country (Wood, 2020).

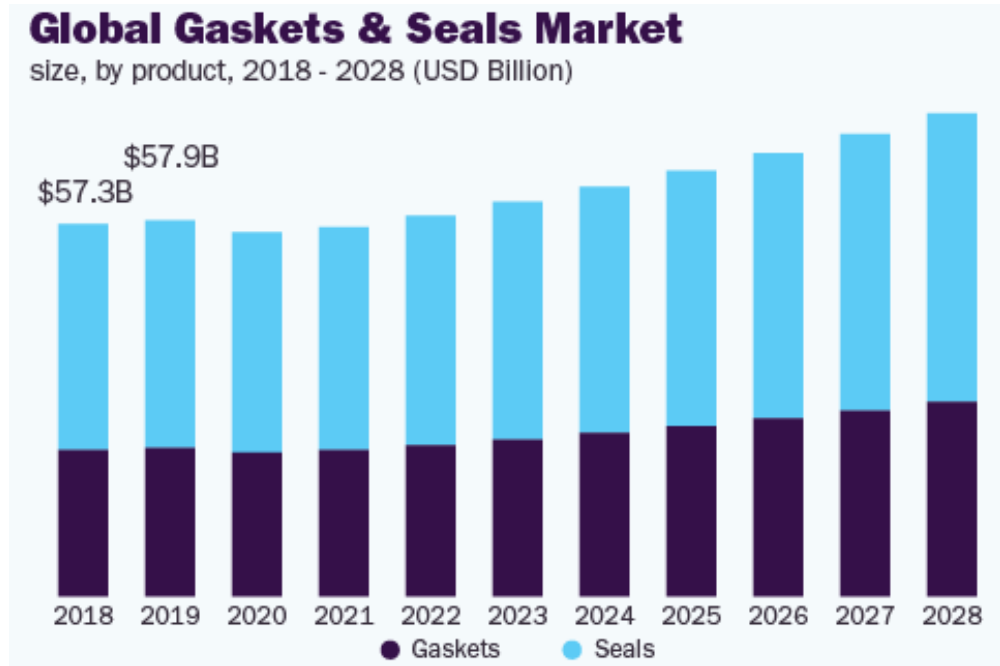


Figure 2.5: Global market for gaskets and seals (Gaskets and Seals Market Size, 2021)

2.2.1 Gasket materials selection

The gasket can be categorized based on the materials used to make it. Nowadays, the gasket can be made with metal, non-metal, polymer, and hybrid, and each gasket is designed for some specific function. The metal gasket can be constructed with stainless steel, titanium, copper, rhenium, aluminium, etc. Generally, a metal gasket can restrain corrosion resistance, apply in high thermal and pressure applications. Besides, the metal gasket has good thermal exchange properties (Aibada *et al.*, 2017).

Polymeric gaskets are produced from synthetic materials in the industry with medium corrosion resistance. It can be categorized by Pyrophyllite, Polytetrafluoroethylene (PTFE), Ethylene-Propylene-Diene (EPDM), Fluoroelastomer, Silicon rubber, Polyethylene, Chloroprene, etc. Pyrophyllite is applied in high volume press due to its good pressure transmitting efficiency. Furthermore, PTFE is widely used in gasket application as it is good thermal stability and compressibility, but a decrease in mechanical strength in higher temperatures. In contrast, Silicon rubber is excellent in temperature and environmental condition resistance. Furthermore, it is stable and easily shaped in a different shape for various applications. In addition, EPDM has fair chemical stability but is low in tensile strength and easily stretched. EPDM sealing gasket is used in tunnel joints, polymer electrolyte membrane fuel cells, and stacks. Fluoroelastomer gasket is a good performance in elevated temperature and excellent chemical stability at the same time. Chloroprene is mainly used in sound isolation on windows due to its good ozone resistance and weathering resistance. (Aibada *et al.*, 2017)

The non-metal gasket can be found in corrosion resistance applications, and it is suitable for use in low to high pressure and temperature environment. A non-metal gasket can be customized into different shapes and sizes and mostly as the alternative to replace the metal gasket for their limitation. The material of non-metal gasket can be made with silicone, graphite, nitrile butadiene, non-asbestos, cork, and others. Silicon has a superior heat resistance and is usually used in electrical insulation. However, silicon experience chemical degradation and increase in hardness over time. The graphite gasket is suitable for

electromagnetic interference shielding as it is sensitive toward electricity and temperature. Nitrile butadiene rubber is another common gasket where it can resist the normal diluted acids and alkaline. However, it is suitable for low tensile strength and low torque applications (Aibada *et al.*, 2017). Generally, non-metallic gasket normally is appearing in homogeneous or composite, filled up by several materials such as fibre, binder, filler, and coating. In addition, typical gasket thickness for non-metallic are 1/32" in North America, 1/16", and 1/8" in Europe. The non-metallic gasket thickness for Asia are 0.75mm, 1.0mm, 1.5mm, 2.0mm, and 3.0mm but gasket is able to adjusted to specific thickness per requested. (Charlene Jones, Mike Shorts, 2017)

Semi-metallic gaskets are a combination of soft and hard materials in the gasket. The soft materials are like fillers, insertions, and facings together with the metal component to enhance the properties of the gasket. Metal gaskets provide the structural strength while the non-metal is giving resilience property for a proper sealing characteristic. There are many synthetic composites or mineral based elastomer are inserted into metallic profile, or cast on metallic surface, or encapsulated partially or completely on the surface of metal. The properties of semi-metallic gaskets are there can perform under low to high temperature and pressure. Figure 2.5 shows examples of semi-metallic gaskets (Charlene Jones, Mike Shorts, 2017).

Figure 2.6 (a) presents metal reinforced with non-metallic gasket. The core metal is made with thin 316L stainless, nickel alloy as core or carrier and supported by soft sealing material. The flexible graphite, PTFE, vermiculite is often used as soft materials for resilience purpose. The core thickness usually at 0.002”/ 0.004” and combination of materials are considered with operating temperature, fluids, and pressure. Corrugated gasket is embossed metal coated with soft material. The highlight of this gasket can fit perfectly or better sealing for irregular shape of flanges and this called labyrinth effect. Jacketed gasket is comprised of soft compressible rubber sheet partially or fully encapsulate the metal. The gasket thickness normally is 2mm or 3mm. Kammprofile gasket is grooved metal surface with an outer ring and coated with coated with soft material. The function of outer ring is to fix the core metal on the top of sealing face by utilise the bolts. The spiral wound gasket is comprised of outer ring, filler material, metal “V” winding, and inner ring. The V-shape metal is closed with a suitable filler composite and the highlight of this gasket. The outer ring centralizes the winded metal on the seal while inner ring is to prevent the inward bend of the windings. Lastly, envelope gasket is made up of two parts such as envelope, function as shield and insert, function as filler insertion. It is commonly found in corrosive resistance applicant. The envelop serve as chemical resistance part which normally make up with PTFE while insert materials can be either metal or without metal material. The insert should good in compressibility and recovery for minimize seating stress. (Charlene Jones, Mike Shorts, 2017)

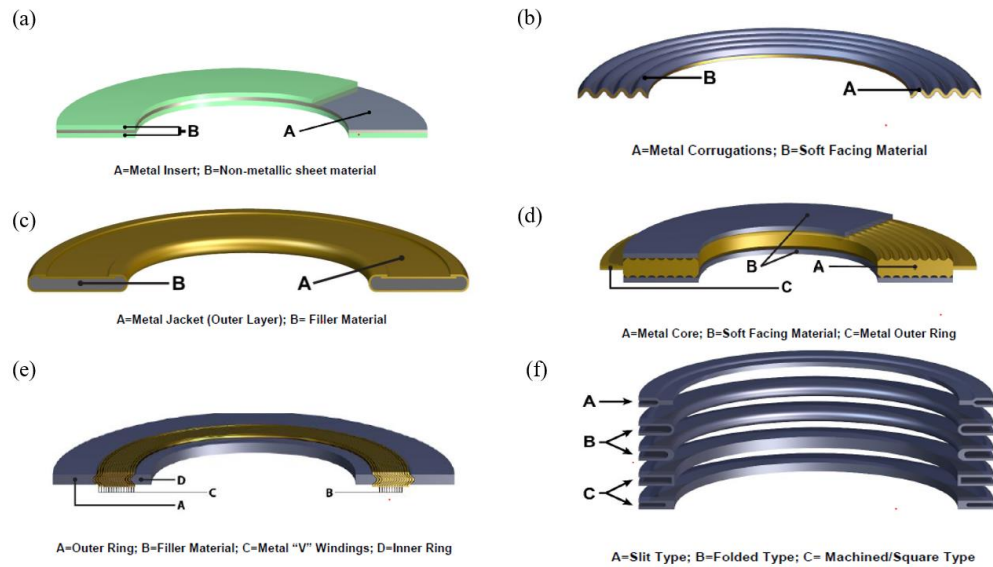


Figure 2.6: Semi-metallic gasket (a) Cross section of metal reinforced with non-metal gasket, (b) Corrugated gaskets, (c) Jacketed gaskets, (d) Kammprofile gasket, (e) Spiral wound gasket, and (d) Envelope gasket (Charlene Jones, Mike Shorts, 2017)

Metallic gasket is made up of single metal or combination of several type of metals. The advantages of metallic gasket are applicable for high temperature and pressure applications. However, higher load is needed to seat on the metallic gasket. The examples of metallic gasket are flat metal gasket, grooved metal gasket, round cross-section solid metal gasket, corrugated metal gasket, and etc. shown in Figure 2.7 (Charlene Jones, Mike Shorts, 2017).

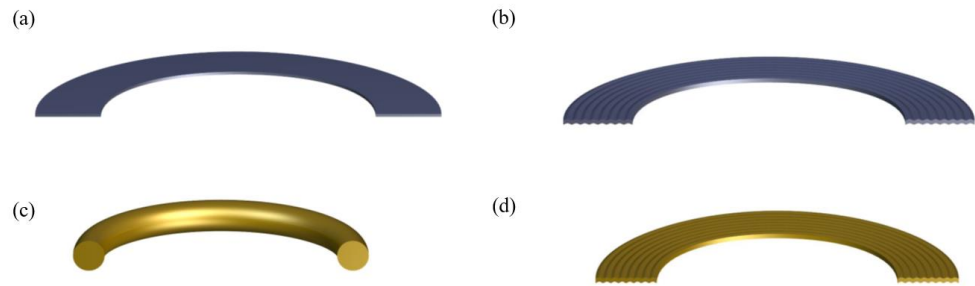


Figure 2.7: Metallic gasket (a) Flat gasket, (b) Grooved metal gasket, (c) round cross-section solid metal gasket, and (d) corrugated metal gasket. (Charlene Jones, Mike Shorts, 2017)

2.2.2. Gasket manufacturing process

The gasket from the industry is made from a large flat piece of rubber or other materials which are normally called “bun”. The process of gasket starts with a bun-splitting machine where it is cut into the desired width. After that, the gasket can be cut into the desired thickness by using a bun splitter machine. Once the specification of the rubber sheet is ready, it is brought to laminating machine where heat and pressure are applied on the surface of the gasket. The gasket side with stickiness can stick on other material's surfaces. Once the size and thickness are specified, computer numerical control (CNC) dies cutting machine is used to stamp the desired gasket shape out from the big rubber sheet. Hence, the gasket is fully done once the gasket is cut from the rubber sheet (Automated Gasket Corporation, 2020).

Furthermore, Dana Automocion S.A provide the process line of gasket manufacturing, to begin with, steel punching by stamping the shape of the desired cylinder head shape out from the steel coils. Next, the Sandwich assembly is where punched steel is stood in the middle of two fibre plates and continues with the calendaring process and produces a coil of materials. Once the process is done, the coils are cut according to the shape profile with a stamp or die tool. Figure 2.8 shows the process line of gasket calendaring and stamping (*Description of production processes, 2012*).



Figure 2.8 Process line of gasket calendaring and stamping (*Description of production processes, 2012*)

Gasket pressing is the next step where it is pressed into the desired thickness. Furthermore, the next steps are assembly and riveting of reinforcement and rings where some pieces of steel are cut into the shape and followed by assembled and riveted reinforcement and rings into the cylinder area. The gasket is pressed again with the reinforcement into specified thickness. The rings are placed around the lubricating fluid hole. Next, the gasket is

undergoing impregnation where the gasket is immersed into a silicone bath to fill up the pore of the fibre materials. Then, the surface finished gasket is cured under a static oven at a high temperature as shown in Figure 2.9. Once it is cured, the gasket undergoes silk-screen printing where the surface of the gasket received surface silicon beading for better sealing purposes where it is shown in Figure 2.10. Once again, it is cured under dynamic ovens and after that, the gaskets are packed for shipping. (*Description of production processes, 2012*)



Figure 2.9: Static curing machine (*Description of production processes, 2012*)



Figure 2.10: Gasket is under silk-screen printing (*Description of production processes, 2012*)

2.3 Waste tire recycling and application

2.3.1 An existing method in rubber recycling

With the rapid development of the automobile industry, a huge amount of waste tires has been generated. Globally it is estimated that 1.5 billion tires are being produced every year and about 4.0 billion tires end up in solid waste streams (Wang *et al.*, 2019). Waste tire is highly resistant to physical, chemical, and biological degradation due to its crosslinking and remain in the environment up to 100 years (Sofi, 2018). Conventional treatments such as landfills and incineration could result in the land occupation and pollutant emission (Wang *et al.*, 2016).

Nowadays, a waste tire can be reused and recycled through different processes such as mechanical (grinding), thermal (pyrolysis), and chemical processes (de-vulcanize). Recycling tire is relatively attractive as it can conserve landfill space. The tire is waste vulcanized rubber which is hardly to decompose in nature. Furthermore, another advantage of recycling rubber is creating beneficial products such as tire-derived fuel which is a higher burning value compared to commercial fuel. Besides, a waste tire can act as filler rubberized asphalt, flooring, railroad ties, etc. (Benefits of Recycling Tires, 2014).

However, vulcanized rubber is hard to re-melt and recycle due to its cross-linked thermoset structure. Cross-linked rubber has better resistance properties to acid, alkaline, chemical solution, and environmental aging which promote rubber to be anti-degradation. Thus, direct application of rubber is not workable, but reinforced waste rubber as filler in composite materials has a great outstanding performance and at the same time reduces the waste of rubber. Research shows that the addition of rubber waste has improved the composite properties such as increasing in tensile strength, modulus of elongation, better thermal insulation, etc. (Nuzaimah *et al.*, 2018). Mechanical grinding can be categorized into ambient grinding, cryogenic grinding, and wet ambient grinding. Waste rubber is breaking down into small particles size mechanically under different processing conditions. Table 2.3 shows a comparison of all three grinding methods (Asaro *et al.*, 2018).

Table 2.3: Comparison of all three grinding methods. (Asaro *et al.*, 2018)

Methods	Process Description	Advantages	Disadvantages
Ambient grinding	Vulcanized rubber breaks down through the mill at ambient temperature.	- Low Cost. - Simple system.	- Heat build-up - The high cost (fine particles) - Cause degradation of rubber.
Cryogenic grinding	Crushing pre-freeze rubber by using impact grinding.	- Smaller particles size. - The morphology of the surface is different. - Low heat build-up.	- High operation cost due to amount of nitrogen use.
Wet grinding	Rubber is grinding with water as lubricant and coolant.	- Very small crump. - Low-cost operation.	- The final ground rubber must dry.

Besides, chemical de-vulcanization is another method to recycle waste by breaking down carbon-sulphur (C-S) or sulphur- sulphur (S-S) chemically. A chemical agent such as disulphides, thiol-amine reagents, hydroxide, or chlorinated hydrocarbon is implemented in rubber de-vulcanized. However, this method is high toxicity and the process of de-vulcanized is complex and still yet fully understand. Diphenyl disulphide (DD) is the most common use agent in de-vulcanization. DD initiates oxidation to break down sulphur crosslinks and reacts with radicals and releases hydrogen sulphite (H_2S) and thiols (R-SH) at the same time. Furthermore, it is found that cross-linking network scission is preferable under high temperatures (Asaro *et al.*, 2018).

Subsequence, pyrolysis is a new form of the tire recycling process to extract hydrocarbon that can be reused in gas or liquid form. Pyrolysis can happen under the temperature of $400^{\circ}C$ with a catalyst or without a catalyst. The main products of waste tire pyrolysis are pyrolysis oil (40-60wt %), gas (5-20wt %), and char (30-40wt %). By this, the produced pyrolysis can be used in the manufacturing of carbon nanotube synthesis, burning fuel, and the residue is made into activated carbon. However, pyrolysis requires large pyrolysis plants with high operating costs due to high temperature and low pressure. Furthermore, the application of pyrolysis product are limited in large-scale manufacturing, and energy balance is not economical (Fazli and Rodrigue, 2020b).

Methods of tire recycling are being associated with several factors such as economic, environmental, and social, ambient grinding is most preferable in our contact due to small particle size, no finishing good drying, and overall cheaper. Thus, it is applicable and reliable to study the compatibility of WTP with NBR in gasket application.

2.3.2 Composition of tire

In the presence of research today, there are many research and practices with partial replacement of cement or natural aggregate with other industrial waste products such as granulated blast slag, coal bottom ash, recycle rubber, recycle aggregate, and others. Thus, many possible suitable materials can be blended with the rubber for cost-saving with acceptable final finishing product strength. Recycling waste is the easiest access able and economical. The content of the car passage tire has 41-48% rubber, 22-28% carbon black, 13-16% of metal, 4-6% textile, and 10-12% additive. Table 2.4 show the composition of car and truck tire (Senin *et al.*, 2016).

Table 2.4 Material composition of car and truck tire (Senin *et al.*, 2016)

Materials	Car/ Passenger (%)	Truck (%)
Rubber/ Elastomer	41-48	41-45
Carbon Black	22-28	20-28
Metal/ Steel	13-16	20-27
Textile	4-6	0-10
Additives	10-12	7-10

Furthermore, the waste tire can be undergoing tire refining (pyrolysis) through high temperature into several kinds of useful resources such as fuel, steel, carbon black, and some fuel gas. Figure 2.11 shows the pyrolysis plan or device for pyrolysis while Figure 2.12 shows composition break down after the pyrolysis process (Senin *et al.*, 2016).



Figure 2.11: Pyrolysis Plan (Senin *et al.*, 2016)

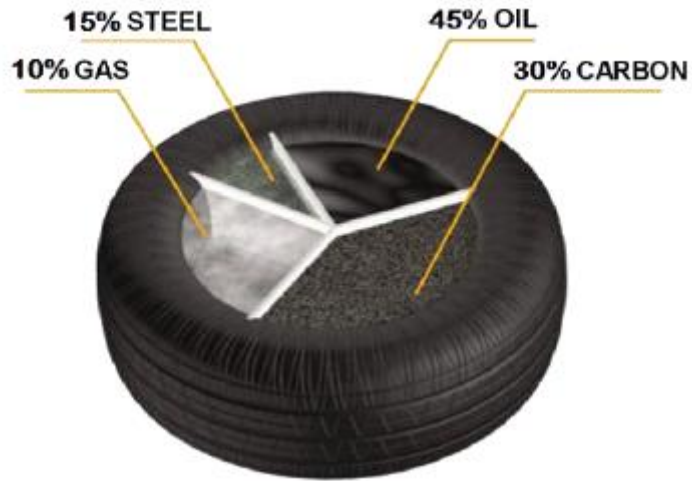


Figure 2.12: Composition breakdown after pyrolysis (Senin *et al.*, 2016)

2.4 Carbon black

Carbon black (CB) is the black colour element produced from the furnace, thermal, and acetylene black through hydrocarbon decomposition and partial combustion. CB is generally fine particulate aggregates as in quasi- graphitic molecular structure. Furthermore, the grade of CB can be classified according to the surface area and measurement of the structure. The smaller size of CB contributes to maximal blackness, but coagulation of CB may cause the resin to become harder. Furthermore, the structure size of CB may affect the dispensability and colour of the resin. The greater structure of CB has better dispensability but with lower blackness. Furthermore, a greater structure has better conductivity. Figure 2.13 shows the CB structure size (Jebur, 2018).

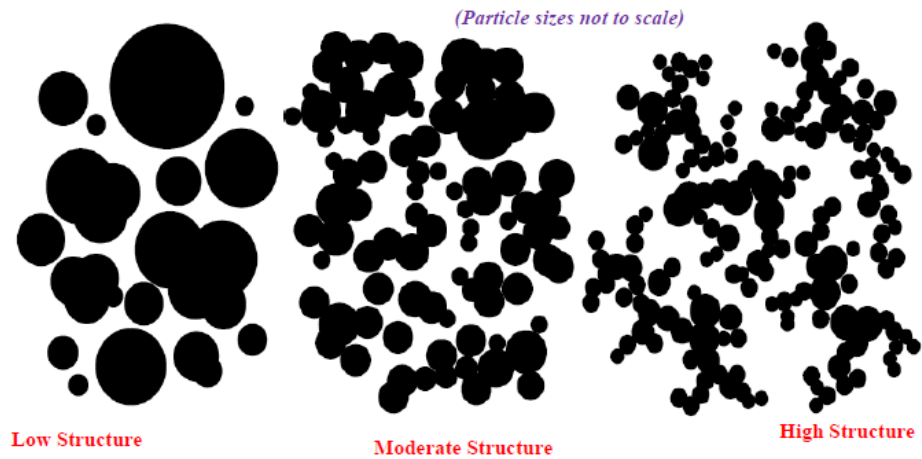


Figure 2.13: Carbon black structural size (Jebur, 2018)

The main application of CB is to act as reinforcement in rubber materials to increase the mechanical and electrical properties. The mechanism of CB is the formation of a filler network physically and the formation of polymer coupling with strong CB. In past, CB functioned as a pigment in black ink, especially in countries like China and India. After that, the CB is further explored as filler in plastic, paints, and elastomer to enhance the electrical, optical, and other mechanical properties. Figure 2.14 shows the global carbon black demand until the year 2018. (Jebur, 2018)

Global carbon black demand by application until year 2018

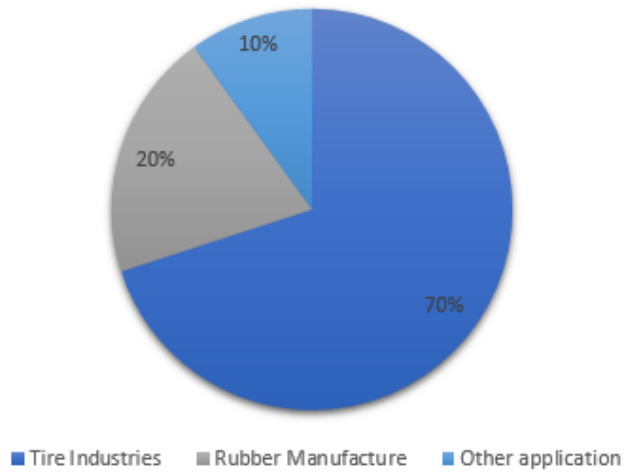


Figure 2.14: Global market demand of carbon black until the year 2018 (Jebur, 2018)

The figure above shows that 70% of CB is used in reinforcing and pigment in automotive tires. Furthermore, CB stabilization and paint are used in films and resins colouring. In addition, 20% of CB is applied in hoses, belts where the functional in pigment in inks, plastics, and coatings. Apart from that, CB can be used in food packaging's such as microwavable meat and meal trays. Figure 2.15 shows the application of CB in a variety of products (Jebur, 2018).



Figure 2.15: Carbon black application in various products (Jebur, 2018).

2.5 Carbon Black/ Nitrile Butadiene Rubber Composite

Nitrile Rubber has a characterization of oil resistance, high abrasion, superior strength, and chemical and solvent resistance. However, neat NBR does not have crystallinity for the self-reinforcement effect. Thus, the addition of carbon black filler in the rubber blend can improve mechanical performance. Carbon black was chosen as reinforcement filler due to compatibility with NBR and different loading of Carbon Black has been tested here. The loading of

Carbon Black is 30phr, 40phr, 50phr, 60phr, and 70phr (Husnan, Ismail and Shuib, 2018).

The result shows that cure time and swelling percentage decrease with increasing CB loading but the minimum torque has increased with the addition of Carbon Black in blending. Furthermore, tensile strength, tensile modulus, hardness, tear resistance, and compression of CB / NBR composite increases with the filler while decreasing elongation at break of the blending and resilience property of the rubber composite. Figure 2.16 shows the cure time of rubber blending with Carbon Black decreases with increasing loading. This is because the recycled NBR contains a remaining cross-link additive and presence curative agent which is sulphur having the crosslinked reaction with carbon black. Furthermore, Figure 2.17 shows increasing in minimum torque value for rubber blending due to increasing glow resistance in rubber blend caused by cross-linked NBR with carbon black and additives (Husnan, Ismail and Shuib, 2018).

Besides, once observation can be done in Figure 2.18 where tensile strength increase with the filler loading as the crosslinking density of the blends has increased. Furthermore, the addition of filler has caused the increase of tensile modulus, compression set, and hardness while decreasing in properties of swelling and elongation at break. As the filler ratio increase, the swelling percentage decrease due to lessening penetration of motor oil into rubber composite. Practically, the density of crosslinking in rubber compound increase and lead to a rise of network elasticity contribution. Restriction extensibility of rubber chains induces by swelling gives a higher difficulty for motor oil to

diffuse into the gaps between rubber molecules. The result is shown in Figure 2.18 (Husnan, Ismail and Shuib, 2018).

In addition, Figure 2.20 shows elongation at break of blend decrease with an increase of filler as due to restriction movement of the chain and the sample fail at lower elongation. Subsequently, tensile modulus shows a trend of increasing with the addition of filler because the filler can increase crosslink density, and thus the rubber blend increases in modulus and hardness (Husnan, Ismail and Shuib, 2018). Figure 2.21 and Figure 2.22 show the result of tensile modulus and hardness of rubber blend increase with the addition of carbon black. The granular CB has active and zigzag surface area which generally increase the entanglements between filler and NBR chain. The body of the rubber composite become rigid and resist penetration components from outside. Thus, the surface tension and hardness of the composite is increase (Al-maamori, Al-Zubaidi and Subeh, 2015).

Moreover, addition of CB can increase the compression set percentage of the rubber composite. The justification is where the entanglement is increased, and chain locomotion is limited. The rubber compound become more rigid, stiffer and rubber is easier to retain their original shape after compression. The data is shows in Figure 2.23. In this research also, CB is showed that it can enhance the property of tear resistance. Figure 2.24 shows the CB loading increase can increase the tear resistance of rubber composite and decrease after 60phr of CB. The loading of CB can increase the complexity of rubber chain but decrease at 60phr when the rubber chain is saturated and cause fragility. Other

than that, resilience property of NBR/CB decrease as shown in Figure 2.25. This is because proportion of CB increase lead to hardening of rubber and chain restriction. The rubber can absorb kinetic energy and become heat energy without changing the shape of rubber. The lower the resilience property, the lower the energy needed for deform materials back to their previous shape. (Al-maamori, Al-Zubaidi and Subeh, 2015)

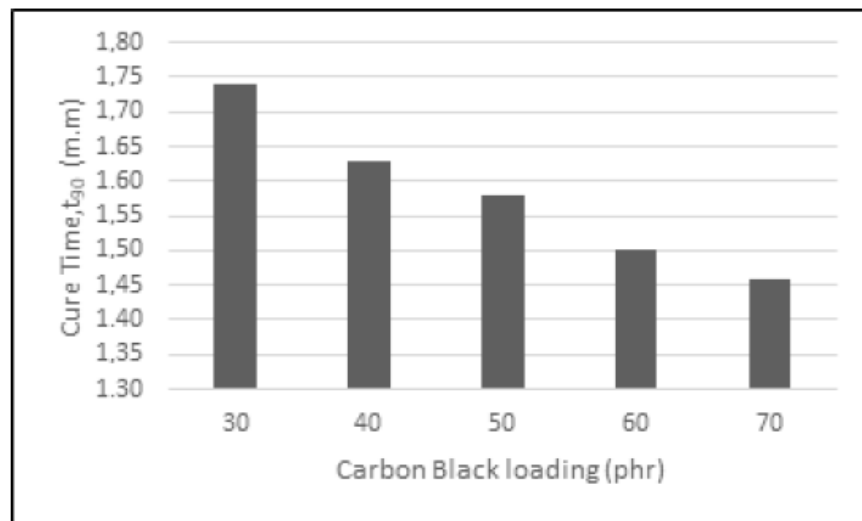


Figure 2.16: Effect of CB loading on Cure Time (Husnan, Ismail and Shuib, 2018).

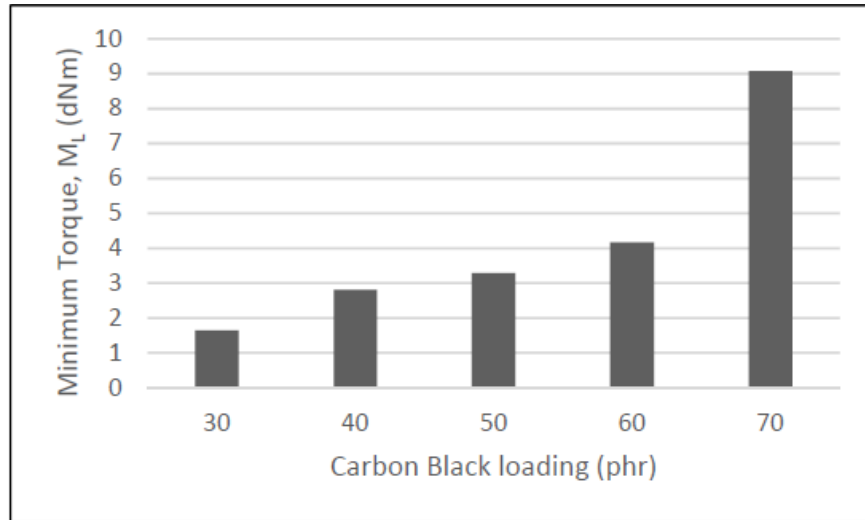


Figure 2.17: Effect of CB loading on minimum torque. (Husnan, Ismail and Shuib, 2018)

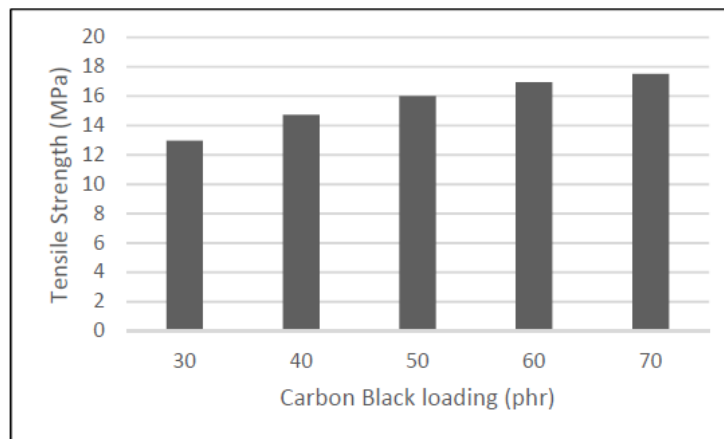


Figure 2.18: Effect of CB loading on Tensile Strength (Husnan, Ismail and Shuib, 2018).

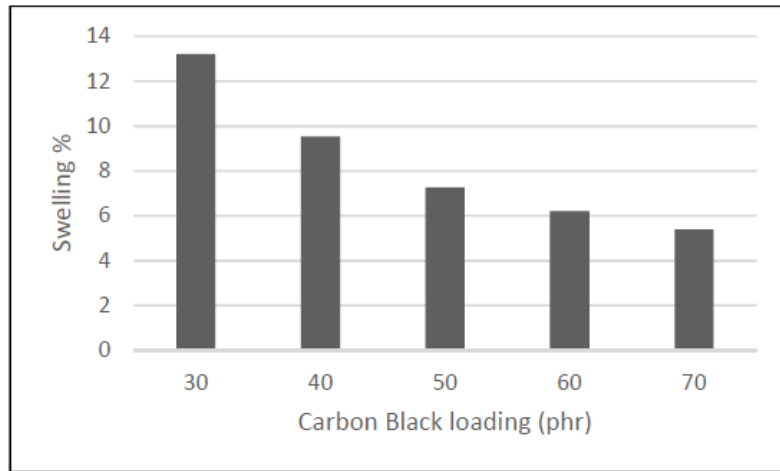


Figure 2.19: Effect of CB loading on composite swelling (Husnan, Ismail and Shuib, 2018).

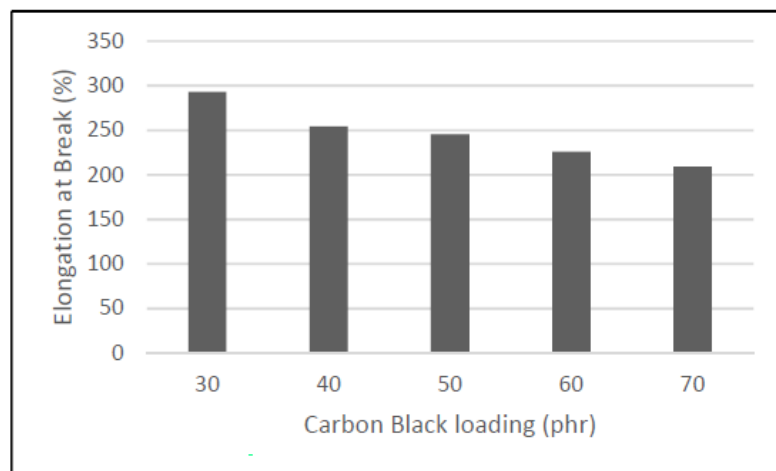


Figure 2.20: Effect of CB loading on Elongation at break (Husnan, Ismail and Shuib, 2018).

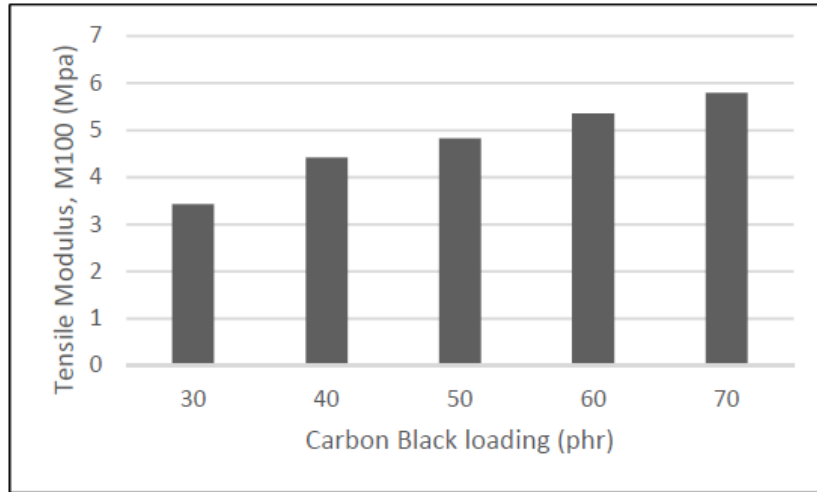


Figure 2.21: Effect of CB loading on Tensile Modulus (Husnan, Ismail and Shuib, 2018).

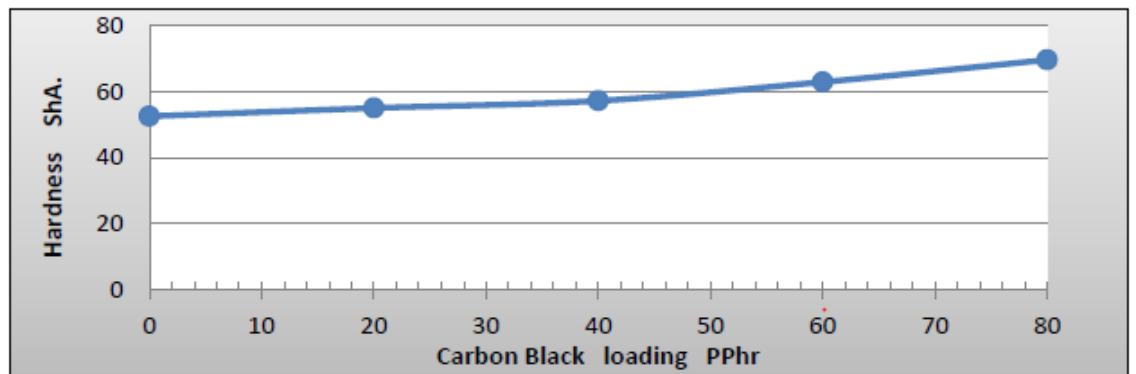


Figure 2.22: Effect of CB loading on the hardness (Al-maamori, Al-Zubaidi and Subeh, 2015).

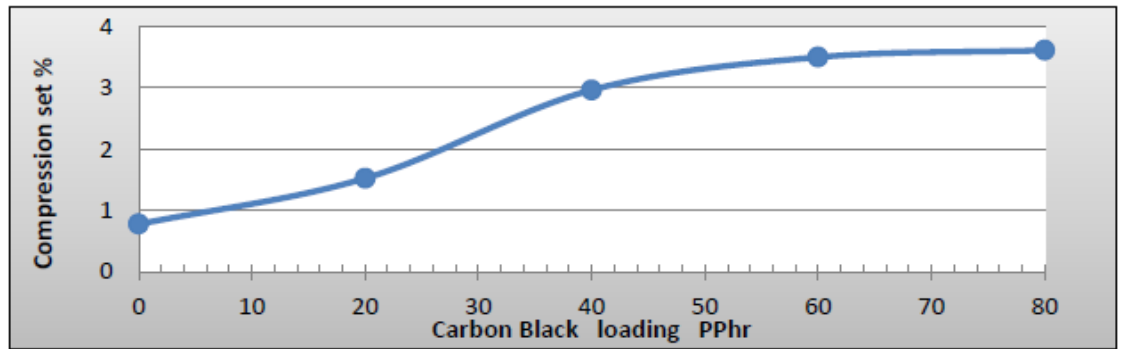


Figure 2.23: Effect of CB loading on Compression set (Al-maamori, Al-Zubaidi and Subeh, 2015).

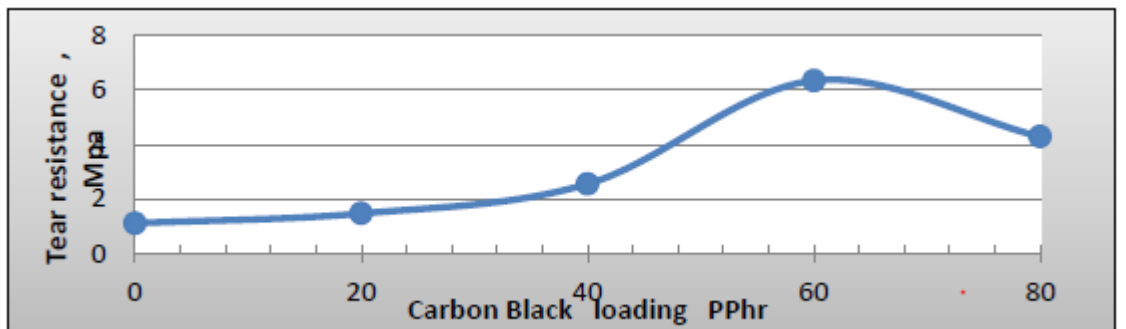


Figure 2.24: Effect of CB on tear resistance (Al-maamori, Al-Zubaidi and Subeh, 2015)

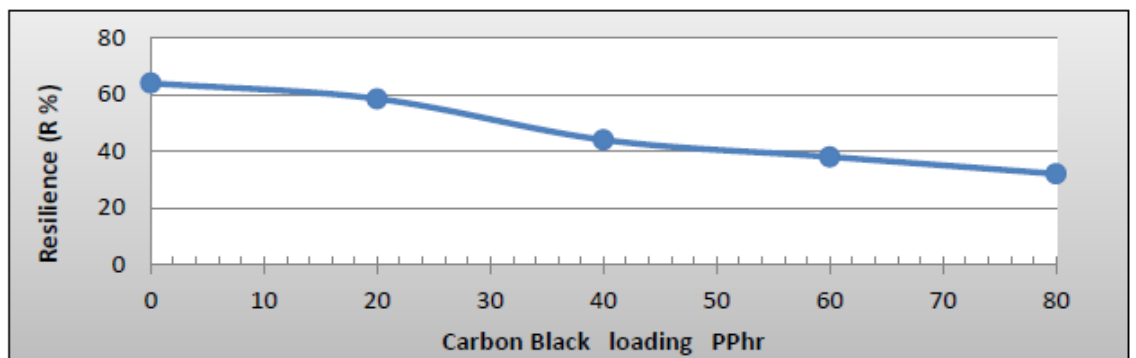


Figure 2.25: Effect of CB on resilience (%) (Al-maamori, Al-Zubaidi and Subeh, 2015).

2.6 Waste tire powder / rubber composite

Vulcanized rubbers have a low elasticity and yield strain, yet the cross-linked structure of rubber is good in shear resistance, high temperature application and as a good environmentally friendly additive. Tire is main source of vulcanized rubber as it has good performance in outdoor application. It can resist to chemical, high temperature, abrasion, and radiations. Despite of excellent outdoor performance, automotive tire has extensive high life span for new tire and large number of un-degradable tire become concern of environmental issues. The tires are being process through the repeat cycles grinding to form WTP (Fazli and Rodrigue, 2020).

In the past study, incorporation of WTP as filler in the rubber increase the Mooney viscosity of the rubber. The viscosity of rubber matrix increase is due to cross linking and chain mobility restriction. The addition of WTP and CB from tire cause the rubber matrix to become stiffer and process ability decrease. Figure 2.26 shows Mooney Viscosity is increase with the loading addition of WTP and CB (Fazli and Rodrigue, 2020).

Besides, mechanical properties of addition grinded tire rubber (GTR) into rubber matrices are investigated. Mechanical properties such as tensile strength, elongation at break, tear strength, abrasion resistance, compression set, and resilience % are investigated and tabulated in Table 2.5. The result shows that NR/ GTR has drop in tensile strength and elongation as the GTR filler portion increase, while mixing of NBR/ GTR has increase in tensile but decrease in

elongation along with filler increase. The rubber composite with lower tensile strength and elongation is due to weak homogeneity and weak adhesive strength in the blending. The higher filler loading attribute to increase of gel fraction with cross linked along the structure of NR and it's become the stress concentrating point as a reason of the decrease of tensile strength and elongation (Fazli and Rodrigue, 2020).

The function of GTR reinforcing filler can diverse the energy intake and alter the tear path through resisting and delaying the growth crack. Thus, reinforced GTR/NBR has higher strength and tear strength is improved. Furthermore, thermal stability rubber is enhanced with the addition of GTR. The weight loss of the rubber is generally reduced with the addition of GTR. The research shows that 50phr of GTR addition can increase rubber residue from 15% to 30%. NBR induced cross linking by GTR has better thermal stability and shifted initial decomposition temperature to higher temperature (Fazli and Rodrigue, 2020).

In addition, solvent is less likely to penetrate rubber reinforced with GTR. The higher crosslinking density imposed less swelling of solvent. Figure 2.27 shows that swelling weight ratio % is reduced with addition of GTR contents. Solvent is less likely to breakthrough vulcanized rubber matrix with high crosslinking density due to chain restriction (Fazli and Rodrigue, 2020).

Furthermore, some research has been carried out to determine the properties enhancement of devulcanized tire rubber in styrene butadiene rubber (SBR). In this research, WTP is undergo treatment before blending. The WTP is devulcanized by using two methods which are mechano-chemical and microwave. 2-mercapto benzothiazole disulphide (MBTS) and Tetramethyl Thiuram Disulphide (TMTD) as the devulcanizing agents together with different microwave treatment periods and temperatures. Then the devulcanized WTP only added with virgin SBR for blending process (Ali *et al.*, 2020).

The literature shows that reinforcement of pre-treated WTP can improve the mechanical properties of the Styrene Butadiene Rubber (SBR). Figure 2.28 show that neat SBR has lower tearing strength compared to reinforced WTP. Furthermore, it is shows that chemically and microwave modified devulcanized waste rubber (DWR) has higher tear strength which conclude that DWR is able it is compatible with SBR. The content of carbon black in the DWR minimize the crack growth and ionizing radiation from gamma ray induces stronger polymer chains. The rubber become more ductility with increase of radiation dose (Ali *et al.*, 2020).

Furthermore, tensile modulus of the SBR can increase with the addition of DWR. Table 2.6 show tensile modules of SBR with various DWR under 100% of elongation and in different irradiation dose. The result shows that neat SBR has lowest tensile strength while (50/50) SBR/DWR-TMTD has the maximum tensile strength follow by (80/20) SBR/DWR-MW as the second highest tensile strength. Cross linking density is the major factor in affecting the tensile strength

(Ali *et al.*, 2020). Figure 2.9 show that tensile strength of different loading of TMTD devulcanized tire powder. The tensile strength increase because DWR has benefit to surface adhesion between virgin rubber and reclaimed rubber (DWR) by inducing co-cross linking (El-Nemr *et al.*, 2020).

Table 2.5: Tensile modulus of 100% elongation of SBR/ various pre-treated tire rubber (Fazli and Rodrigue, 2020).

Blend	GTR Loading	Tensile strength (MPa)	Elongation at Break (%)	Tear Strength (N/mm)	Abrasion Resistance (cc/h)	Compression Set (%)	Resilience (%)
NR/ GTR	20	15.9	500				
	40	13.4	417		Not reported		
	60	11.6	260				
NBR/ GTR	20	4	325	22	4	15.5	30.5
	10	6	310	27	7	17.5	27

Table 2.6: Tensile modulus of 100% elongation of SBR/ various pre-treated tire rubber (Ali *et al.*, 2020).

Modulus at 100% (MPa)	Irradiation dose		
	0	100	200
100 SBR	0.1610	0.2980	0.3420
(80/20) SBR/DWR- MBTS	0.4000	0.4000	0.5900
(80/20) SBR/DWR- TMTD	0.3900	0.3900	0.4800
(50/50) SBR/DWR- TMTD	0.6180	0.6180	0.7200
(80/20) SBR/DWR- MW	0.4000	0.4200	0.5100

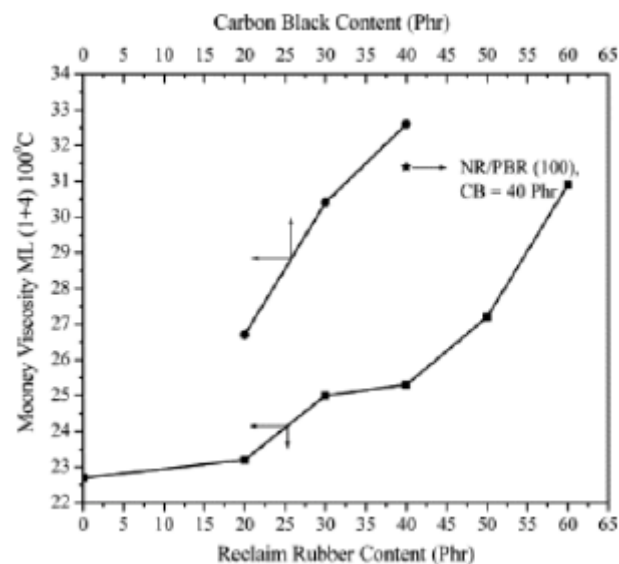


Figure 2.26: Mooney viscosity of NR with WTP and CB (Fazli and Rodrigue, 2020).

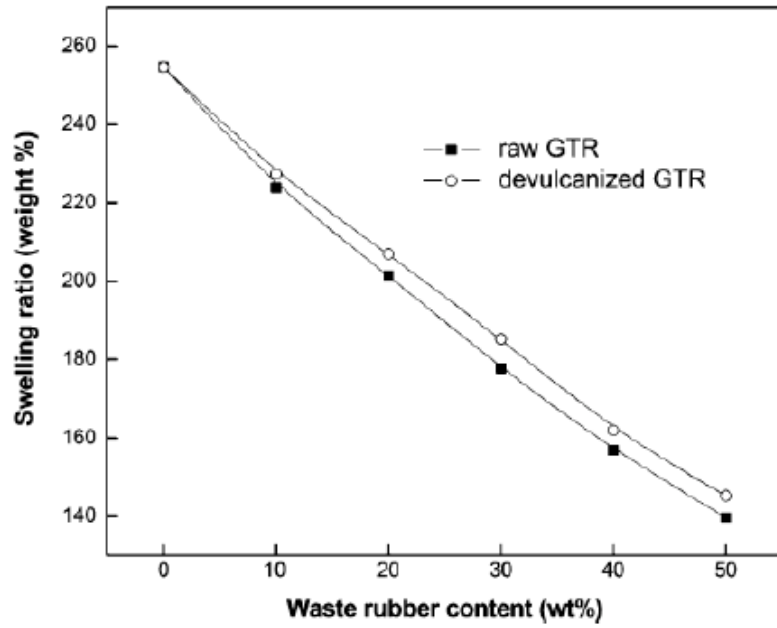


Figure 2.27: Swelling ratio on different loading of raw and devulcanized GTR (Fazli and Rodrigue, 2020).

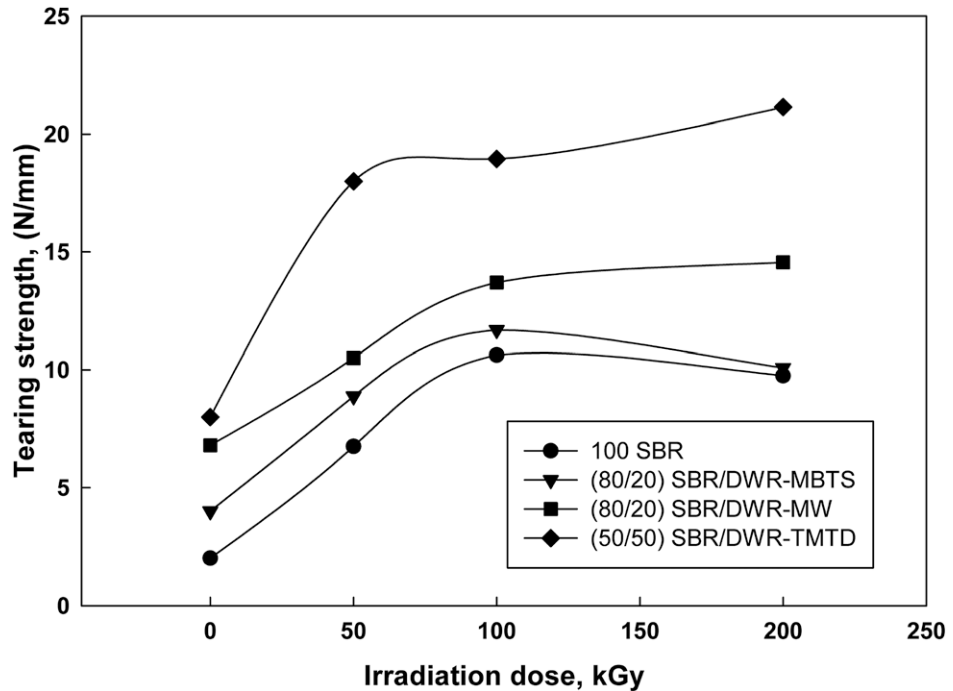


Figure 2.28: Tearing strength of SBR reinforce with different type of DWR under different gamma radiation dose (Ali *et al.*, 2020).

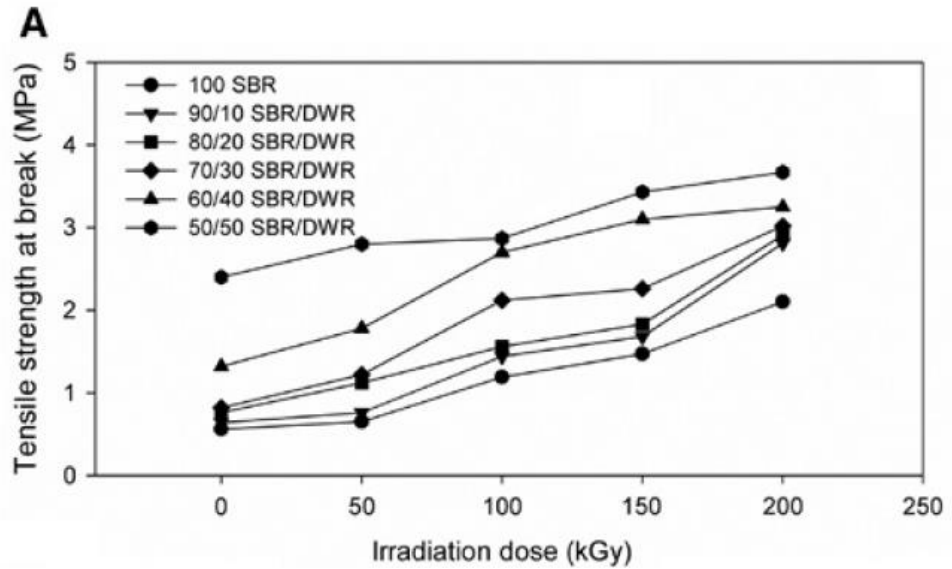


Figure 2.29: Tensile strength of different loading of irradiated SBR with TMTD waste tire powder (El-Nemr *et al.*, 2020).

2.7: Foaming and Curing Parameters

Foaming technology is widely used in industrial applications nowadays due to large contact area and more rapid wettability. Furthermore, foaming performance can be evaluated from foaming ability and foaming stability. Foaming ability is referring to surfactant formation when under exposure of various circumstances. Besides, foaming ability is referring to lifetime and durability of the foam. There are result show that higher viscosity has better durability of the foam while viscosity is influenced by temperature.

In addition, the temperature increase will lead to foaming concentration increase as well. The anionic surfactants or foaming agents increase with the temperature increase because of Brownian motion. The kinematic velocity of the ions increases and there have move frequent collision in between of ions. Thus, the foaming concentration increase.

Other than that, researcher also define the foaming stability under influence of temperature. Generally, half-life of the foam decreases with increase of temperature. The anionic, cationic, and nonionic surfactant half life are decrease drastically when the temperature arises. The data show that at lower temperature from 20⁰C to 30⁰C, the four surfactants reach the maximum half life where the gas diffusion rate is relatively low at this stage. At elevated temperature, the surface viscosity is lower and more rapid liquid drainage happened (Wang *et al.*, 2017).

Besides, the curing behaviour has been identified by addition of nanofiller. Nanofiller increase the viscosity of the rubber as shown in Figure 2.30. The data show the torque is increase with the addition of silica content from 0phr until 40phr. The viscosity forms a barrier for the cell to growth. Thus, the bubble size will be smaller in size. Secondly, the two-steps foaming lead to larger cell size as bubbles continue to growth and then cured. There is no limitation of crosslinking during bubbles growing. Furthermore, the participant of blowing agent able to boost the curing rate due to exothermic decomposition reaction (Bayat *et al.*, 2020).

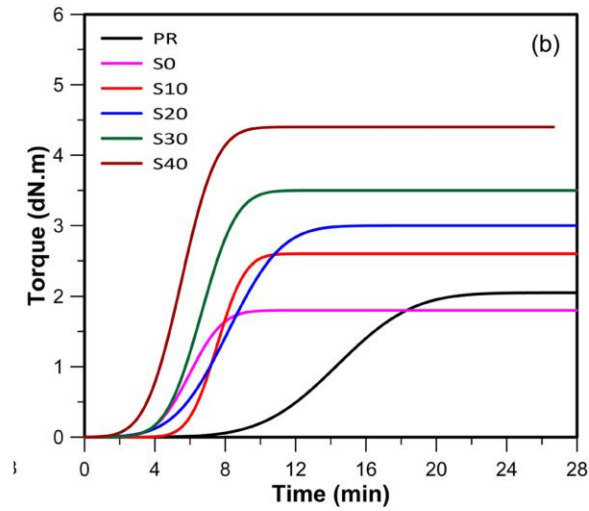


Figure 2.30: Torque vs time at 140°C (Bayat et al., 2020).

Apart from that, curing duration is importance in rubber foaming. It can be divided into three stages which are induction period which is safe processing time. The second stage which under curing reaction which the rubber network become rigid and stiffer due to crosslinking reaction happened. After this stage, the rubber tends to become mature and overcuring. The rubber will have reversible reaction in this stage. Figure 2.31 shows the three stages of curing with time.

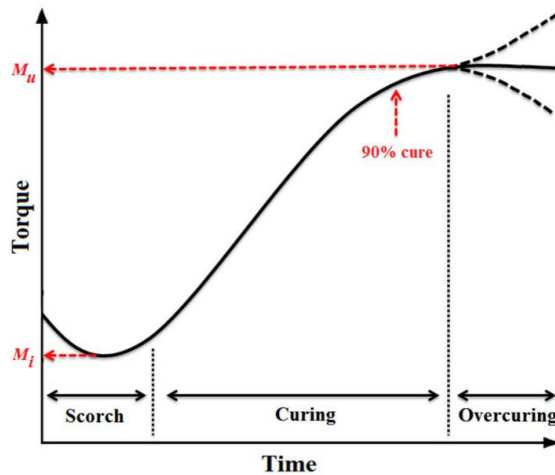


Figure 2.31: Rubber vulcanization curve rate

2.8 Introduction to the rolling method in gasket coating production.

Coating process is a more challenging process and it require high process accuracy. Coating requires high thickness control, pattern formation and uniformity. Furthermore, coating can be done with single layer or multiply layer of materials on the surface of the substrate. Thus, there are different type of coating technique available to cater wide range of coating materials and substrate while achieving the final products performance with cheaper cost. The final products shall have uniform and desired thickness, stable and good adhesion to the sample surface. Besides, processes such as metering, transferring, and fixing are applied in all coating technique (Shim, 2018).

Metering is a controlling process where amount of desire material is coated on the surface of the substrate. Metering coating process can be referred to free-meniscus coating, pre-metering coating, and post-metering coating. Free-meniscus coating is referring to dip coating or where substrate is withdrawn from the liquid. The rheology properties of the liquid, substrate geometry, and substrate speed is the dependent for the coating thickness. Furthermore, pre-metering coating technique refer to the slot coating and curtain coating where the liquid volume is fixed before feed into metering die. Post-metering coating is where excessive of liquid are apply on the substrate and removal of excessive liquid by using knife or air-knife afterward (Shim, 2018).

Transferring is mentioned where the liquid is coated on the surface of the substrate and formation of a coating layer. The process can be completed by applying a series of rollers, spray, direct extrusion, or immersion of substrate on the liquid. Afterward, fixing is a process where liquid transferred is fixed on the substrate through drying, pressing, curing and others. Roll coating can be differentiated with number of rollers used in the application. Figure 2.32 shows the example of roll coating with post-metering process. The liquid is transfer on the substrate and excessive of the liquid is removed. The thickness of the gasket is determined by the gap of the knife with the surface of the substrate. Once the liquid is transfer to the substrate, the fixing is taken place by curing (Shim, 2018).

Besides that, the roll coating can be set up according to Figure 2.33. The fabric picks up the substrate from the applicator roller. The applicator roller and metering roller are rotate in opposite direction to ensure the amount of the substrate picked up and doctor blade is used to clean up the remaining coating liquid on the surface of the metering roller to prevent coating defects. Lastly, the backup roller is used to support the coated layer from the applicator roller (Butt, 2022).

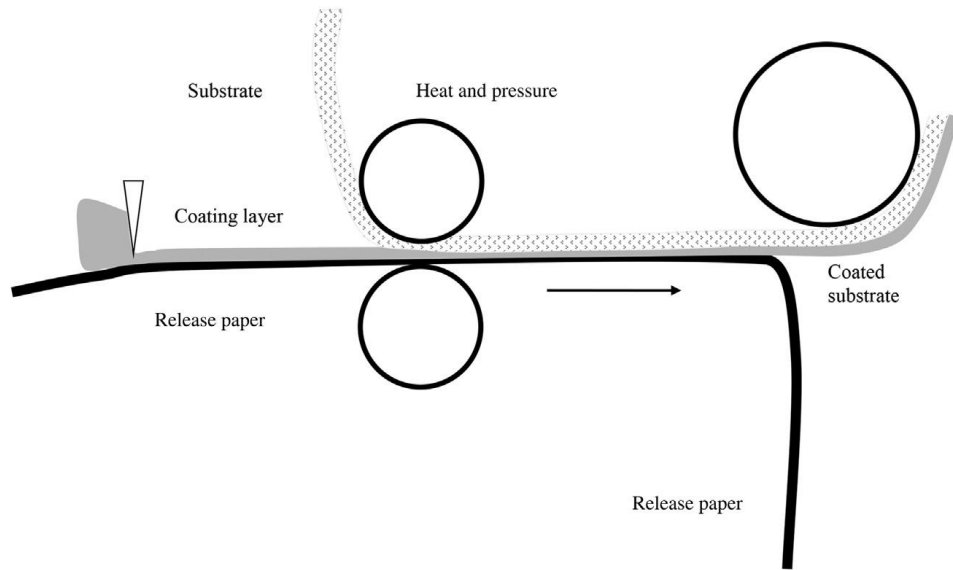


Figure 2.32: Calendaring rolling process of the rubber (Shim, 2018).

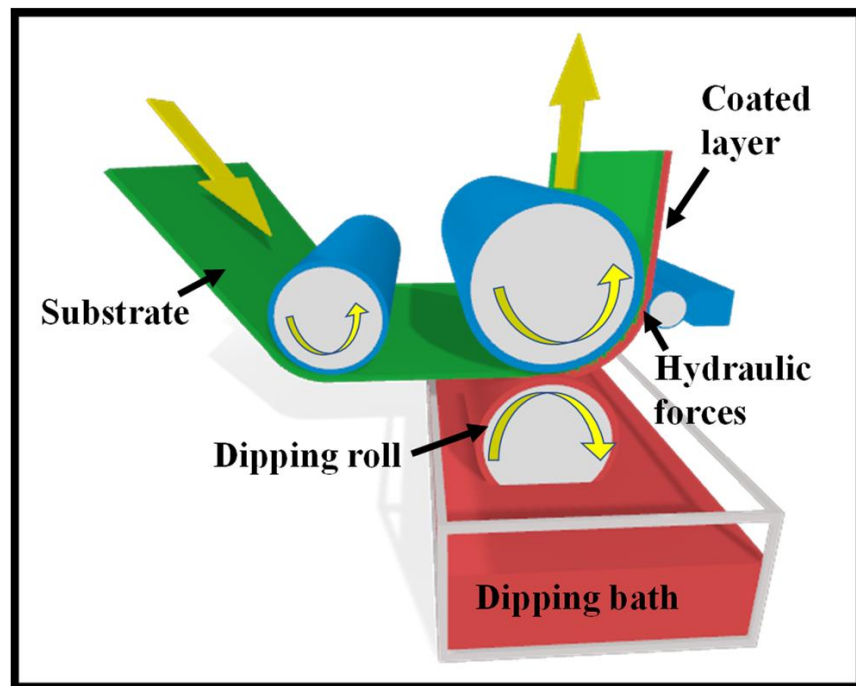


Figure 2.33: Roll coating set up (Butt, 2022).

Furthermore, roll coating is suitable for coating applications where it can be coated on one side, both sides, or even laminated with multiple later substrates on the surface. The use of three rollers is sufficient for single side coating while four rollers calendar is suitable for extremely thin coating, and it can apply both size coating techniques simultaneously. The advantage of taking calendar as a coating method as it has maximum rates, speedy, accurate, and consistent thickness measurement, products, processing range versatility, etc (Rosato, Rosato and Rosato, 2004).

2.9 Principle of rolling process and rolling defect in rubber.

Rolling manufacturing is widely used in sheet manufacturing and media transfer, especially in papermaking, sheet making, and printing process. However, the rolling methodology might come with defects on the finishing composite. The material is push in the between of the two rolls and the frictional force is applied on the surface of material and roller when the material is pulled into the rollers (Chu *et al.*, 2019).

As for rolling process, shear strain and stresses will be occurred, and it is depending on rolling velocity and the distance before the solidification happen. However, casting film does not have any stress and strain build up. Besides, Furthermore, rolling gasket always has higher chemical links as compared to casting gasket and the polymer structure and crystallinity rate are different in

casting and rolling. The chemical link is relatively important in rolling process as presence of shear strains on the surface of rolling conditions will induce diffusion and promote addition copolymerization reaction (Serrat *et al.*, 2012).

In gasket casting process, the crystallization of the gasket is affected by cooling rate, and it is more homogeneous structure because heat transfer evenly on the upper surface of the sample through convection. Apart from that, peeling force is more dependent on the mechanical properties (Serrat *et al.*, 2012).

Rolling manufacturing is widely used in sheet manufacturing and media transfer, especially in papermaking, sheet making, and printing process. However, the rolling methodology might come with defects on the finishing composite. There is some deflection mainly due to roll force which results in thicker at the centre of the roll sheet and thinner at the edges. This deflection is named as crown camber. Furthermore, other defects such as mill spring where the thickness of the rolled sheet is thicker than desired thickness and roll elastic deformation are where uneven thickness across the sheet. The result of the deflected sheet has thinner edges and thicker in the centre. The long edges of the sheet are elongated and compressed more than the centre and the tension is applied at the middle of the sheet. Besides, rolling can cause edge defects where tensile deformation happened at the edge of the sheet (Jansto and Stalheim., 2020).

CHAPTER 3

METHODOLOGY AND MATERIAL

The detail of the raw materials used to development the coating materials for gasket, and the complete methodology for the research work are described in this chapter. In summary, the coating material was developed by dissolving NBR rubber in the Methyl Ethyl Ketone (MEK) solvent and other compounding ingredients was added to prepare the coating compounds with different formulation. In phase 1, the researcher formulation is used for optimization of processing parameters such as foaming and curing temperature and time. The phase 1 optimization is carried out simultaneously with phase 2 optimization of compounding formulations. The given formulation is manipulated with filler, sulphur and plasticizer loading. In the Phase 3, optimization of the coating techniques was carried out by comparing coating technique through casting and rolling methods to obtain desired thickness and texture of the final coating material. The finished coating gasket was characterized and mechanical testing such as oil absorption test, gel fraction, thermal aging test, Thermogravimetric analysis (TGA), peeling test, hardness test, and Scanning electron microscopy (SEM) analysis was carried out to evaluate the required properties as per standard. Figure 3.1 shows the research flow chart for the preparation and testing of NBR/WTP coating materials for gasket application.

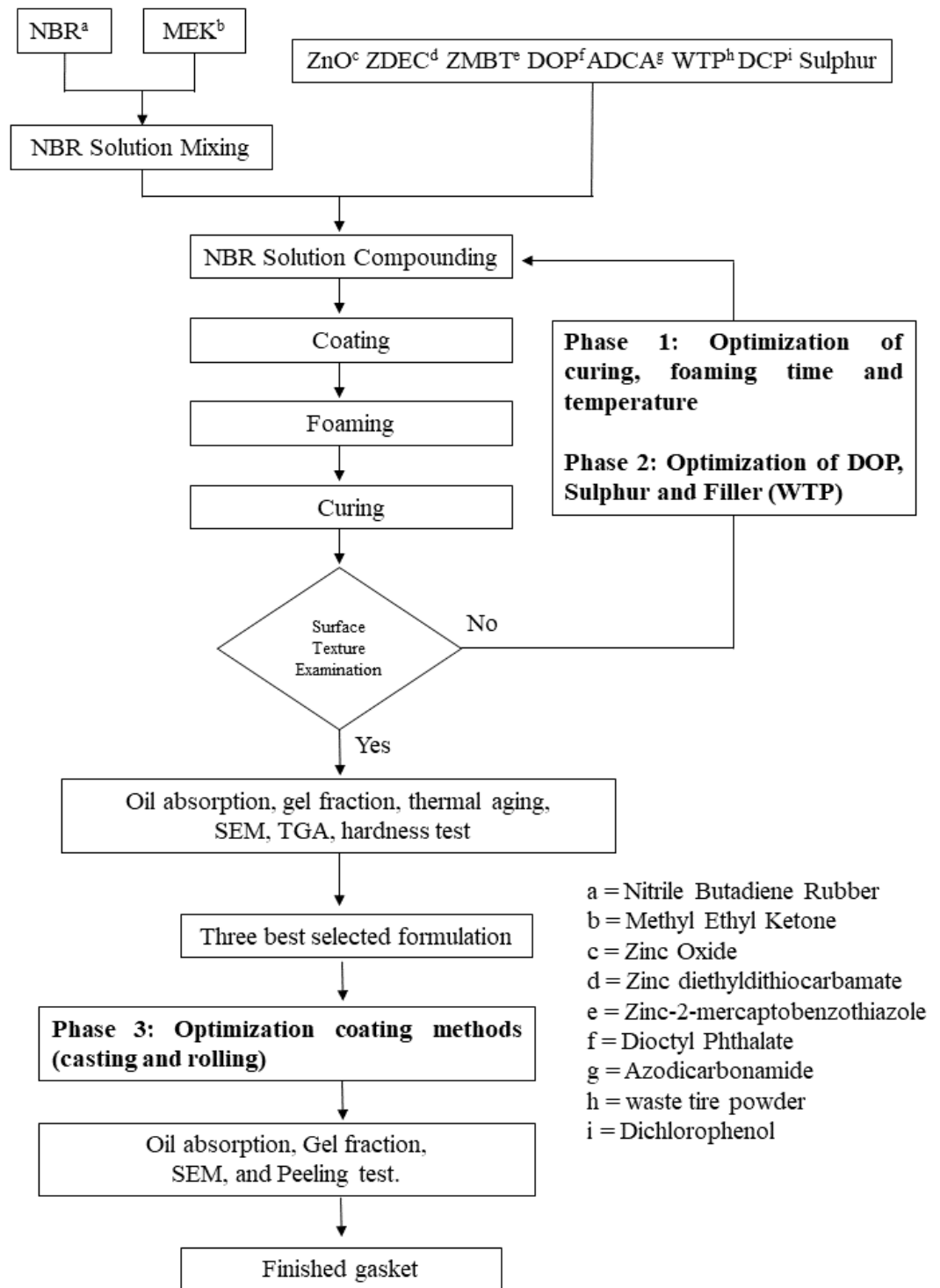


Figure 3.1: Compounding flow chart of NBR/WTP.

3.1 Compounding materials

The major compounding materials that been used in the research were nitrile butadiene rubber (NBR) as the matrix and the waste tire powder (WTP) as filler. Other compounding ingredients used are Zinc Oxide (ZnO), Zinc diethyldithiocarbamate (ZDEC), Zinc-2-mercaptobenzothiazole (ZMBT), Dioctyl Phthalate (DOP), Azodicarbonamide (ADCA), Dicumyl peroxide (DCP), and Sulphur. Table 3.1 show the list of suppliers and the respective function of all the raw materials used in this research. All materials were purchased and used as it is.

Table 3.1: Functions of compounding ingredients and distributor.

Chemical	Function	Distributor
Azodicarbonamide (ADCA)	Foaming agent	UP Packing Sdn. Bhd
Dicumyl peroxide (DCP)	Curing agent	Sigma-Aldrich (M) Sdn.Bhd
Dioctyl Phthalate (DOP)	Plasticizer	Sigma-Aldrich (M) Sdn.Bhd
Methyl Ethyl Ketone (MEK)	Solvent	Next Gene Scientific Sdn. Bhd.
Nitrile Butadiene Rubber (NBR)	Rubber matrix	Zarm scientific & supplies sdn bhd
Sulphur	Cross-linking agent	Next Gene Scientific Sdn. Bhd.
Waste tire powder (WTP)	Reinforce filler	Sunrich Integrated Sdn.Bhd
Zinc Oxide (ZnO)	Vulcanization activator	Labchem Sdn Bhd
Zinc-2-mercaptobenzothiazole (ZMBT)	Primary curing accelerators	Tokyo Chemical Industry Co.LTD
Zinc diethyldithiocarbamate (ZDEC)	Secondary curing accelerators	SIGMA-ALDRICH.Co

Besides, there were several chemicals that used in performance testing such as oil absorption test and gel absorption test were provided. These chemicals were automotive engine oil, and toluene. The automotive engine oil is Castrol 20W-50 while toluene supplied by Chemiz (M) Sdn.Bhd.

3.2 Preliminary experiments

3.2.1 Identify total content of WTP loading in formulation

Before executing the real experiment, some preliminary experiment was carried out to determine the amount of WTP filler content that can be compounded with NBR to obtain the gasket texture. The experiments were carried out by using compounding formulation as shown in Table 3.2 with manipulating the loading of WTP. The total WTP loading was varied from 15phr, 30phr, 35phr, 40phr, 50phr, 60phr, 70phr, and 80phr. From the physical observation, coating material containing 80phr WTP has even distribution of WTP and the WTP particles seems to cover the overall surface of the gasket. Below that 80phr WTP showed exposed area and the overall gasket materials are not covered by WTP. Thus, the WTP loading for the research was set to 80phr and 90phr from this observation. Figure 3.2 show the gasket sheet produced through trial run with different WTP loading.

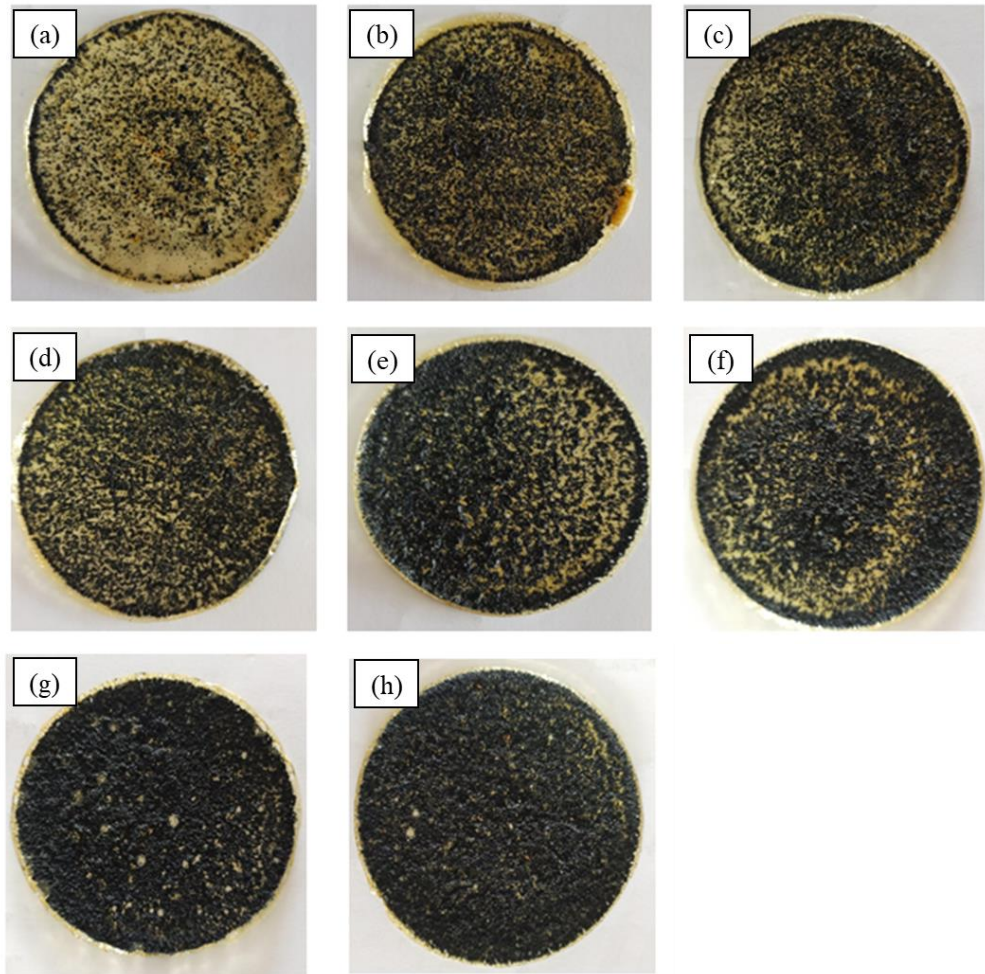


Figure 3.2: Gasket compounding with different WTP loading. (a) 15phr, (b) 30phr, (c) 35phr, (d) 40phr, (e) 50phr, (f) 60phr, (g) 70phr, and (h) 80phr.

3.2.2 Optimum weight of NBR/WTP blend in petri dish

The thickness of the desired coating material was optimized by casting a specific amount of the NBR mixture at the first stage before the foaming and curing process. Mass of the NBR mixture was fixed at 5g, 10g, and 15g to be coated on a gasket paper in a petri dish. The desired thickness of the coating

material for the application as gasket material is around 0.6 ± 0.1 mm in thickness. Figures 3.3 (a-c) showed the physical appearance of the NBR mixture containing 80phr of WTP at different casting amounts. The physical observation showed that 5g of the mixture produced a thin coating layer that has many voids and is unevenly dispersed throughout the gasket paper. The thickness of the coating material produced was 0.362 mm which is too thin for gasket material application. Meanwhile, when 10g of the mixture was used, a slightly thicker coating sample was produced with a thickness of 0.567 mm. gasket sample produced with 10g of casting mixture was much more suitable as it showed even distribution of fillers, good surface texture with no pored or voids and suitable thickness to be used as a gasket material. In addition, from Figure 3.3 (c), coating material with 15g mixture produced a very thick layer of coating. The coating material was under cured and contains numerous air bubbles and voids. The thickness measurement was 0.741 mm which is not suitable for gasket application. Thus, the optimum amount of mixture selected for the casting process for Phase 1 was 10 g based on the physical observation, the thickness of the coating, and the surface texture produced.

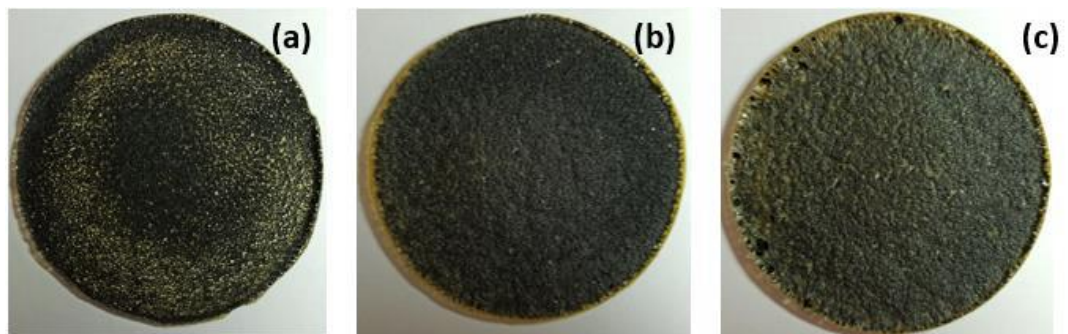


Figure 3.3: NBR/ WTP Gasket sheet with different weights (a) 5g, (b) 10g, and (c) 15g.

3.3 NBR solution compounding steps

3.3.1 Dissolution of NBR

Dissolution of NBR was completed by cutting the NBR dry rubber into small pieces and immersed in the MEK solvent. The volume of MEK is three time of NBR weight (Wong, 2013). After that, the NBR solution was seal and kept at room temperature for 24hrs. The NBR solution are then diluted with further addition of MEK to prepare the NBR solution for compounding with other ingredients. The volume of MEK is five time the weight of NBR and the mixture was sealed and kept in refrigerator.

3.3.2 NBR solution compounding.

NBR solution blend with additive by using IKA RW 20 Digital with ~ 500 rpm for 30mins. Subsequences, other compounding ingredient such as ZnO, ZDEC, ZMBT, DOP, ADCA, DCP & waste tire powder was added one by one. Lastly, Sulphur is added as the last component to prevent curing of rubber during mixing. Compounding formulation that used in experiment was tabulated in Table 3.2 by referencing to Journal Title Research of NBR foaming coating (Wong, 2013). Figure 3.4 shows the setup of compounding done using mechanical stirrer. The loading of WTP was varied between 80 and 90phr upon preliminary results showed good dispersion of WTP in NBR above 80 phr.

Table 3.2 Compounding Formulation for NBR / WTP compounds

Materials	Total solid content (%)	Formulation (phr)	Dry weight (g)	Actual weight (g)
NBR	12.5	100	25.00	200.00
ZnO	100	1	0.25	0.25
ZDEC	100	1	0.25	0.25
ZMBT	100	0.5	0.125	0.125
DOP	-	<u>10 / 15</u>	2.50	2.50
DCP	100	2	0.50	0.50
ADCA	100	9	2.25	2.25
WTP	100	<u>80 / 90</u>	20.00	20.00
Sulphur	100	<u>1 / 2</u>	0.25	0.25



Figure 3.4: Compounding blending by using IKA RW 20 Digital

3.4 Experimental design for optimization of NBR/WTP

There were three optimizations that has been done in this research to determine the optimum combination of formulation, curing and foaming parameters and coating techniques. The first optimization was done on foaming and curing parameter on combination of formulation. The suitable foaming and curing duration and temperatures were identified by using surface appearance study. The second phase optimization was done on formulation compounding by manipulate the loading of sulphur, DOP and WTP. In this phase, the gasket samples were tested with oil absorption test, gel-fraction, thermal aging test, TGA, SEM, and hardness test. Afterward, three best formulations from oil absorption test were selected for third phase optimization where casting method was changed to rolling method.

3.4.1 Phase 1: Optimization of foaming and curing parameters.

The suggested formulation showed in Table 3.2 was blended and casted on the gasket paper. The 10g of solution was undergoing curing and foaming by using Oven model UNB 500. The foaming and curing parameters were showed in Table 3.3 and Table 3.4. The tables showed the combination of possible treatment temperature (°C) and time (mins) for the rubber mixture foaming and curing time.

Table 3.3: Phase 1 manipulation factors

Factors	Level 1	Level 2
Temperature (°C)	T ₁ : 70; T ₂ :130	T ₁ : 80; T ₂ :130
Time (min)	t ₁ : 20; t ₂ : 30	t ₁ : 20; t ₂ : 40

Table 3.4: Phase 1 Treatment condition

Treatment Conditions (TC)	Temperature (°C)	Time (min)
A	T ₁ : 70; T ₂ :130	t ₁ : 20; t ₂ : 30
B	T ₁ : 70; T ₂ :130	t ₁ : 20; t ₂ : 40
C	T ₁ : 80; T ₂ :130	t ₁ : 20; t ₂ : 30
D	T ₁ : 80; T ₂ :130	t ₁ : 20; t ₂ : 40

3.4.2 Phase 2: Optimization of filler, plasticizer, and cross-linking agent

After the curing and foaming parameter, the second stage of optimization was optimization of compounding formulation by manipulating the content of WTP, DOP, and sulfur. Level 1 formulation combination was selected from researcher Wong, year 2013. However, Level 2 formulation was requested by UP Packing Sdn Bhd (gasket material producing company – in collaboration for research work) to identify the effect of WTP, DOP and sulfur loading on the performance of the gasket. Table 3.5 shows manipulation factors and Table 3.6 shows possible combination of formulations from WTP, DOP and sulfur content manipulation. Then, all these possible formulations were implied in formulation

showed in Table 3.2 for compounding. Next, the finished compounded gaskets were tested by Oil absorption, Gel-fraction, Thermal Aging, SEM, TGA, and Hardness test.

Table 3.5: Phase 2 manipulation factors

Factors	Level 1	Level 2
DOP (phr)	10	15
WTP (phr)	80	90
Sulphur (phr)	1	2

Table 3.6: Phase 2 Treatment Condition

Treatment Conditions (TC)	DOP (phr)	WTP (phr)	Sulphur (phr)
D10-W80-S1	10	80	1
D10-W90-S1	10	90	1
D10-W80-S2	10	80	2
D10-W90-S2	10	90	2
D15-W80-S1	15	80	1
D15-W90-S1	15	90	1
D15-W90-S2	15	90	2
D15-W80-S2	15	80	2

3.4.3 Phase 3: Optimization of coating methods

Phase 3 optimization was the manipulation of coating technique and the comparison of casting and rolling had been made. The coating parameters such as number of adhesion coating, and thickness of coating must be established to ensure the formation of thin, continuous, and smooth coating on the metal plate. The visual inspection such as finish coating material will be conducted using naked eyes to observe the finish surface. Furthermore, the quality of the roll and cast gasket will be tested on oil absorption, gel fraction, peeling test and microstructure will be observed through SEM. Figure 3.5 showed gasket coated by using rolling method and Figure 3.6 as casting gasket in the petri dish.

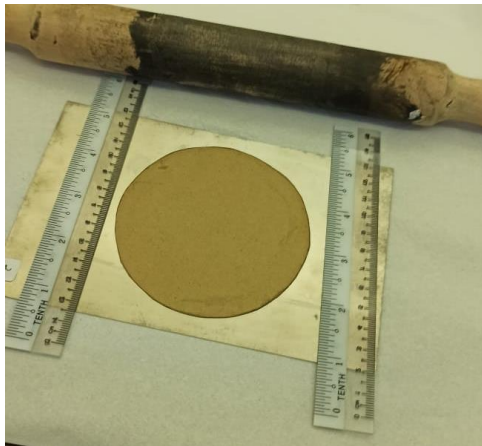


Figure 3.5: Gasket rolling method.

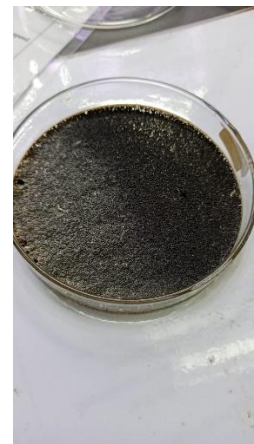


Figure 3.6: Casting gasket.

3.5 Characterization Testing

3.5.1 Particle Size Analysis (PSA)

Particle Size Analysis of waste tire powder and carbon black was carried out by using Malvern Analyzer from DKSH Technology Sdn. Bhd. Particle Size analysis is an analysis to measure the particle size of the particles existed in proportions of the total amount of particles in the sample particle group. In this particle size analysis, volume, area, length, and number of particles used as standards to measure the distribution of different sizes in liquid. The cumulative distribution of particles passing the sieve showed the percentage of the amount of particle from specific size of particles or below than that of Mastersizer 2000, Hydro 2000MU (A) was used to determine the particle size distribution of the waste tire powder and carbon black.

3.5.2 Scanning electron microscopy (SEM)

Scanning electron microscopy (SEM) was used to observe the surface morphology of waste tire powder, carbon black and the tensile fractured morphology of NBR/ WTP composites at accelerating voltage of 2 kV. Prior to scanning, the sample was placed on a disc and held in the place using a double-sided carbon type then coated with platinum particles to avoid sample changing. JOEL JSM 6701F model of equipment was used in this study. Surface morphology such as the particle shape, structure, and surface roughness of the

WTP and carbon black particles were observed. Meanwhile, for the composites, the surface roughness, matrix tearing, filler dispersion and distribution as well as filler adhesion on the NBR matrix were analyzed.

3.5.3 Thermal gravimetric analysis (TGA)

Thermal gravimetric analysis (TGA) was used to determine the decomposition temperature and the thermal stability of waste tire powder and carbon black. The carbon content in WTP was determined through TGA method by heating the WTP from room temperature to 900°C under nitrogen gas purging and held at 900°C. The measurement was carried out under the nitrogen atmosphere using a heating rate of 20°C / minute from 0°C to 900°C using Mettler Toledo TGA SDTA851 E.

3.5.4 Oil absorption test

Oil absorption test was used to determine the oil resistance property of NBR/WTP gasket according to ASTM F146. The samples will be prepared at 2 cm x 2 cm dimension and the initial weight and thickness will be measured and recorded. Then, the sample will be immersed in Engine Oil at 150°C for 5 hours. Afterward, the sample will be removed and dried with tissues. Next, the final weight and thickness of gasket pieces were measured and recorded. The weight

and thickness changes of samples were measured and calculated by using Equation 3.1.

$$\text{Changes in Mass or Thickness} = \frac{\text{Final reading} - \text{Initial reading}}{\text{Initial reading}} \times 100\% \quad (\text{Equation 3.1})$$

3.5.5 Gel fraction / solvent extraction test

Solvent extraction was carried out to determine the gel content in the samples by immersing the gasket samples in toluene at 120°C for 24 hours using Soxhlet apparatus. The composite specimens and wire mesh was prepared into square size of 1cm x 1cm and 3cm x 3cm accordingly. After that, weight of the samples (W1) and weight of wire meshes (W2) were measured and recorded. Next, the samples wrapped into the wire mesh, respectively. Once it is done, the wrapped samples were placed inside thimble for extraction. After 24 hours of immersion, the samples will be taken out and dried in oven at 60°C until constant weight was obtained (W3). The gel fraction can be calculated by using Equation 3.2.

$$\text{Gel fraction} = \frac{(W3 - W2 - W1)}{W1} \times 100\% \quad (\text{Equation 3.2})$$

where:

W1 = Initial weight of sample

W2 = Weight of wire mesh

W3 = Final weight of dried samples with wire mesh

3.5.6 Thermal aging test

Thermal aging properties was evaluated by referring to ASTM D573-99 standard test method for rubber deterioration in an air oven. The gasket samples were placed in an air oven at 108°C for 72 hours using Aging Oven Chamber, Model VAT 60, ASLI test equipment. Afterward, the oil absorption property of thermal aged sample was study. The effect of aging on the strength and physical properties of the samples was compared with the un-aged gasket samples.

3.5.7 Peeling test

Peel test was used to exam the adhesive strength between two substrates bonded together. The substrates can either be flexible or rigid on one side. Besides, adhesive strength was a measurement on samples resistance to separate the coating materials from the gasket base paper. The coating on gasket was applied by using sandwich method where the coating material was casted and rolled on the gasket paper and another pieces of gasket paper was stick on the top. The peeling test was done by using Tinius Olsen H10KS-0748 with 450N load cell with a crosshead speed of 20 mm/min. The samples were clamped on each side of tensile machine and five samples were used in the experiment and average tensile strength were recorded.

CHAPTER 4

RESULT AND DISCUSSION

This chapter presents the result and analysis that has been done from the characterization and testing of waste tire powder (WTP) and nitrile butadiene rubber with waste tire powder (NBR/WTP) composites. Research and analysis that has been done on WTP is Particle Size Analysis (PSA), Scanning Electron Microscope (SEM), and Thermal Gravimetric Analysis (TGA). Furthermore, characterization on Carbon Black N330 is done by using PSA, TGA, and SEM. While the characterization analysis that has been done for NBR/WTP compounding as coating material are surface texture analysis, Scanning Electron Microscope (SEM), Thermal Gravimetric Analysis (TGA), oil absorption, gel-fraction, thermal aging test, hardness test, and peeling test.

4.1 Characterization of filler materials waste tire powder and carbon black

4.1.1 Particle size analysis (PSA)

The particle size and shape of the fillers are one of the major factors in determining the processing and final properties of particulate filled composite materials. Filler generally comes with a variety of shapes and sizes which

provide different adhesive and interaction properties of filler with the polymer. Furthermore, filler size can determine the dispersion of filler in the polymer composite. The segregation, agglomeration, and aggregation of filler particles can affect the filler dispersion in polymer matrix and reduce the overall finishing properties of the products (Rothon, 2017).

Aggregation usually happened when the small particles strongly stick together (stronger filler – filler interaction) by intergrowth or fusion of the particles. Meanwhile, agglomeration of fillers happens when primary or individual particles and aggregates attach by the weak force where it can be broken down easily. Figure 4.1 shows an illustration of particles primary, aggregates, and agglomerates (Rothon, 2017).

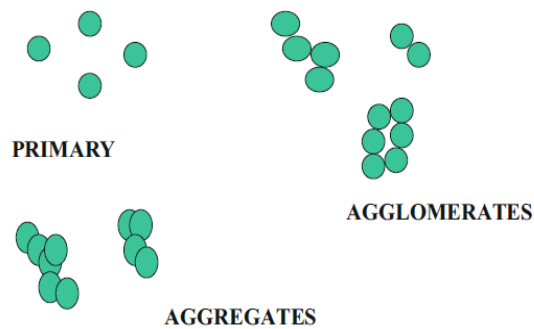


Figure 4.1: Concept of aggregate, agglomerate, and primary. (Rothon, 2017)

Besides the stronger filler-filler interaction which causes agglomeration and aggregate, segregation may happen due to different particles size of fillers or particles having very broad particle size distribution. The larger size particles tend to move further along the slope surface and end at the side wall while the

smaller particles remain at the centre region. Such phenomenon could affect the difference in the quality of the composite products and difficulties to control the processing due to difficulties to effectively disperse the filler particles homogeneously throughout the polymer matrix. Figure 4.2 shows a solid flow time lap during the hopper filling process (Zhang *et al.*, 2018).

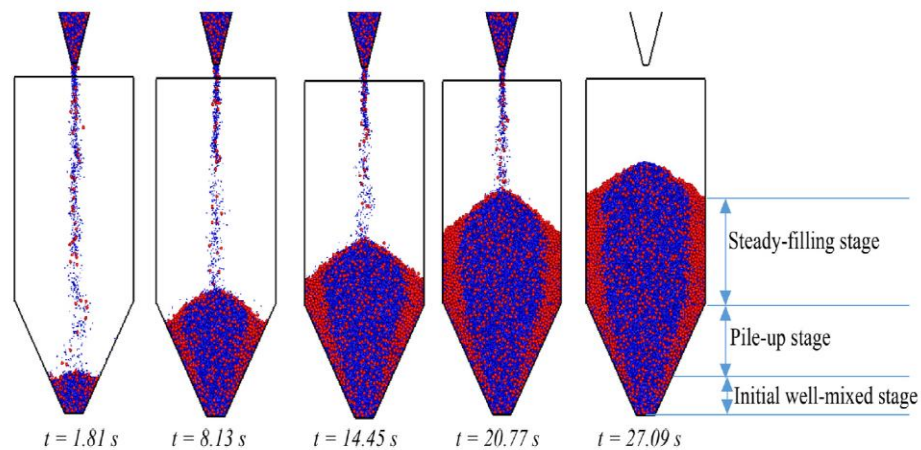


Figure 4.2: Solid flow time lap during hopper filling process. (Zhang *et al.*, 2018)

Figure 4.3 and Figure 4.4 shows the particle size distribution curves of WTP and CB. The interpretation from the result shows that WTP has single and narrower particle size distribution. WTP has been sieved with a 500 μm sieve prior to compounding to control the particle size distribution. The dominion size of the filler is 339.653 μm and the graph remains at the centre as the distribution is equally balanced and filler volume distribution mainly as 339.653 μm . On the other hand, data show that CB N330 has a bigger particles size as compared to WTP. CB N330 has a slightly broader particle size distribution and a volume distribution of 1025.7355 μm . The graph also showed skewed to the left

distribution with some smaller particles in CB N330. Thus, segregation tends to happen when there is a difference in particulate size in the compounding. This is one of the reasons of the poor dispersion of CB in rubber. Secondly, CB as the coating materials which causes destabilization of latex compounds and producing poor surface texture of the gasket materials. Interparticle van der Waal's forces in CB cause the destabilization of rubber matrix and weak in dispersion. Surface modification is needed for better CB application in rubber (Fang *et al.*, 2020).

Furthermore, the specific surface area (SSA) is another justification to analyse the effectiveness of filler in polymer reinforcement. SSA is the measurement as surface area per unit weight of filler with unit m^2g^{-1} . SSA is easier for comparison with the same density and shape materials. The higher the SSA, the smaller the particle size and more exposed area available for interaction with matrix (Rothon, 2017). Table 4.1 shows SSA for CB is $0.04 \text{ m}^2\text{g}^{-1}$ while WTP is $0.023 \text{ m}^2\text{g}^{-1}$. CB has a higher SSA as compared with WTP even it has a bigger particle size. This is because CB and WTP have different density and particle shape. In addition, WTP has a flat surface as it is processed through cryogenic grinding.

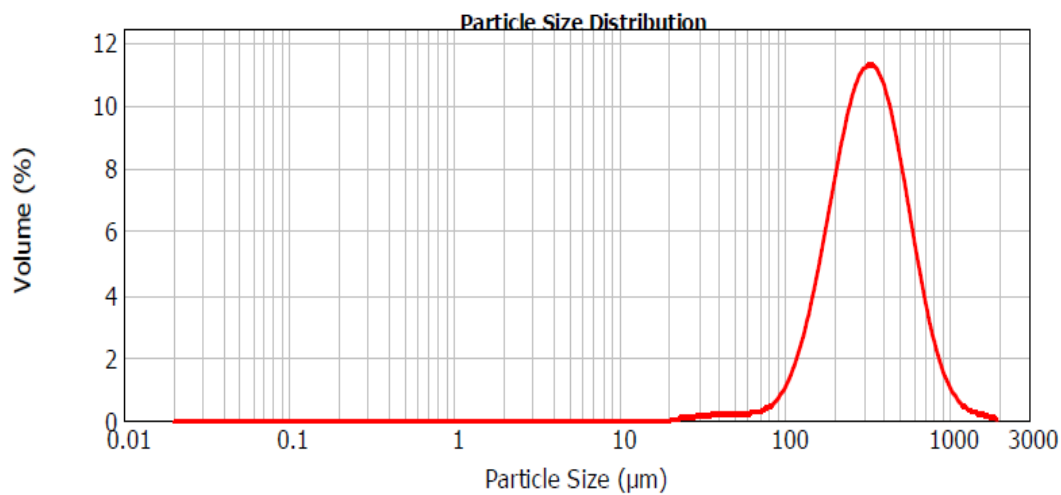


Figure 4.3: Particle size graph of waste tire powder.

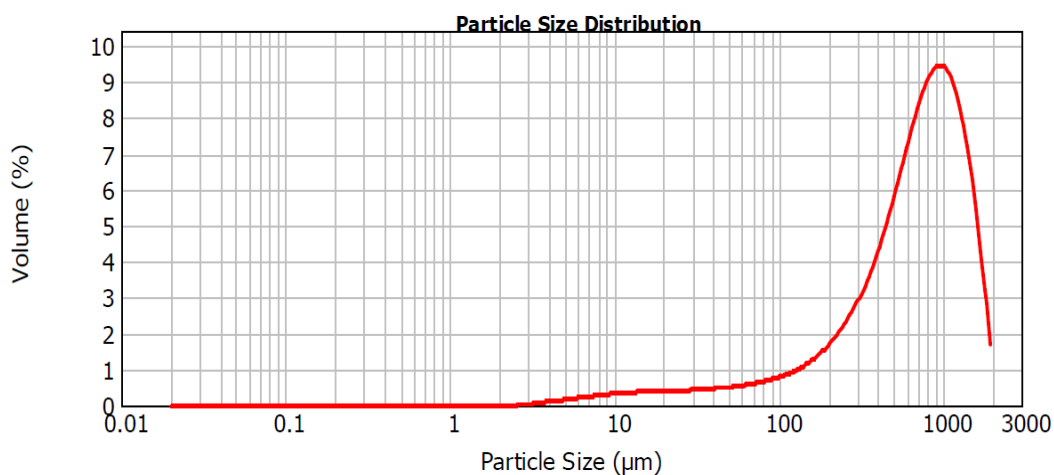


Figure 4.4: Particle size graph of carbon black.

Table 4.1: PSA Data of WTP

Component	Specific Surface Area, m ² /g	Mean Diameter, μm	Particle size range, μm
WTP	0.023	321.72	21.43 – 2046.61
CB	0.040	712.93	2.698 – 2046

4.1.2 Thermal Gravimetric Analysis (TGA)

Thermal gravimetric analysis is a technique to measure the quantity and frequency of multiple weights of samples under thermal heating at controlled atmosphere such as nitrogen gas purging atmosphere. Thus, the thermal stability and composition properties of the samples can be identified through TGA. Furthermore, weight loss and gain are attributed to several factors. Weight gain of samples is due to oxidation while weight loss is most likely due to decomposition, dehydration, desorption, etc. The information and properties of the samples can be interpreted through TGA curves provided by the decomposition mechanism of the polymers (Ng *et al.*, 2018).

Figure 4.5 display the thermal decomposition curve of WTP and CB over a temperature plot. WTP has a single-stage thermal degradation while CB does not have significant weight loss in the TGA. In addition, the curve shows that thermal degradation of WTP started at temperature 260°C with mass loss of 3.2725% and ended at temperature 510°C with mass loss of 57.70%. The sample continues slight degradation until temperature 900°C. Previous study on the thermal degradation of WTP was done by Alias and Mohd Rafee, (2020) where single-stage thermal degradation of WTP begins at 340°C and ended at 460°C while degradation midpoint is at 398°C to form oil, gas, and char. WTP degradation at 200°C to 300°C due to decomposition of additives such as oil and stearic acid. Furthermore, 380°C to 480°C due to degradation of the primary ingredient of the tire such as natural rubber, styrene-butadiene rubber, etc.

Lastly, the decomposition of polybutadiene happens at 410°C to 500°C (Alias and Mohd Rafee, 2020).

Subsequently, CB is used as filler in many reinforced polymer materials nowadays. The reason for the application of CB as it has better thermal stability and generally increases the thermal stability of the polymer composite. The research shows that epoxy with higher CB loading has a higher initial decomposition temperature and the final decomposition which will produce char which is CB (Bera, Acharya, and Mishra, 2018). Thus, carbon black is the end decomposition product from thermal degradation and Figure 4.5 show that CB is stable and doesn't experience degradation in a nitrogen environment.

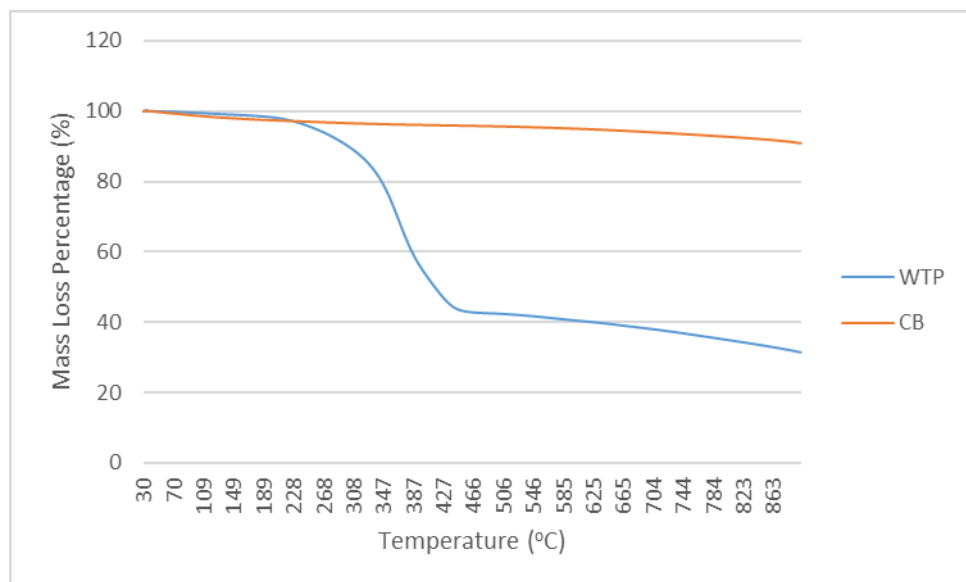


Figure 4.5: Mass loss of CB and WTP under Thermal Gravimetric Analysis

4.1.3 SEM of CB and WTP

Carbon Black is a micro or nanoscale carbon particle produced through thermal decomposition or partially burning of hydrocarbon. The structure of CB is made up of numerous spherical particle that fused together to form the fillers that is lower cost and able to improve the mechanical properties of composite through blending. However, there are some cons of application of CB filler due to high aspect ratio. The high surface energy of CB nanoparticles tends to agglomeration and formation of segregation in the filler rubber compounding. This phenomenon shows that CB filler has a poor surface bonding with the rubber chain. Furthermore, the poor adhesion and dispersion of CB will generally become a greater issue to the rubber properties when the volume fraction of micro or nanoparticles fillers increase. (Cougo *et al.*, 2019) As per mention above, interparticle van der Waal's force existence cause the weak in dispersion (Fang *et al.*, 2020). Figure 4.6 shows the primaries of CB are agglomerate which will give negative impact to the mechanical properties under 500X and 1000X magnification.

Besides, filler aggregate happens due to poor dispersion of filler and wide range of particles size (Sanjuan-Navarro, Moliner-Martínez and Campíns-Falcó, 2021). Figure 4.6 (b) shows CB filler dispersion under 1000X magnification. The CB particulate with variety of size and smaller particles tend to stick with bigger size of filler. Moreover, the PSA analysis shows the CB has larger range of particle size which has higher possibility to form filler aggregates.

Surface morphology is determined by using SEM analysis. Figure 4.7 shows surface of WTP under 500X and 1000X magnification. The images show that cryogenic grinded WTP has a smooth surface and lesser surface area which leads to poor binding ability with rubber matrix. However, cryogenic grinding provide occlusion or less obstacles in compounding due to smooth surface. Thus, cryogenic grinding has lower viscosity flow and sulphur migration into granulate from rubber is easier, cross-linking density is increase. In contrast, the ambient grinding is better interaction with rubber matrix due to irregular and ambiguous surface (Cougo *et al.*, 2019). Figure 4.6 shows CB filler agglomeration happens due to stronger surface energy on the filler itself.

The surface of cryogenic grinded WTP does not have complex surface such as micro cracks, and pores as part of strength of cryogenic grinding method. The micro complex structure on the fine particle will absorption ambient gases will trigger oxidation of the polymer (Yerezhep *et al.*, 2021).

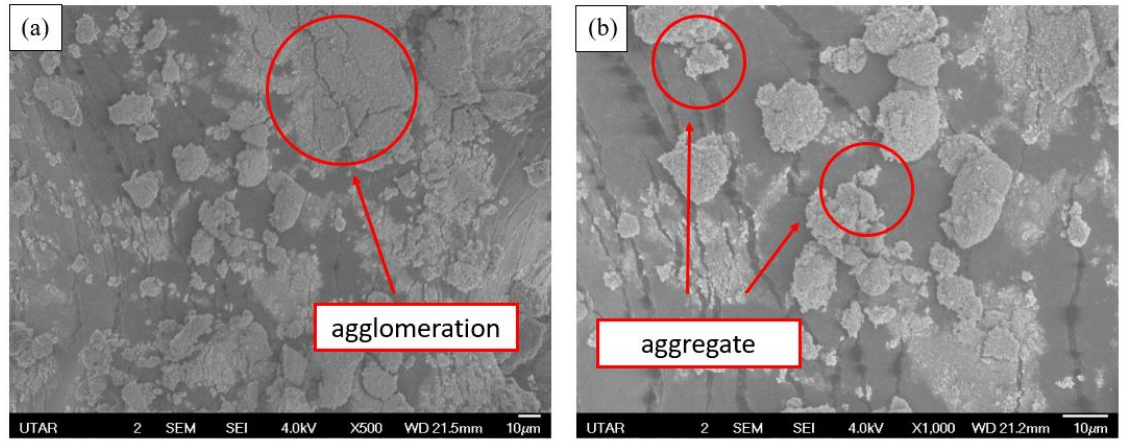


Figure 4.6: SEM image of CB particle under (a) 500X, (b) 1000X magnification.

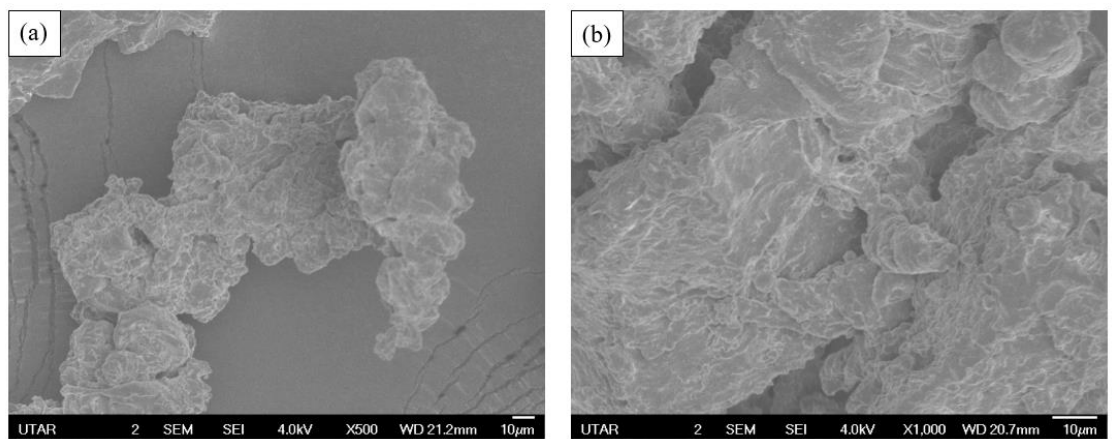


Figure 4.7: SEM image of WTP under (a) 500X, (b) 1000X magnification.

4.2 Characterization of NBR/ WTP for Phase 1 and 2

4.2.1 Compound weight for curing and foaming of NBR/ WTP

First and foremost, the NBR/WTP compounds were casted on the petri dish with a fixed diameter of 9.5cm and a total area of 70.88cm². The compound weights are varied to study the effect on the thickness of the gasket material produced after casting. Optimum compound weight is required to produce gasket materials with desired thickness. Based on the standard specification of gasket materials, the thicknesses of a normal non-metallic gasket (soft) used in the North American region are 1/32'' (0.79mm), 1/16'' (1.59mm), and 1/8'' (3.18mm). Meanwhile, standard thickness of gaskets used in Asia and European regions varies from 0.75mm, 1.0mm, 1.5mm, 2.0mm, and 3.0mm. However, gasket materials with different thickness are also available in the market depending on the specific applications requirement (Charlene Jones, Mike Shorts, 2017).

In comparison to thick gasket materials, the thinner gaskets are more preferred and recommended as gasket cut from the sheets if the flange arrangement is allowed. The thin gaskets are thick enough to compromise unevenness of the flange surface as compared to the thicker gaskets. This is because the thinner gasket can withstand higher bolt load to prevent the bolt to loss its stress. Besides, the thinner surface has less explored inner fluid and internal pressure (Charlene Jones, Mike Shorts, 2017).

The relationship and characteristics of thin and thick gaskets are further discussed. A thicker gasket has higher compression amount which is able for better flange's strain and swelling absorption. In contrast, a thinner gasket has smaller penetration leakage and allows for a higher seal resistance. Furthermore, a thinner gasket has lower creep relaxation as compared to a thicker gasket, which causes a thinner gasket to have better long-term stability. Other than that, a thinner gasket is durable when facing compression failure contact pressure. Thus, the thinner the gasket, the better external force tolerance. Therefore, a thinner gasket is preferable in principle. However, a thicker gasket is applied when large swelling and strain in the flange is needed and considering of surface roughness of flanges. Table 4.2 show the comparison between the characteristic of gasket with different thickness (Asuka Matsushita, 2018).

Table 4.2: Characteristic of thin and thick gasket

Characteristic	Gasket thickness	
	Thin	Thick
Compression amount	Little	Large
Seal Property	Strong	Weak
Creep relaxation	Little	Large
Compression failure contract pressure	Strong	Weak

The desired thickness of the gasket is affected by the casting weight of NBR/ WTP compounds in the fixed volume of the petri dish before foaming and curing stages. Mass of compounds were varied from 5g, 10g, and 15g and are cast on a separate gasket paper with a thickness of 0.4mm. The desired coated mass compound is selected after the surface observation.

Figure 4.8 (a-c) show the different physical appearance of 80phr NBR/WTP compounds casted at different weight. Figure 4.8 (a) shows the gasket produced through casting of 5g NBR/WTP compound, which has a thin coating surface and many voids on the surface of the gasket. However, the WTP dispersion is uneven and the compound unable to cover the entire surface of the gasket paper evenly. The thickness of the gasket material produced by casting 5g of the compound is 0.362mm which is too thin for the gasket usage. On the other hand, casting of 10g of the compound produced a 0.567mm thickness gasket which is slightly thicker. Figure 4.8 (b) shows the appearance of the gasket casted using 10g of the compounds which has more even WTP dispersion, and the amount of compound used is sufficient to cover the entire surface of the gasket paper evenly with fewer empty spaces, and good surface texture. Meanwhile, increasing the weight of casting compound to 15g, the thickness of the gasket produced is 0.741mm. Figure 4.8 (c) show that the surface of the gasket which is not completely cured and contains numerous large air bubbles and empty pore. Physical observation also showed that the texture of the gasket is rubberier rather than foam structure which is not suitable for gasket application. Thus, the thickness of the gasket is too thick for the gasket application. With that it can be said that 10g of casting compound is sufficient

to produced gasket material with desired thickness and surface texture with adequate WTP dispersion throughout the gasket surface.

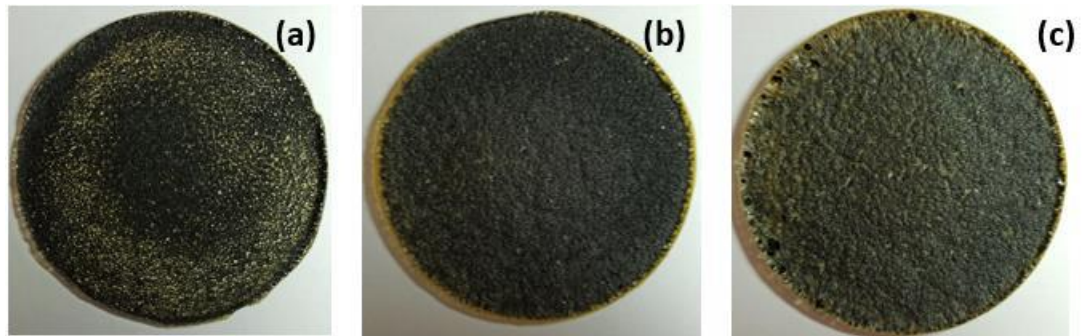


Figure 4.8: NBR/ WTP gasket samples with (a) 5g, (b) 10g and (c) 15g.

4.2.2 Surface texture observation

Surface texture observation is the analysis to identify the physical appearance of the readily made gaskets by using naked eyes. The physical appearance of the gasket should have an even, smooth, and continuous surface finishing. Surface with voids or filler agglomeration should be eliminated from our selection. In this study, the surface texture can be affected by several factors such as temperature and processing time of foaming and curing. Besides, the addition and composition of filler and other additives such as WTP, DOP, and sulphur can also affect the surface finish of gasket.

The gaskets with treatment A undergo foaming at 70°C (20mins), curing parameters are 130°C (30mins) while treatment B undergo foaming at 70°C (20mins), and curing at 130°C (40mins). The gasket in compounding treatment C undergo foaming at 80°C (20mins), curing parameters are 130°C (30mins), and treatment D parameters are foaming at 80°C (20mins), and curing at 130°C (40mins). Table 4.3 summarize the acceptable gaskets after identification through physical observation at different compounding formulations and treatment conditions. The table shows eight formulations with different treatment A, B, C, and D. The formulation D10-W90-S1 (A), D10-W90-S1 (C), D10-W80-S2 (C), D10-W90-S2 (A), D15-W90-S1 (A), D15-W90-S1 (B), D15-W80-S2 (A) and D15-W80-S2 (C) present a smooth and even surface coating while the rest have uneven surface and numerous pores.

Furthermore, Figure 4.9 (a - h) display the pictures of selected treated formulation gasket appearance out of all possible formulation while Figure 4.10 (a-d) show the samples with poor filler dispersion, voids, and uneven surface texture. Hence, the good surface gaskets texture is selected for the second optimization of compounding. Several characterizations are used to choose better formulation combination.

Table 4.3: Acceptable surface texture among all compounding with different treatments.

Formulations	A	B	C	D
D10-W80-S1	-	-	-	-
D10-W90-S1	Acceptable	-	Acceptable	-
D10-W80-S2	-	-	Acceptable	-
D10-W90-S2	Acceptable	-	-	-
D15-W80-S1	-	-	-	-
D15-W90-S1	Acceptable	Acceptable	-	-
D15-W90-S2	-	-	-	-
D15-W80-S2	Acceptable	-	Acceptable	-

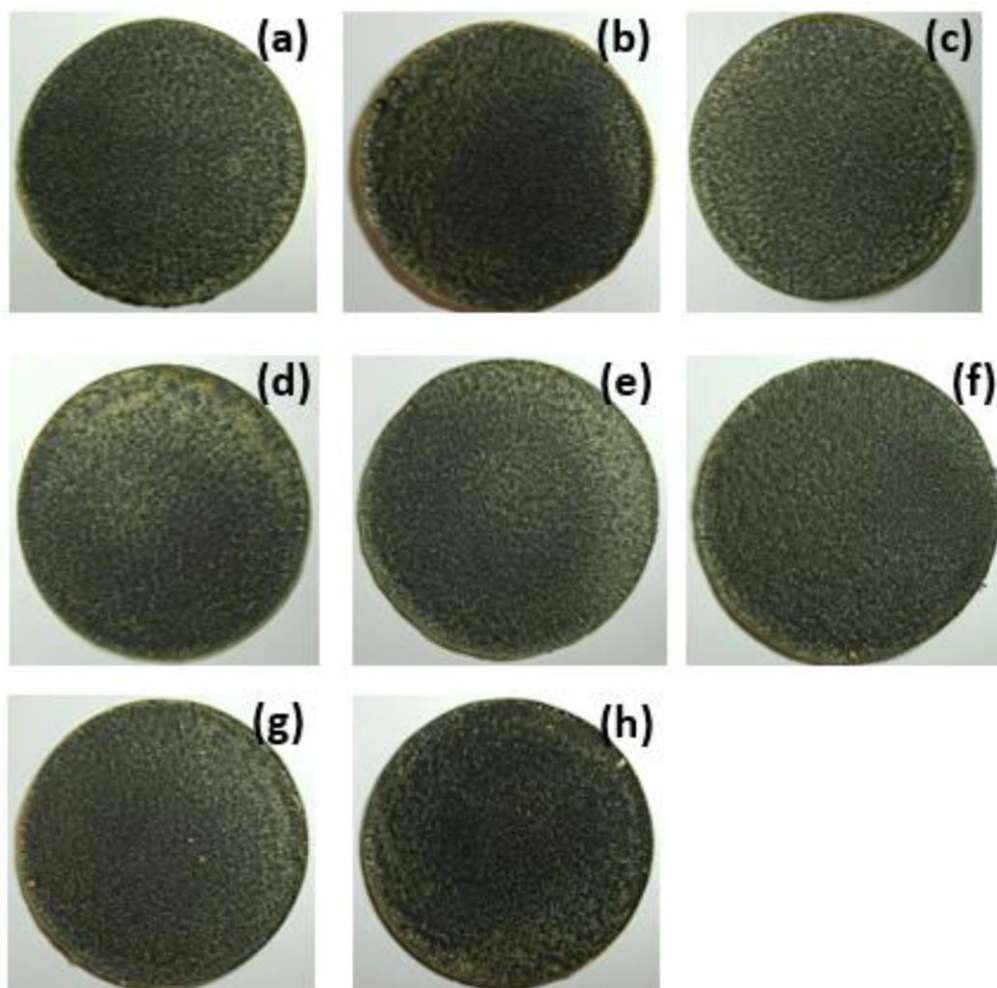


Figure 4.9: Physical appearance for acceptable formulation and treatment:

- | | | |
|-------------------|-------------------|-------------------|
| a) D10-W90-S1 (A) | d) D10-W90-S2 (A) | g) D15-W80-S2 (A) |
| b) D10-W90-S1 (C) | e) D15-W90-S1 (A) | h) D15-W80-S2 (C) |
| c) D10-W80-S2 (C) | f) D15-W90-S1 (B) | |

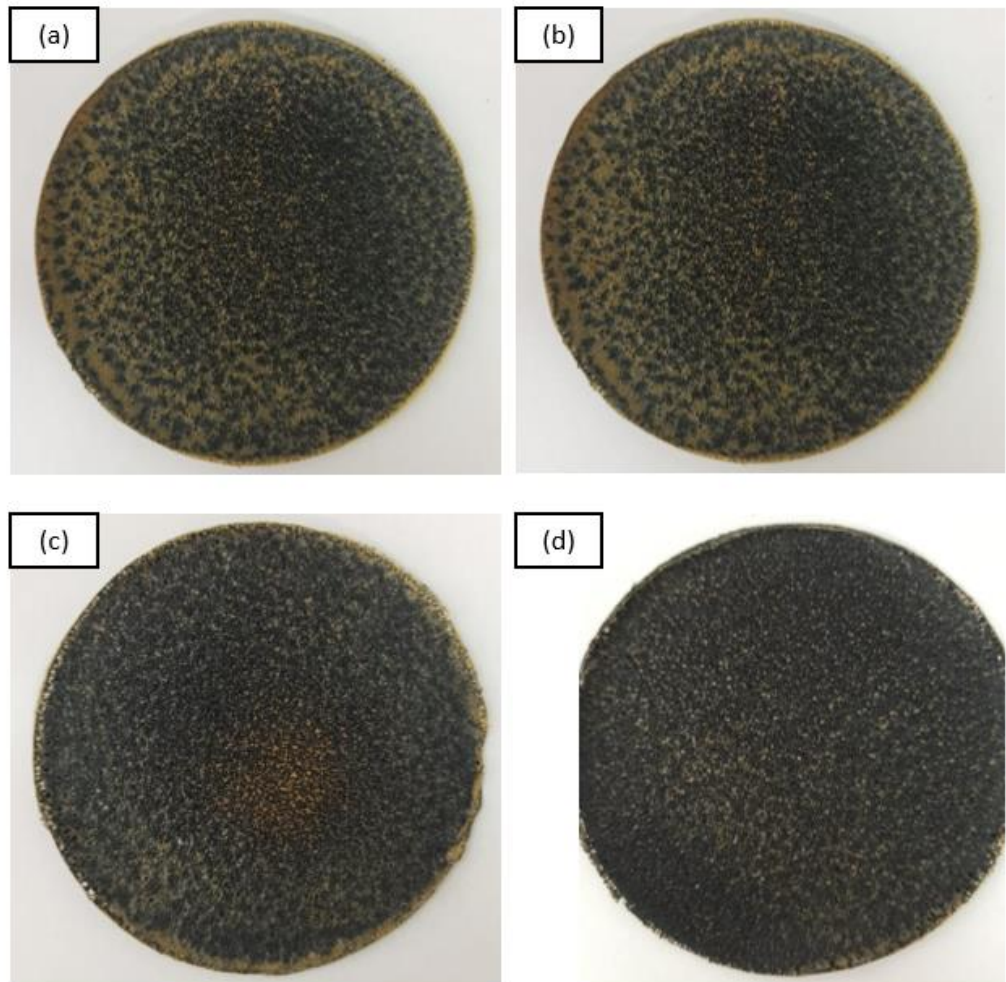


Figure 4.10: The formulation with void surfaces.

(a): D10W90S1 (C)

(b): D10W80S2 (D)

(c): D15W80S1 (C)

(d): D15W90S2 (D)

4.2.3 Oil absorption test

The oil resistance test of rubber is essential to measure the ability of rubber to perform well in an oily environment or involved with oily application. The measurement of the oil resistance indicates whether the rubber will swell or be weakened by the penetration of oil molecules in between the molecular structure of the rubber. Natural rubber will disintegrate when the rubber is exposed for a long period in the oil. Besides, oil-resistance elastomer only absorbs a little oil, especially in higher temperatures. However, most oil resistance end uses rubber can tolerate appreciable swelling and increase in rubber volume (Ciulllo and Hewitt, 1996). Table 4.4 shows the composition of sulphur, WTP, and DOP in each of the formulations. In addition, a specification requirement such as 15% mass changes and 10% thickness are given by UP Packing Sdn. Bhd. Such requirements become our guidelines and the percentage of changes are tolerable.

The oil absorption test was carried out to investigate the application of new formulation of NBR/ WTP gasket under controlled temperature at 150°C. Several factors will affect the swelling properties of rubber. Crosslinking density can be the factor that affects the portion of oil absorption. The vacant between the crosslink can intake the oil or solvent and the low fluid absorption polymer molecules are limited by the formation of a three-dimension network form in between polymers. Further explanation whereby the cross-linking agent is shortening then chain length of the polymer and form a denser network for lower fluids intake. The network structure becomes denser and the polymers tend to become harder and have better oil absorption resistance (Zielińska *et al.*, 2016).

Thus, as sulfur loading is increased, the better the oil resistance properties. Figure 4.12 shows that D10-W90-S2 (A), D15-W90-S2 (A) and D15-W90-S2 (B), and D15-W80-S2 (C) with 2phr sulfur loading have given a lesser mass increase with 16.01%, 16.08%, and 15.54%. Meanwhile, formulation D10-W90-S1 (A), D15-W90-S1 (A) and D15-W90-S1 (B) with 1phr of sulfur given a larger mass increase with 18.78%, 19.89%, and 22.23% respectively. The higher mass changes due to oil absorption at lower sulfur loading of 1phr is in line with the findings of previous researchers. Increasing sulfur content results in higher crosslinking which prevents the oil molecules to penetrate the gasket materials.

In addition, reinforcement by fillers also plays an importance role in the oil absorption of a polymeric system. A study by Mustafa *et al.* 2009, shows that percentage of oil uptake is increasing fast at the initial stage due to the affinity of the rubber and slowly increase when rubber is saturated with the oil. On the other hand, the oil swelling percentage decreases with the increase of filler content in the rubber. The study shows that CB-filled SBR and CB-filled NBR have a lower percentage of oil absorption with the filler loading is increased. The presents of fillers blocks the oil absorption pathway which prevents the oil molecules to penetrate into the rubber molecular structure (Mostafa *et al.*, 2009).

Figure 4.11 shows the schematic diagram of rubber under the oil absorption process. The expanding or shrinking of rubber is contributed by pressure acting in between rubber network structure and oil. Theoretically, filler content increases the density of crosslinking in rubber compounding and thus the rubber is become more elastic and these crosslinks restrict the expansion of the

network and the oil is hard to diffuse into the gap in between rubber molecules. (Mostafa *et al.*, 2009) Furthermore, filler behaves as an obstacle to the diffusion of liquid to the rubber molecules. Thus, the higher reinforce filler, the more obstacles are created to reduce the oil absorption of rubber (Zielińska *et al.*, 2016).

Table 4.4 shows that most of the compounding formulations having 90phr of WTP instead of 80phr of WTP due to gasket surface selection. Furthermore, Table 4.4 shows 90phr WTP has less mass gain and thickness changes. Formulation D10-W90-S1 (C) have 14.45% of mass changes, 3.61% of thickness changes, and D10-W90-S2 (A) has 16.01% mass changes, 4.45% thickness changes. Both formulations are complying with the specification given which are < 15% mass changes and < 10% thickness changes. On the other hand, formulations with 80phr are expelled from selection as either mass or thickness are not an intolerable region. Furthermore, results show negative thickness or reduction in thickness because rubber tends to collapse rather than expand under the oil test. The phenomena demonstrated under Figure 4.11 (Mostafa *et al.*, 2009).

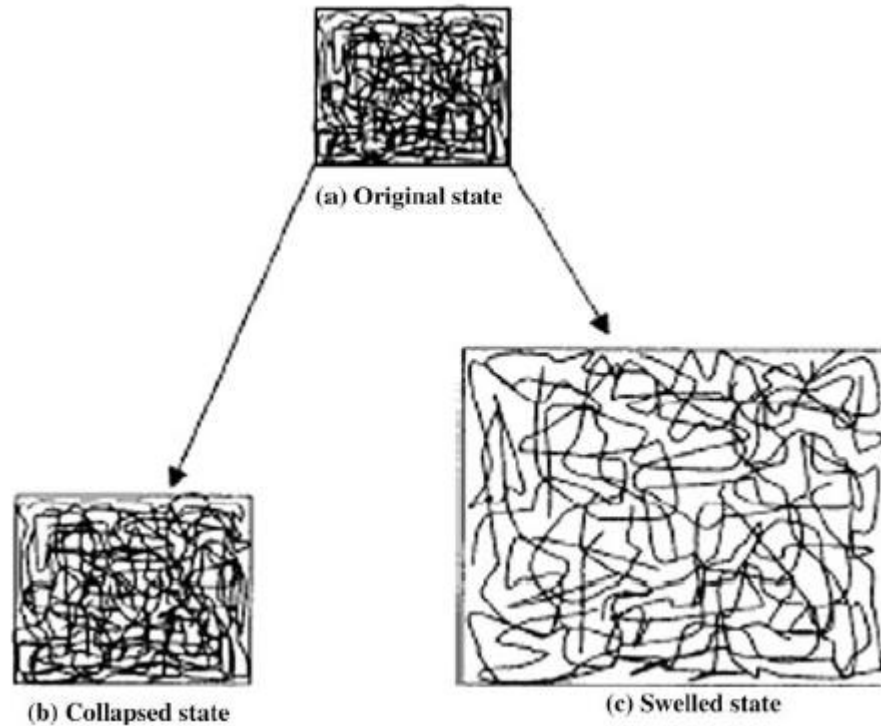


Figure 4.11: Schematic diagram of swelling and collapse of rubber.
(Mostafa *et al.*, 2009)

Besides, plasticizers are an important element in the rubber industry, which functions to act as a lubricant to reduce the viscosity of rubber and improve the rubber processing, properties, and filler dispersion. Other than that, lower Mooney viscosity by adding plasticizer can give better protection on equipment and reduce the processing costs. However, despite many advantages of having plasticizer in rubber compounding, there are some weaknesses such as crosslinking density of rubber will decrease with the addition of plasticizer. Thus, the rubber will decrease in hardness and increase in elongation which shows the plasticizer effect (Xu *et al.*, 2020).

Table 4.4 show that four formulations apply 10phr of DOP and another five formulations are using 15phr of DOP. DOP is a low molecular weight substances that able to promote plasticity and flexibility of the rubber blend. The glass transition temperature is reduced where polymer chains are disintegrate by addition of DOP (Foroughi-Dahr *et al.*, 2017). Furthermore, DOP can enhance filler dispersion by modified the surface of the graphene. Besides, DOP and graphite surface has good π - π interaction and bonding. The final modified graphite surface has smoother and thicker surface (Duy *et al.*, 2022). Thus, the higher the DOP content, the better is the processing and filler dispersion but the crosslinking of the rubber will decrease. The rubber tends to become more flexible and lower in mechanical strength. Hence, the oil absorption properties will increase as crosslinking of rubber is decreased. The result shows that formulation D15-W90-S1 (A), D15-W90-S1 (B), D15-W90-S2 (A), and D15-W90-S2 (B), are having higher oil absorption compared to lower DOP content. They have 19.89%, 22.23%, 16.08% and 17.36% mass changes respectively. Furthermore, formulation D10-W90-S1 (C) and D10-W90-S2 (A) have lower oil absorption content as shown in Table 4.4. D10-W90-S1 (C) and D10-W90-S2 (A) have 14.45% and 16.01% mass changes.

Table 4.4: Mass and thickness changes in NBR/WTP for each formulation.

Formulations	Sulphur (phr)	WTP (phr)	DOP (phr)	Mass Increase (%)	Thickness Increase (negative) (%)
D10-W90-S1 (A)	1	90	10	18.78	6.83
D10-W90-S1 (C)	1	90	10	14.45	3.61
D10-W80-S2 (C)	2	80	10	19.97	6.68
D10-W90-S2 (A)	2	90	10	16.01	4.45
D15-W90-S1 (A)	1	90	15	19.89	9.83
D15-W90-S1 (B)	1	90	15	22.23	5.44
D15-W90-S2 (A)	2	90	15	16.08	9.74
D15-W90-S2 (B)	2	90	15	17.36	13.40
D15-W80-S2 (C)	2	80	15	15.54	10.81

4.2.4 Gel Fraction / Solvent Absorption Test

Gel fraction test was conducted to measure the amount of the extractable materials from the rubber compounds upon exposure to solvent. The solvent will penetrate the rubber's crosslink network and cause the rubber to swell. Exposed pathway may allow the escape of non-vulcanized molecules to the solvent. Aromatic toluene is used as a solvent as a polar group of NBR ($C\equiv N$) has higher interaction with aromatic solvent than nonpolar solvent (Indrajati and Dewi,

2017). The initial mass and final mass after solvent extraction are to be measured and the mass lost is relatively due to extraction through the solvent. Furthermore, crosslinking density can be depicted from the number of extractable materials. Compounding with a higher crosslink density has a low percentage mass loss due to material's extraction to the solvent.

One of the main factors that affect the rate of swelling is the reinforcement of fillers. Filler can restrict chain movement of rubber and induce the higher crosslinking density of the rubber. Thus, crosslinking density of filled rubber is higher than unfilled rubber and the gel fraction of the rubber composite is relatively lower as it has a higher crosslinking density. High crosslinking results in rigid rubber network system which restrict the solvent penetration (Liang, 2017). Besides, the composition of compounding ingredients also affects the crosslink density of the rubber system.

The crosslinking density also increases when the compounding formulation consist of extra composition of curatives. Meanwhile, the crosslink may decrease due to addition of triglyceride-based oil as plasticizers which consumes the curatives. Thus, the addition of sulphur conceptually reduces the gel fraction of rubber, whereas the increase of plasticizer such as DOP will increase the gel fraction of rubber (Li *et al.*, 2016). Similarly, another study also reported the reduction of swelling ratio of NBR composites with increasing sulphur loading as the crosslinking density of compounding was increased. The rubber becomes rigid and the extensibility of the rubber chain has been restricted

and thus, the solvent is more difficult to penetrate into the rubber matrix (Alshabatat and Abouel-Kasem, 2021).

Table 4.5 show the percentage mass changes of NBR/WTP with various formulations in toluene conducted at 120°C. The swelling percentage of gasket shows decreasing trend as the mass of the samples were reduced upon immersion in toluene. The reduction in mass of the samples was due to the extraction of non-crosslinked NBR molecules and soluble components. The (C≡N) group of NBR has high chemical interaction when contacted with toluene. However, the addition of filler and sulphur can increase the chemical resistance properties of NBR. The result in Table 4.5 shows a comparison of solvent gel fraction results of the gasket with different loading of sulphur, WTP, and DOP.

Among all the compositions, the D10-W90-S2 (A) shows the least mass changes among all compounding. This is due to the compound has the highest WTP loading of 90phr as filler, highest sulphur loading of 2phr, and lower DOP loading of 10phr as plasticizer. The high loading of WTP and sulphur as well as the lower DOP loading results in formation of more crosslinking which leads to least solvent extraction effect and mass reduction. This result is in line with previous researchers reporting on reduced swelling of rubber with increasing filler and sulphur loading, and reduced plasticisers. The mass changes for formulation D10-W90-S2 (A) are 14.022%, followed by gasket with D15-W90-S2 (B) composition, which consists of 2phr of sulphur, 90phr of WTP, and 15phr of DOP. The mass change for the compounding is 14.221%. In contrast, formulation D15-W90-S1 (B) has the highest mass changes with 18.904%. The

formulation consists of 1phr of sulphur, 90phr of WTP, and 15phr of DOP. The lower sulphur loading, and higher plasticizer loading causes low crosslink density of the rubber and thus increased solvent extraction, and highest mass loss percentage.

Table 4.5: Mass changes for NBR/WTP under solvent for a different formulation

Formulations	Sulphur (phr)	WTP (phr)	DOP (phr)	Mass Changes % (negative)
D10-W90-S1 (A)	1	90	10	16.078
D10-W90-S1 (C)	1	90	10	16.243
D10-W80-S2 (C)	2	80	10	17.470
D10-W90-S2 (A)	2	90	10	14.022
D15-W90-S1 (A)	1	90	15	17.069
D15-W90-S1 (B)	1	90	15	18.904
D15-W90-S2 (A)	2	90	15	15.463
D15-W90-S2 (B)	2	90	15	14.221
D15-W80-S2 (C)	2	80	15	14.463

4.2.5 Thermal ageing test

The thermal aging test was conducted to determine the long-term aging effect of polymer composite due to a strong oxidation reaction that might cause the decrease and degradation in polymer performance. Generally, fibres are stable under high temperatures, but rubber matrix and interface will be the key for properties deterioration and alter the glass transition temperature of the composite. Polymer aging may occur by physical and chemical aging. Physical aging is reversible whereby the polymer is prolonged exposed under high temperature and causes changing of molecular conformation but remain structural integrity of the rubber matrix. On the other hand, chemical aging is irreversible aging that causes changes in rubber molecular weight. The aging is mainly due to de-polymerization, manipulation of crosslinking density, and oxidation of the rubber in high elevated temperatures (García-Moreno *et al.*, 2019).

In this experiment, the effect of sulphur, DOP, and WTP loading in rubber NBR/ WTP to resist the thermal aging under a controlled environment. The rubber NBR/ WTP is undergoing thermal aging in the air at 108°C for 72 hrs. Then the properties of rubber after aging are tested with an oil absorption test under 150°C for 5 hrs. The result in Table 4.6 shows a comparison of aged and unaged NBR/ WTP rubber composites with different DOP, WTP, and sulphur content. Generally, NBR/ WTP with higher loading of sulphur will have a less mass increase in oil absorption which is applied in aged or unaged NBR/ WTP. As sulphur content increase, the crosslinking density will increase which

as well generate more sulphide bonds in the rubber matrix. The mobility of the rubber chain is restricted and less swelling will occur (Alshabatat and Abouel-Kasem, 2021).

Table 4.6 indicates that formulation D10-W90-S2 (A) has lower thermal age as compared to other formulation because it has higher sulfur and filler loading and lowest DOP loading which generate more cross-linking density for the NBR matrix. Subsequently, aging characterizing will lead NBR/ WTP composite in losing some additives and fillers beside oxidation reaction happen include crosslinking and chain scission. In this contact, loss of additive will affect the properties of the rubber, and an increase of crosslinking density will enhance the properties of rubber indirectly. However, the overloading of sulphur will cause a reduction in strength. For the longer aging period, the cross-linking of curatives will increase and more oxidation and more chain scissions will take place. (Alshabatat and Abouel-Kasem, 2021)

In our study, aged NBR/ WTP has higher mass loss compared to unaged NBR/WTP as indicated in Table 4.6. This is due to mass loss of some additives and reduction of the crosslinking density of the compound. As filler and additives loss can cause reduction of strength and properties of the NBR composite. Thus, thermal aged NBR/ WTP generally has higher oil absorption percentage compared to unaged NBR/ WTP. The data comparison of oil absorption test under thermal aging and non-thermal aging show that formulations D10-W90-S1 (A), D10-W90-S1 (C), D10-W80-S2 (C), D10-W90-S2 (A), D15-W90-S1 (B), D15-W90-S2 (A), D15-W90-S2 (B), and D15-W80-

S2 (C) has higher thermal aged oil absorption compared to non-thermal aged oil absorption.

In addition, formulation D10-W90-S2 (A) showed nearly similar oil absorption mass increase percentage. However, D15-W90-S1 (A) show lesser oil mass absorption compared to unaged NBR. The consolidation phase happens when the post-curing reaction happens when the temperature increase. Cross-linking density further increase as NBR molecular chain activities have been reactivated under high-temperature exposure. However, degradation after consolidation happens due to matrix deterioration. Transition temperature decrease and cracking happen on the rubber-filler matrix during the curing process and debonding happens. Oxidation will happen when oxygen can enter the new paths during thermal aging (García-Moreno *et al.*, 2019).

Table 4.6: Comparison of aged and unaged NBR/WTP with different formulations.

Formulations	Sulphur (phr)	WTP (phr)	DOP (phr)	Unaged Mass Increase (%)	Aged Mass Increase (%)
D10-W90-S1 (A)	1	90	10	18.78	25.86
D10-W90-S1 (C)	1	90	10	14.45	19.46
D10-W80-S2 (C)	2	80	10	19.97	23.09
D10-W90-S2 (A)	2	90	10	16.01	16.52
D15-W90-S1 (A)	1	90	15	19.89	17.87
D15-W90-S1 (B)	1	90	15	22.23	25.27
D15-W90-S2 (A)	2	90	15	16.08	17.98
D15-W90-S2 (B)	2	90	15	17.36	25.09
D15-W80-S2 (C)	2	80	15	15.54	17.36

4.2.6 Thermogravimetric analysis of NBR/WTP

Thermogravimetric analysis is used to analyze the stability of the samples under a high thermal environment. A sample of NBR/ WTP is undergoing continually weighed and heated under inert gases environment. Nitrogen gas is used so that the sample will only decompose, and oxidation will not take place. Lastly, the mass changes of the sample are recorded from time to time until the ending of combustion. Figure 4.11 and Table 4.7 show thermal stability data and mass changes of NBR/ WTP at different temperatures. The

thermal degradation of NBR/ WTP has three steps degradation starting from 148°C and ending at 468°C where constant mass is achieved.

Thermal degradation of NBR/WTP has three stages of degradation. The initial phase of degradation or dehydration of NBR happens at the temperature of 110°C till 200°C to release volatile liquids and some mass loss is attributed to the degradation of low-temperature volatile composites. (Pruneda *et al.*, 2005) Subsequently, the second stage of thermal degradation occurs at temperatures 250°C to 367°C. The thermal degradation happens due to DOP plasticizer desorption. The function of DOP is to reduce the modulus of rubber and soften the rigid rubber into semi-rigid rubber. Hence, the glass transition temperature of the compounding will decrease with the addition of DOP content. Therefore, the higher the DOP loading, the higher the mass loss of the compound in stage two thermal degradation. (Chen *et al.*, 2021) Table 4.7 show that formulation D15-W90-S1 (A), D15-W90-S2 (A), and D15-W90-S2 (B) which contain 15phr of DOP has a higher percentage of mass loss of 14% compared to D10-W90-S1 (A), D10-W90-S1 (C), D10-W80-S2 (C), and D10-W90-S2 (A) which has 10phr of DOP with 13% of mass loss at temperature 270°C.

The third stage of thermal degradation happens at temperature 367°C to 468°C and slightly degrade until temperature 900°C. Here is the degradation of rubbers components including NBR, SBR, and Polybutadiene found in WTP as discussed in section 4.2.2. Neat NBR starts to degrade at temperature 360°C follow by other rubber at 380°C – 480°C. (Alneamah and Almaamori, 2015) To be specific, Materials loss at temperature 436°C is attributed to decompose of

styrene-butadiene rubber (SBR). The mass loss of high boiling point substances and carbon black is beyond temperature 500°C. Theoretically, mass loss of WTP reinforces rubber can enhance the thermal stability of the compounding. (Silva *et al.*, 2020)

However, the rubber mixture at temperature 360°C shows that 80phr of WTP has lower mass loss compared to 90phr of WTP filler. The formulation D10-W80-S2 (C) and D15-W80-S2 (C) with 80phr WTP present a 36.5275% and 37.7203% of mass loss at 360°C respectively duly due to heterogeneous morphology of filler and NBR. Furthermore, the research shows that neat WTP has 32wt% of final char residue after the thermal degradation which is similar to experimental WTP residue at 900°C. (Alneamah and Almaamori, 2015)

Moreover, the role of sulfur can slightly improve the thermal stability of the rubber. The increase of sulfur loading can increase the C-S-C bond. Hence, more activation energy is needed for thermal decomposition when the cross-link density is increased. As compared in the data shown in Table 4.7 formulations D10-W90-S1 (A), D10-W90-S1 (C), D15-W90-S1 (A) and D15-W90-S1 (B) are having a higher mass loss in 900°C with 79.0833%, 79.4053%, 78.3439%, and 80.592% respectively while other formulations with higher sulfur loading have 78% of mass loss. Thus, this indicates that 2phr of sulfur has better thermal stability than 1phr of sulfur. (El-Nemr, 2011) As for final mass loss in 900°C, the residue is nearly the same as the content of minerals in each formulation are relatively equal, and the remaining WTP only contains 22% of char after thermal degradation.

Table 4.7: TGA for various NBR/ WTP formulations, CB and WTP.

Formulations	Temperature at 50% mass loss, T50% (°C)	Total mass loss at 130°C (%)	Total mass loss at 270°C (%)	Total mass loss at 360°C (%)	Total mass loss at 900°C (%)
D10-W90-S1 (A)	399.83	1.8582	13.4609	38.1627	79.0833
D10-W90-S1 (C)	396.67	1.9443	13.9143	38.9365	79.4053
D10-W80-S2 (C)	409.00	1.6610	13.5320	36.5275	78.8348
D10-W90-S2 (A)	400.00	1.9450	13.4344	38.1400	78.2452
D15-W90-S1 (A)	397.83	1.9469	14.9675	40.6060	78.3439
D15-W90-S1 (B)	404.17	1.4809	13.7967	36.8258	80.592
D15-W90-S2 (A)	396.83	1.8671	14.0675	39.3919	78.2281
D15-W90-S2 (B)	401.27	1.8410	14.0362	38.9270	78.2375
D15-W80-S2 (C)	402.33	1.6110	13.6568	37.7203	78.5558
WTP	415.67	0.7981	6.1580	26.5922	68.5479
CB	>900	1.7827	3.1639	3.7594	9.1069

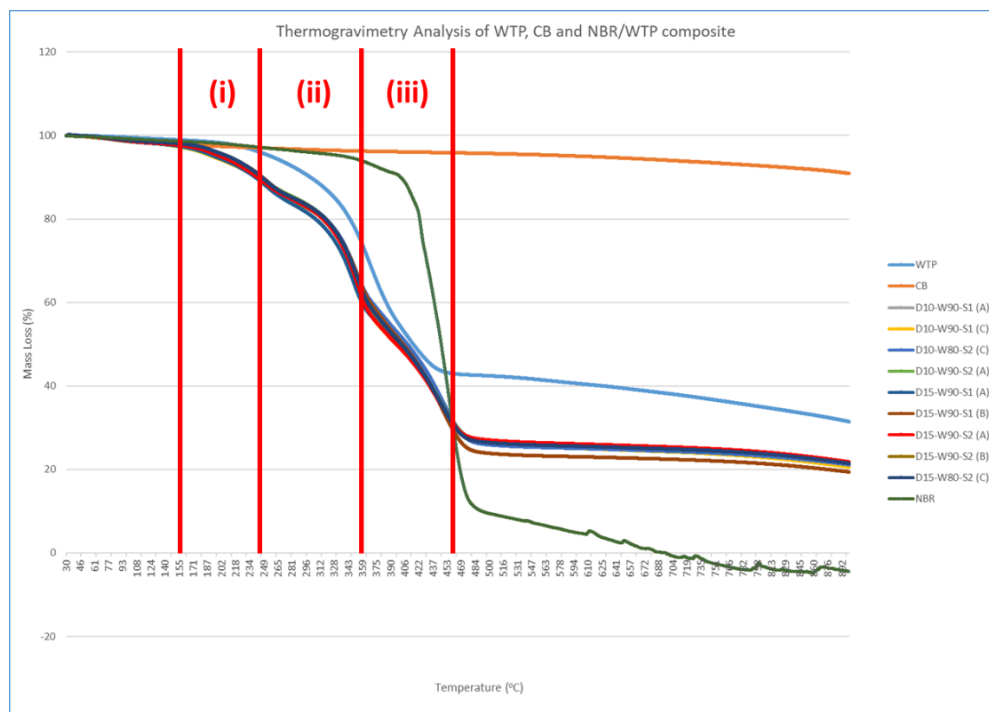


Figure 4.11: TGA curves for various NBR/ WTP formulations, CB and WTP.

4.2.7 Scanning electron microscope (SEM)

Scanning electron microscope is a method to analyse the surface morphology of gasket samples after foaming and curing. In the compounding formulation, ADCA is used as foaming agent, DCP acts as curing agent, sulphur is as cross-linking agent, ZnO is a vulcanization agent, while ZMBT and ZDEC are curing accelerator. Furthermore, SEM is used to justify the foaming and curing parameters. In addition, foaming process and conditions are relatively importance in controlling foaming density, cellular structure and it will affect the foams properties indirectly. However, the cell size and cell distribution in

rubber foams are generally hard control than thermoplastic foams as foaming and curing are happened simultaneously.

Table 4.8: Formulations of NBR/WTP for SEM.

Formulations	Sulphur (phr)	WTP (phr)	DOP (phr)
D10-W90-S1 (A)	1	90	10
D10-W90-S1 (C)	1	90	10
D10-W80-S2 (C)	2	80	10
D10-W90-S2 (A)	2	90	10
D15-W90-S1 (A)	1	90	15
D15-W90-S1 (B)	1	90	15
D15-W90-S2 (A)	2	90	15
D15-W90-S2 (B)	2	90	15
D15-W80-S2 (C)	2	80	15

Foaming and curing can be carried separately which is foaming first and follow by curing or it can happen simultaneously. For examples, rubber is foam at 90°C and cure at 140°C which is considered as two steps while single steps refer to rubber is foam and cure at 140°C. The single step foam and cure is giving a smaller cell size but higher cell density. Furthermore, higher foaming temperature has lower cell growth but higher cell distribution. Figure 4.12 show the different of single step and double step foaming to foaming density of the rubber. The high temperature restricted the cell growth as it is cure and cell coalescence is reduced.

However, the experiment was carried out by using two steps curing and comparison of foaming temperature 70°C and 80°C are studied. Figure 4.13 shows image comparison of different foaming temperature under 200X magnification. Figure 4.13 (a) shows foaming temperature at 70°C which represent Treatment A and B while Figure 4.13 (b) shows foaming temperature 80°C which represent Treatment C and D. As part of the research, the result in Figure 4.13 (b) shows the D10-W90-S1 (C) has higher cell concentration but smaller in cell size while Figure 4.13 (a) shows that D10-W90-S1 (A) has smaller density but larger in cell size. Formulation D10-W90-S1 (C) has smaller cell size as compared to D10-W90-S1 (A) because nitrile butadiene rubber continues to growth until rubber viscosity increase. The reason is curing doesn't happen in temperature less than 90°C, thus the rubber can continue to growth in cell size and stopped when temperature and viscosity increase (Bayat *et al.*, 2020).

Beside foaming and curing temperature and duration, filler also plays an importance role to determine the cell size and density. The filler addition is able reduce cell size and increase cell density in the rubber. Figure 4.14 shows the SEM image of compounding formulation that consists of 90phr of WTP while Figure 4.15 shows SEM image of compounding with 80phr of WTP under 200X magnification. Figure 4.14 consists of formulation D10-W90-S1, D10-W90-S2, D15-W90-S1, and D15-W90-S2 which have small cell size and higher cell density. In contrast, Figure 4.15 represents formulation D10-W80-S2, and D15-W80-S2 which have bigger cell size and lower cell density due to its lower in filler content.

Besides, the research done by Silva and other on year 2020 show that addition of waste tire rubber into polyurethane reduce the composite cell size and increase the density under magnification of SEM. The addition of waste tire rubber induces the nucleation effect during curing. Thus, the rubber microstructure has more foaming cell as compared to neat polyurethane. Furthermore, viscosity of the mixture increase due to filler loading cause more bubbles nucleation and thus, the foaming density increase and cell size decrease (Silva *et al.*, 2020) Figure 14 shows series of formulation with higher rubber filler has smaller cell size and uniform distributed while Figure 15 shows formulation D10-W80-S2 and D15-W80-S2 which has larger grain size and distribution is uneven.

Furthermore, cell density increase as filler increase is because of nucleating effect of silica. Moreover, one steps curing has higher cell density compared to two steps foaming and curing as it provides sufficient energy for nucleation. Figure 4.12 shows cell density increase with silica content and one step curing is higher than two steps curing (Bayat *et al.*, 2020). Moreover, rubber cross linking is referred to formation of covalent bonds that hold the rubber together. Formation of covalent bonds mainly due to present of sulphur in the rubber. The sulphur can form mono-sulphide (-S-), disulphide (-S-S-), and polysulfide (-S_x- where X ≥ 3).

Furthermore, crosslinking density is determined by crosslinking agent such as sulphur, and fillers content for rubber-filler interactions. The low vulcanization rubber tends to have less crosslink chains formation and it is

vulnerable to collapse due to external factors. In contrast, high vulcanization increases the crosslinking chains, and the degree of free chains are decrease. The chain length and dangling chains are become shorter and there have better molecular chains interaction (Rostami-Tapeh-esmaeil *et al.*, 2021).

Figure 4.16 shows SEM images for higher sulphur loading (2phr) (a) D10-W90-S2, and (b) D15-W90-S2. Meanwhile, Figure 4.17 shows SEM images for lower sulphur loading (1phr) for (a) D10-W90-S1 and (b) D15-W90-S1. Both SEM images are under 500X magnification. There are more struts are observed in between of filler and rubber as compared to D10-W90-S1 and D15-W90-S1. The high curing rate is limited the chain mobility and changed the structural properties of the rubber. The properties of the vulcanized rubber are discussed previously and in Hardness Test.

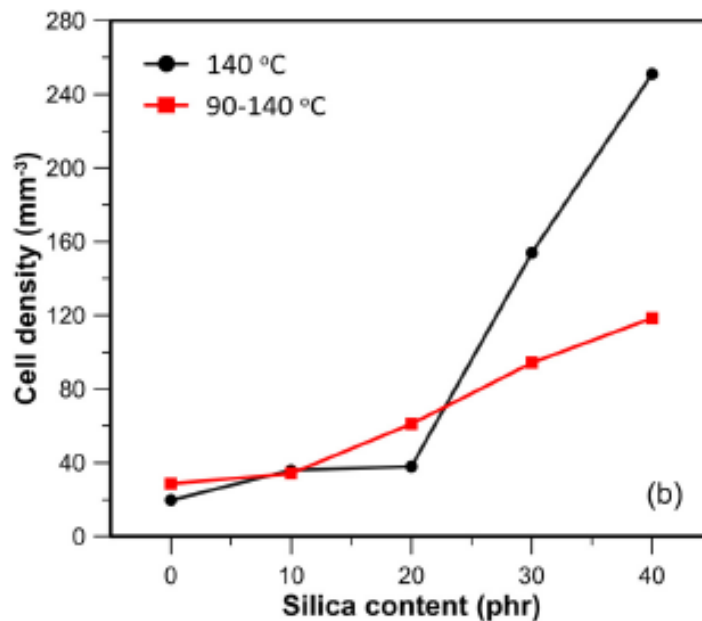


Figure 4.12: Cell density increase with filler (silica) content (Bayat *et al.*, 2020).

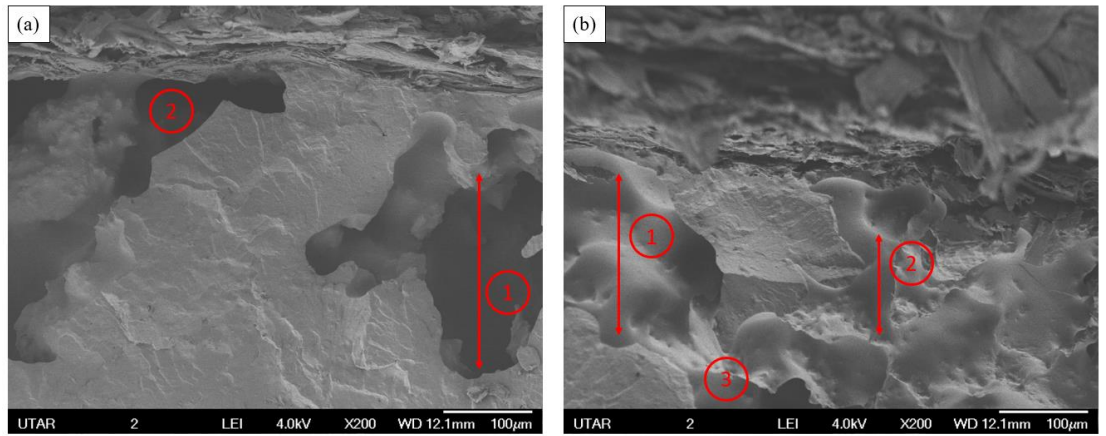


Figure 4.13: Comparison of surface morphology of foaming temperature (a) 70°C, and (b) 80°C under 200X magnification.

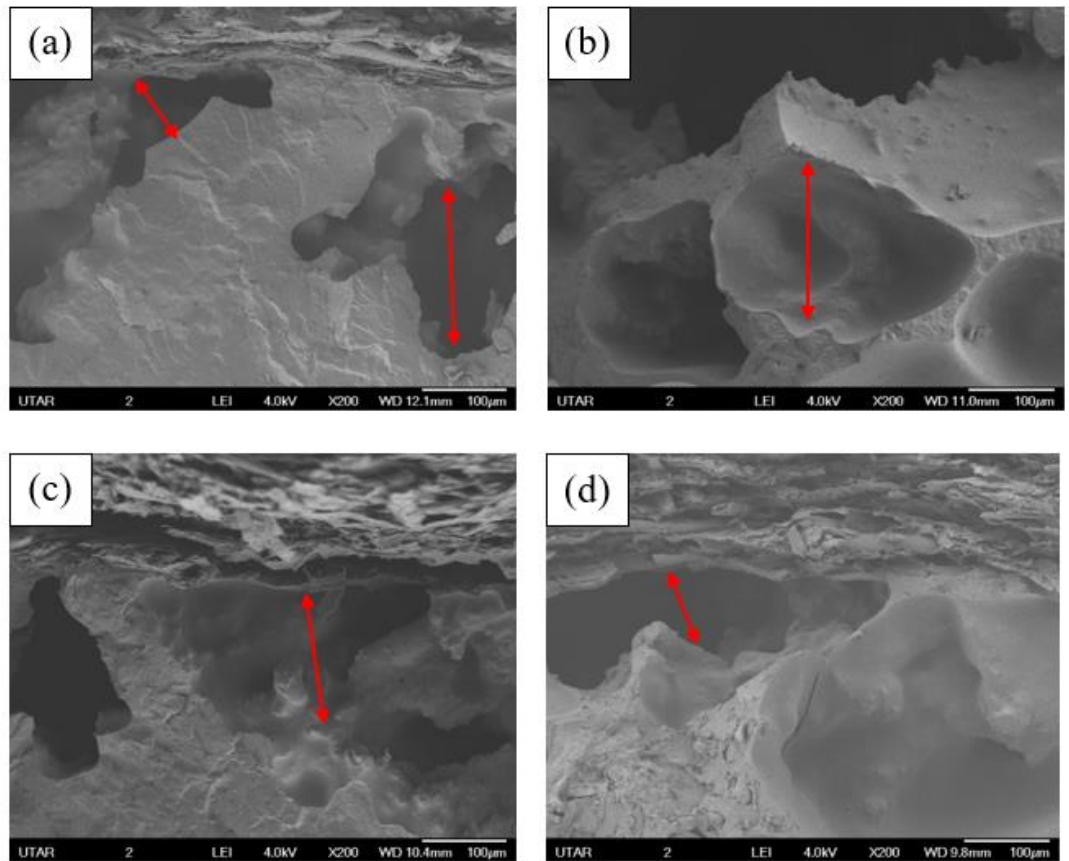


Figure 4.14: Gasket formulation with 90phr of WTP (a) D10-W90-S1 (b) D10-W90-S2 (c) D15-W90-S1 (d) D15-W90-S2 under 200X magnification.

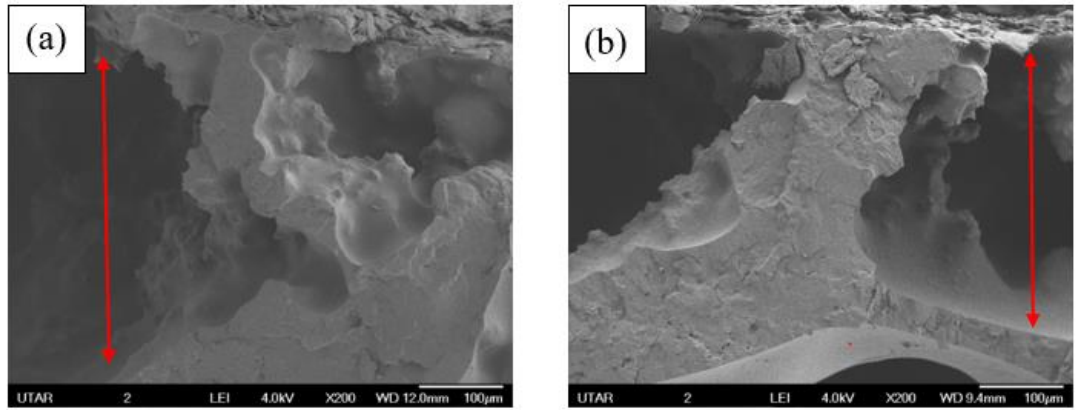


Figure 4.15: Gasket formulation with 80phr of WTP (a) D10-W80-S2 (b) D15-W80-S2 under 200X magnification.

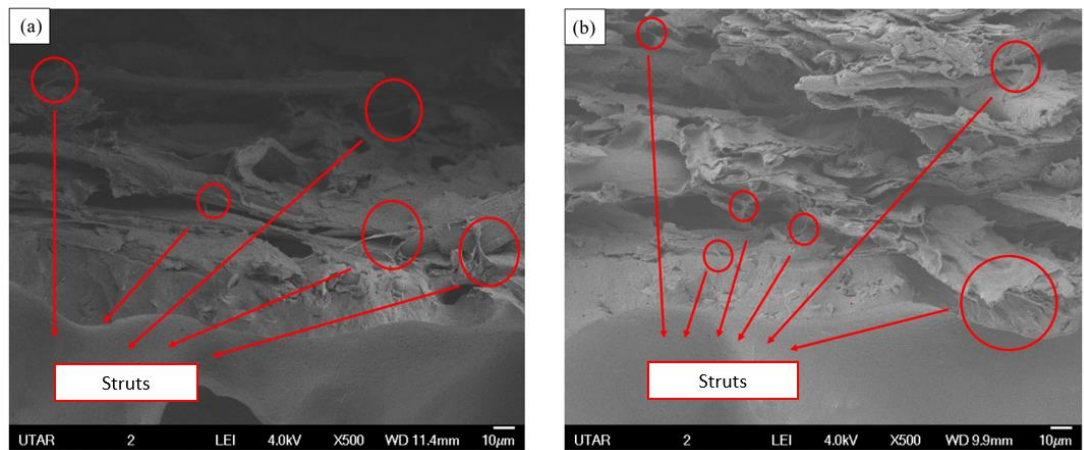


Figure 4.16: Gasket formulation with higher sulphur (2phr) (a) D10-W90-S2 (b) D15-W90-S2 under 500X magnification.

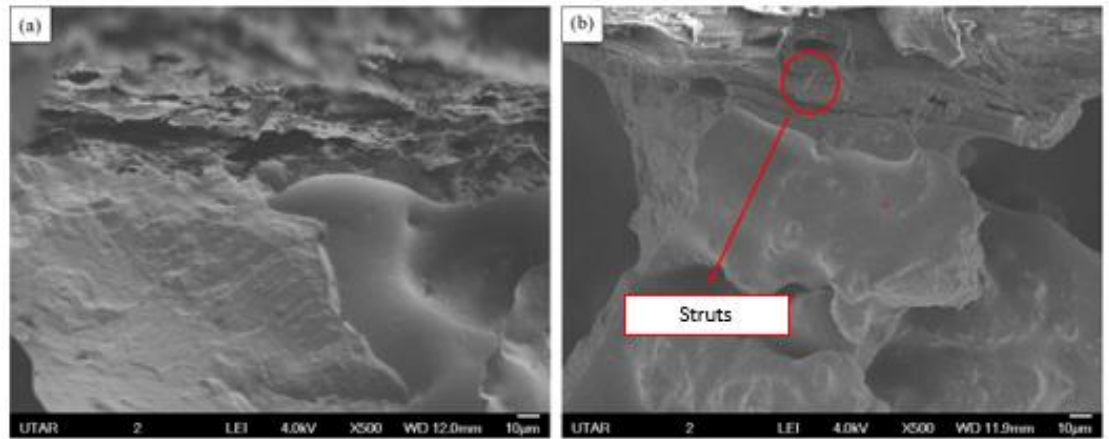


Figure 4.17: Gasket formulation with lesser sulphur (1phr) (a) D10-W90-S1 (b) D15-W90-S1 under 500X magnification.

4.2.8 Hardness test (Shore A)

Gasket samples hardness is tested with Shore A hardness with ASTM D2240 standard. The hardness reading is taken by using an analog durometer and the reading is tabulated in Table 4.9. The analogy of the testing method is depending on the penetration of the indenter into the material when force is applied. Furthermore, the hardness value is reflecting the viscoelastic and elastic modulus of the sample. However, the geometry of the indenter and the force applied can affect the hardness values of the sample (American Society for Testing and Materials. ASTM., 2017).

The composite NBR/ WTP hardness has been identified by using a hardness durometer and the result is tabulated in Table 4.9 and Figure 4.24 for hardness value comparison with different compositions of DOP, sulphur, and WTP. Filler act as reinforcement in the rubber composite materials by creating

rubber – filler interaction. As filler loading increases, more total crosslinking density in the rubber composite. Furthermore, the filler can restrict the mobilization of the rubber chain, thus the rubber becomes more rigid and harder (Kim *et al.*, 2020).

In contrast, formulation with lesser WTP has a lower hardness value, 80phr of WTP is softer than 90phr of WTP. In the experiment, D10-W80-S2 (C) has a hardness value of 52.4, and D15-W80-S2 (C) has a hardness value of 52. On the other hand, formulation with 90phr of WTP such as D10-W90-S2 (A), D15-W90-S1 (A), D15-W90-S2 (A) and D15-W90-S2 (B) has hardness values at 53 and 54. D10-W90-S2 (A) shows a significant highest hardness value due to the influence of WTP loading apart from DOP and sulphur loading addition.

In addition, the hardness of the compounding can be determined from a sulphur additive perspective. Sulphur in compounding will form a cross-linking reaction between rubber and sulphur which happens at carbon-carbon double bonds. Furthermore, accelerators can speed up the cross-linking reaction by minimizing the free sulphur amount in the compounding. (Tamási and Kollár, 2018) The hardness of the compounding containing a different portion of sulphur is determined and significantly shown by D10-W90-S2 (A) and D10-W90-S1 (A). D10-W90-S2 (A) has a 54.6 hardness value compared to D10-W90-S1 (A) which has a hardness value of 52. D10-W90-S2 (A) has 2phr of sulphur while D10-W90-S1 (A) has 1phr of sulphur.

Besides, DOP is made to reduce the modulus and lower the glass transition temperature of the rubber at performance temperature. Young's modulus of rubber decreases with the increase of DOP. Thus, the rubber rigidity will decrease and the rubber tends to be softer (Chen *et al.*, 2021). Other than that, plasticizers will decrease the crosslinking density during the curing process. The double bond of the plasticizer will intake crosslinking agents resulting in low crosslinking in rubber and reducing the mechanical and hardness of rubber (Xu *et al.*, 2020). Hence, the lower plasticizer has better rigidity than rubber. Table 4.9 shows that formulation with 10phr of DOP has a higher hardness value. Formulation D10-W90-S1 (C) and D10-W90-S2 (A) have hardness values of 53 and 54.6 respectively which are higher than 15phr of DOP. In contrast, formulation D15-W90-S1 (B) and D15-W80-S2 (C) have hardness values of 52.

Table 4.9: Comparison of hardness value with sulphur, DOP, and WTP content.

Formulations	Sulphur (phr)	WTP (phr)	DOP (phr)	Hardness Value
D10-W90-S1 (A)	1	90	10	52.0
D10-W90-S1 (C)	1	90	10	53.0
D10-W80-S2 (C)	2	80	10	52.4
D10-W90-S2 (A)	2	90	10	54.6
D15-W90-S1 (A)	1	90	15	53.0
D15-W90-S1 (B)	1	90	15	52.6
D15-W90-S2 (A)	2	90	15	53.2
D15-W90-S2 (B)	2	90	15	53.4
D15-W80-S2 (C)	2	80	15	52.0

4.2.9 Formulation selection

Several characterization and testing had been done for gasket formulations justification. The gasket is gone through an oil absorption test, solvent absorption test, thermal aging test, hardness test, and SEM for surface morphology observing. Table 4.10 shows the three most outstanding performance and theoretical preferable gasket formulations.

There are three formulations selected from the oil absorption test, the listing is selected from the least oil absorption. D10-W90-S1 (C) has 14.45% mass increasing, followed by D10-W90-S2 (A) with 16.01% of mass increasing and D15-W80-S2 (C) with 15.54% of mass increasing. However, the theoretical desire formulation is D10-W90-S2 (A) as it has higher loading of filler (WTP), cross-linking agent (sulphur), and least amount of plasticizer (DOP). Furthermore, thermal aging followed by an oil absorption test at 150°C is done on NBR/WTP. The result shows that D10-W90-S2 (A) is still the optimum and theoretical as it has higher crosslinking density to avoid materials loss such as additives and filler.

Apart from that, D10-W90-S2 (A) has better performance in TGA. The formulation for D10-W90-S2 consists of 2phr of sulphur, 90phr of WTP, and 10phr of DOP. Higher sulphur loading indicates more activation energy needed for thermal decomposition and SBR in WTP has higher thermal stability and lease DOP can remain the crosslinking and rigidity of the rubber. Besides, formulation D10-W90-S2 (A) is chosen based on the hardness test as it has

higher rigidity compared to other formulations. Mid-range hardness values such as 40A-55A are used indoor seals, gaskets, silicone masking, etc. while higher hardness (60A) is used for grommets, rubber brushes, O-rings, tire treads, and others. (Lechner, 2020) Other than that, D10-W90-S2 (A) shows the least solvent swelling under Gel Fraction analysis. It has optimum loading for sulphur and WTP which creates more crosslinking density and lowest DOP content which will consume the curatives.

The SEM analysis show that formulation with higher loading of filler (WTP) give a better advantage. The higher loading of WTP has higher viscosity and has smaller cell growth but bigger cell density. Furthermore, higher sulphur content is essential for higher cross-linking density and the chain length and struts are shorter for better molecular interaction. Subsequently, higher cross-linking restricted the rubber matrix deformation and strengthen the properties of the rubber. Treatments condition A and B are preferable as it has foaming temperature 70°C than Treatments condition C and D as they have 80°C foaming temperature. Higher foaming temperature has smaller cell size but higher cell density which cause more oil traps in the cell.

Besides, curing duration is optimum at 30min which compile with Treatment A and C. As increase in curing time, the curing agent will continue to discompose and increase the crosslinking network density (Rostami-Tapehesmaeil *et al.*, 2021). Figure 4.25 shows over curing of rubber after a period and some reversion of equilibrium of cross-linking density will happen to the rubbers. However, properties of the NBR/WTP decrease after over curing

period. Generally, NBR/ WTP D15-W90-S1 (A) has better properties in oil resistance, gel fraction, and thermal aging than D15-W90-S1 (B) which has shorter cured duration. Furthermore, D15-W90-S1 (A) has smaller foam cell size because of lower curing temperature. Table 4.11 shows comparison of formulation D15-W90-S1 (A) and D15-W90-S1 (B) to indicate the effect of curing duration to the properties of the rubber mixture.

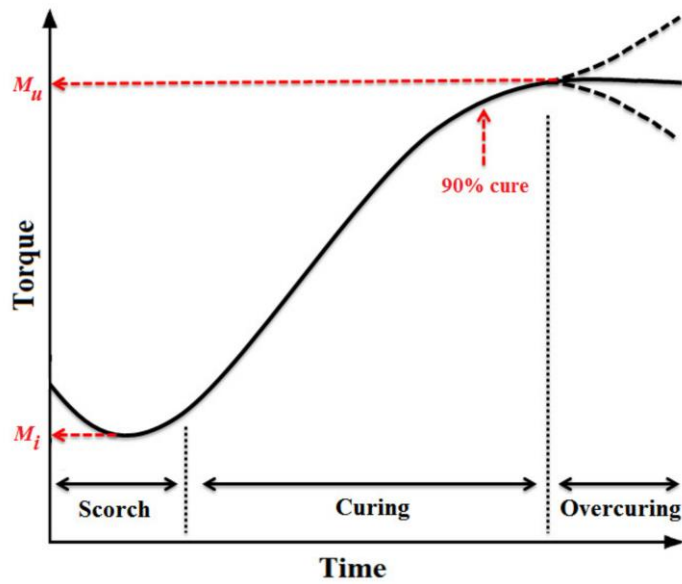


Figure 4.25: Torque over curing time (Rostami-Tapeh-esmaeil et al., 2021).

Table 4.10: Formulation selection from various experimental testing.

Testing	Preferred Formulation 1	Preferred Formulation 2	Preferred Formulation 3	Theoretical Desire
Oil absorption test	D10-W90-S1 (C)	D10-W90-S2 (A)	D15-W80-S2 (C)	D10-W90-S2 (A)
Gel-fraction	D10-W90-S2 (A)	D15-W90-S2 (B)	D15-W80-S2 (C)	D10-W90-S2 (A)
Thermal Ageing Test	D10-W90-S2 (A)	D10-W90-S1 (A)	D15-W80-S2 (C)	D10-W90-S2 (A)
TGA	D10-W90-S2 (A)	D15-W80-S2 (C)	D10-W90-S1 (C)	D10-W90-S2 (A)
SEM	-	-	-	D10-W90-S2 (A)
Hardness Test	D10-W90-S2 (A)	D15-W90-S2 (B)	D15-W90-S2 (A)	D10-W90-S2 (A)

Table 4.11: Formulation comparison D15-W90-S1 (A) and D15-W90-S1 (B)

Formulation	D15-W90-S1 (A)	D15-W90-S1 (B)
Oil absorption test	19.89% mass changes	22.23% mass changes
Gel-fraction	17.07% mass changes	18.90% mass changes
Thermal Ageing Test	17.87% mass changes	25.27% mass changes
TGA	78.34% final mass lost	80.59% final mass lost
SEM	Smaller cell distribution	Larger cell distribution
Hardness Test	53 Shore (A)	52.6 Shore (A)

4.3 Characterization of NBR/ WTP for Phase 3 Optimization- Rolling

Method.

In the experiment design, the coating method is to modify from casting to the rolling method by applying the calendaring concept. Figure 4.26 shows the lab scale calendaring method where 10g samples of the rubber mixture are poured on the top of the gasket paper. Then, the roller is pressing the rubber mixture throughout the gasket paper. The function of the rulers is to adjust the thickness of the gasket compounding. Table 4.12 shows the thickness of the gasket under different stack numbers of rulers. Figure 4.27 shows the completed gasket after foaming and curing.

Figure 4.27 (a) shows that two stacks of rulers are unable to coat the NBR/WTP on the surface of the gasket due to a shorter gap in between gasket paper and roller. Besides, three stacks of rulers with the height of 2.396 mm produce 0.637 mm thickness coating while 4 stacks of rulers with 3.139 mm produce 0.728 mm thickness of gasket after foaming and curing. Figure 4.27 (b) shows gasket produced by three rulers stacking while Figure 4.27 (c) shows gasket produced by four ruler stacking rolling process. In conclusion, three stacks of rulers are used as a rolling method because the thickness of the gasket produced is approximately to the casting gasket's thickness. The casting gasket's thickness is 0.567 mm.

Table 4.12: Gasket thickness with the different numbers of a stack of rulers.

Number of rulers	Height of the rulers (mm)	Gasket Thickness (mm)
2	1.408	-
3	2.396	0.637
4	3.139	0.728

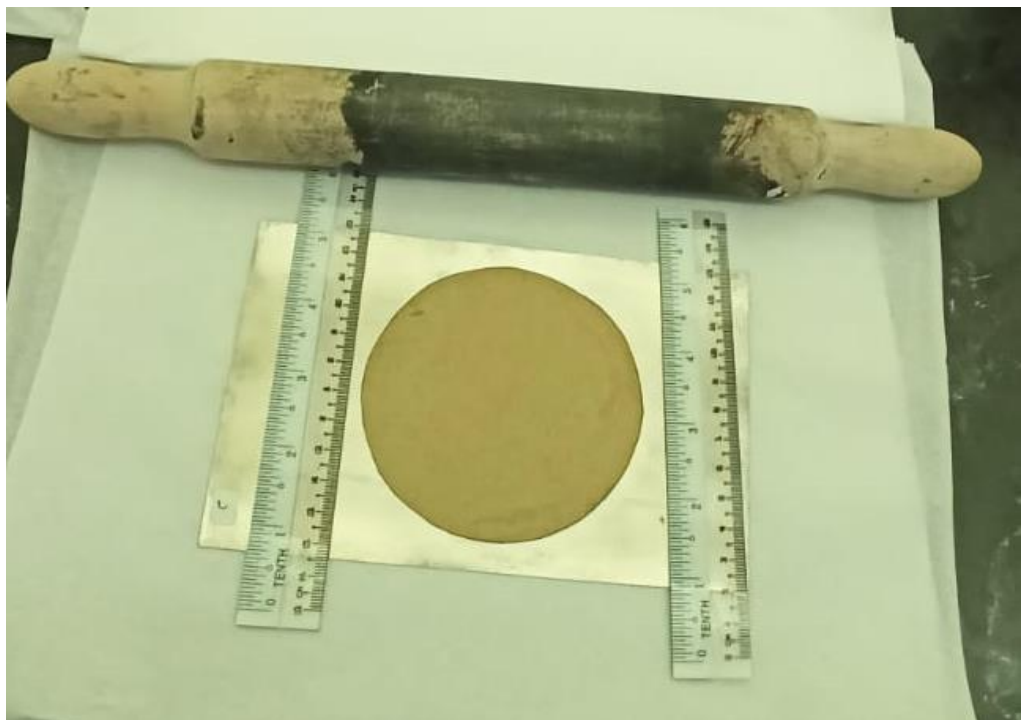


Figure 4.26: Gasket calendaring modelling in the lab-scale

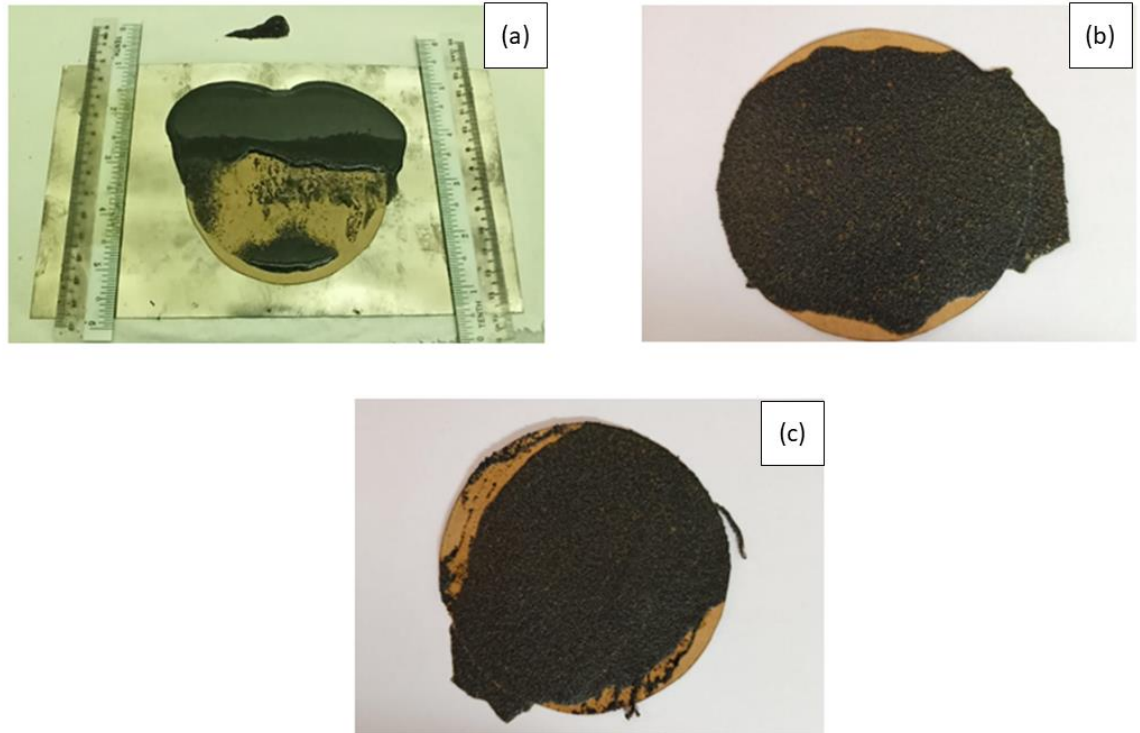


Figure 4.27: Gaskets surface upon completion after curing and foaming.

4.3.1 Selected formulations for rolling method with 3 stacks of rulers.

A pre-selected formulation such as D10-W90-S1 (C), D10-W90-S2 (A), and D15-W80-S2 (C) are applied in phase 3 optimization. The reason where these three formulations been selected because they have least oil absorption under oil test. The objective of Phase 3 optimization is to understand the differences between the rolling and casting method in gasket compounding. The three formulations above are applied and foam and cure under each pre-designed treatment and performance of the gasket are tested by using oil absorption test, solvent absorption test, peeling test, and the surface is observed by using the scanning electron microscope.

4.4. Characterization of NBR/WTP formulation by using rolling method.

4.4.1 Oil absorption test

Frequently, rolling is used as a processing method to produce some sheet products due to advantages of speed, maximum rates, consistency thickness, accuracy, and suitability for a variety of sheet products (Joo *et al.*, 2011). However, there are many defect and correction that must be made to get a perfect and fine rubber sheet in our application. Properties of oil absorption of the gasket as a comparison to justify the application of rolling and casting in gasket manufacturing by using NBR reinforce with WTP.

The rolled gasket is gone through an oil absorption test at 150°C in the medium of engine oil, the changes of weight and thickness are measured, and the data is compared with the casting gasket under the same parameter oil absorption testing. Table 4.13 shows the comparison data for both rolling and casting percentage changes in mass and thickness. Figure 4.28 show differences in mass percentage changes of the gasket in rolling and casting methods while Figure 4.29 shows differences in thickness percentage changes in rolling and casting methods.

The result shows that rolled gasket has higher mass absorption compared to the casted gasket. Rolled gasket formulation D10-W90-S1 (C), D10-W90-S2 (A) and D15-W80-S2 (C) has 26.32%, 17.13%, and 22.32% of mass percentage increase compared to casted gasket formulation D10-W90-S1 (C), D10-W90-S2

(A) and D15-W80-S2 (C) which has 14.45%, 16.02%, and 15.54% mass percentage increase. The rolled gasket has a higher mass percentage increase as compared to the casted gasket is due to the deformation of the fluid during the coating process. However, rolled gasket formulation D10-W90-S2 (A) shows the least increase as it has a higher composition of WTP, sulphur, and with the least DOP which provides the gasket with higher crosslinking density.

The second formulation D15-W80-S2 (C) has the second least increased oil absorption as the sulphur loading is remained the highest loading of sulphur but lower in WTP and higher in DOP. As discussed in Section 4.2.3 where curatives can shorten the chain and denser the rubber matrix network. The rubber matrix becomes rigid and improves in oil absorption resistance (Zielińska *et al.*, 2016). D10-W90-S1 (C) has slightly higher mass absorption because it has lesser curative. However, the advantage of higher fillers can form a barrier for the oil absorption and lesser DOP can retain the number of curatives as DOP can break down the curative agent.

Polymers are categorized as viscoelastic which inherit the properties of viscous and elastic behaviour. The properties of a viscoelastic polymer are displacement of the molecule will slightly move when small forces act on it and return to their original position when the force is removed. However, the nature of the viscoelastic can be imposed by shear and elongation force when the polymer is rolled (Drobny, 2014). Other than that, filler segregation may happen, and flattening may happen in the rolling process (Darmawan *et al.*, 2018).

Next, the thickness of the rolled gasket shows fewer changes compared to the casted gasket. The reading of the thickness change with D10-W90-S1 (C), D10-W90-S2 (A), and D15-W80-S2 (C) for rolled gasket are -4.19%, -0.78%, and -3.42% while the thickness for casted gaskets is -3.61%, -4.45% and -10.8%. The negative changes in gasket thickness are due to rubber than collapsed instead of expanding in the oil absorption test as discussed in Section 4.2.3. The rolled gasket has a lesser change in the matrix because the sheet can be deformed in the lateral direction where stress is imposed on the centre of the sheet. The rubber mixture is less spread on the side and accumulated at the ends of the sheet as discussed in Section 2.9. Thus, less NBR rubber contain stimulated per sample space for oil stimulated. Furthermore, the function of curatives and filler can restrict the mobility of the NBR chain network for further collapse.

Table 4.13: Formulation comparison of mass and thickness changes for rolling and casting.

Formulations	Sulphur (phr)	WTP (phr)	DOP (phr)	Mass	Mass	Thickness	Thickness
				changes in Rolling (%)	changes in Casting (%)	changes in Rolling (%)	changes in Casting (%)
D10-W90-S1 (C)	1	90	10	26.32	14.45	-4.19	-3.61
D10-W90-S2 (A)	2	90	10	17.13	16.02	-0.78	-4.45
D15-W80-S2 (C)	2	80	15	22.32	15.54	-3.42	-10.8

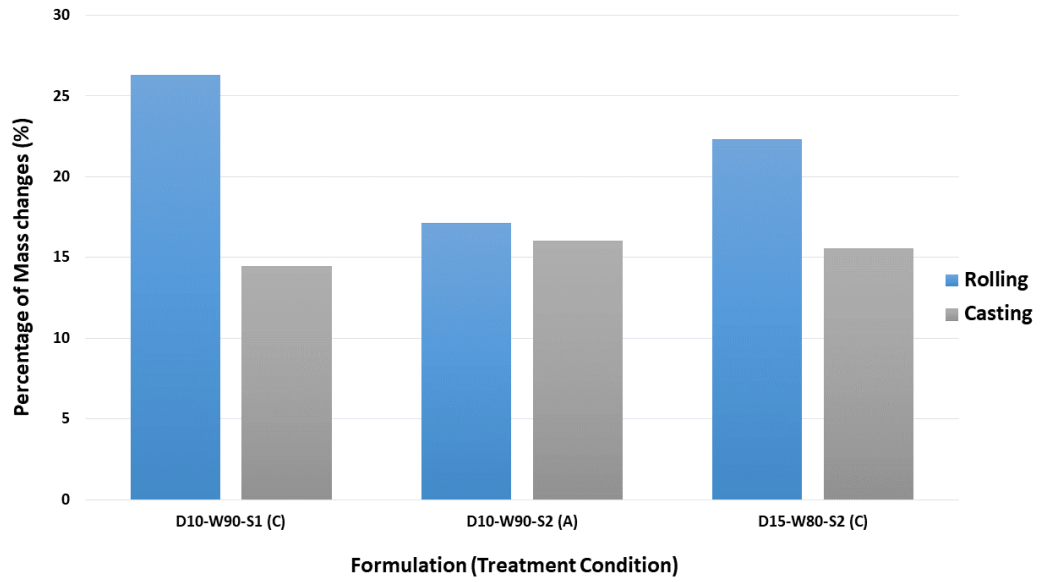


Figure 4.28: Comparison of mass changes in percentage for rolling and casting methods.

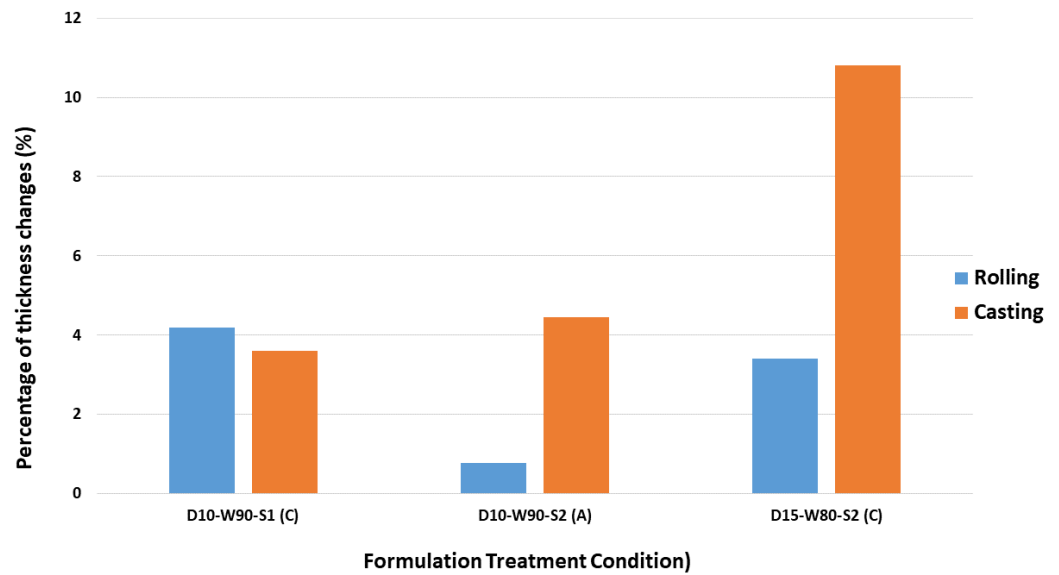


Figure 4.29: Comparison of thickness changes in percentage for rolling and casting methods.

4.4.2 Gel fraction / solvent extraction test

Next, a comparison of rolled and cast gasket under gel fraction or solvent extraction has been made. In this study, the resistance of the rubber compound toward solvent is measured through mass lost due to dissolution in the solvent. In Section 4.2.4, we understand that aromatic toluene is used as a solvent for the extraction of the polar group of NBR ($C\equiv N$). The solvent will soak into the rubber matrix and interact with the nitrile (Indrajati and Dewi, 2017). The mass loss of rolled gaskets and cast gaskets for formulations D10-W90-S1 (C), D10-W90-S2 (A), and D15-W80-S2 (C) is tabulated in Table 4.14 and shown in Figure 4.30.

Both rolled and cast gaskets results show that D10-W90-S2 (A) is the least mass changes among all formulations as it has higher crosslinking density as discussed in Section 4.2.4. It has the highest loading of WTP and sulphur and least DOP among other formulations. Curative can increase the crosslinking density and make the rubber rigid, and the chain extensibility is restricted. The solvent is harder to penetrate the rubber matrix (Alshabatat and Abouel-Kasem, 2021). Hence, D10-W90-S1 (C) has lower mass changes percentage in gel fraction followed by D15-W80-S2 (C).

Secondly, filler WTP can form obstacles and induce higher crosslinking density to control the mobilization of the rubber chain. Furthermore, extra triglyceride DOP will consume the curative (Li *et al.*, 2016). Hence, crosslinking density will decrease if DOP content is excessive in the compounding. However,

D10-W90-S1 (C) still has a higher gel fraction as compared to D15-W80-S2 (C) because sulphur shows a dominion effect in crosslinking, and DOP content is slightly different in the overall compounding formulation.

Besides, another fact is that rolled gasket has a higher gel fraction percentage as compared to the casted gasket. D10-W90-S1 (C) increase from 16.24% to 38.73%, D10-W90-S2 (A) increase from 14.02% to 36.62% and D15-W80-S2 (C) increase from 14.42% to 37.02%. The reason behind of gel fraction increase is because deformation of structure and chain when force and strain are applied on the surface of the gasket. The deformation of rubber is affected by pressure and force. Figure 4.31 shows the numerical simulation for the stress distribution on the width cross-section of the rubber by Tian et al. The middle of the gasket rubber in the width direction is subjected to higher stress and the elastic recovery of rubber will be greater at this point. Thus, the calendared sheet is unable to have a uniform surface as stress distribution in the roll gap is uneven (Tian *et al.*, 2021).

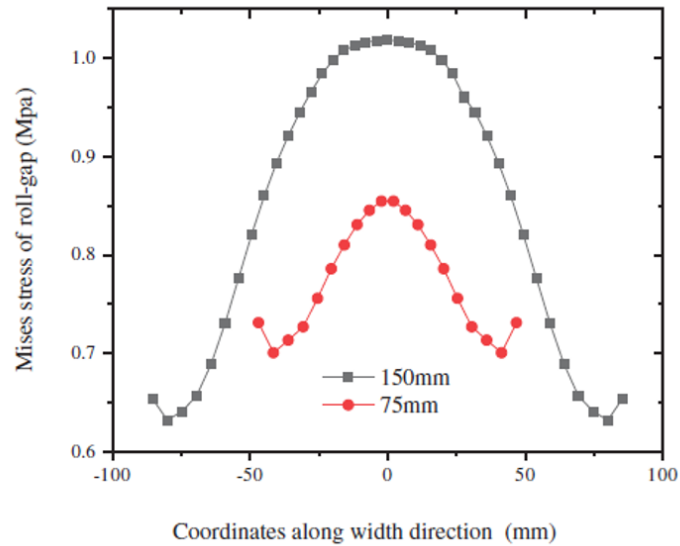


Figure 4.30: Numerical stimulation stress distribution on the width cross-section (Tian *et al.*, 2021).

Furthermore, shear strains and stress can be justified from the perspective of thermos-mechanical history. From the study, the rolling velocity can affect the temperature along with the interface and the extruded products. Besides, the shear stress and shear strain are only present in the interface of the rolled sheet and nil in the casted sheet. The condition of strain and stress are affected by roller velocity and the distance of solidification before the interface. Theoretically, the chemical density link is more significant in calendaring as compared to casting. This is because the presence of shear strains on the interface during the calendaring process will attribute addition of copolymerization reaction, but elongation will be nil as solidification happens very fast right after calendaring (Serrat *et al.*, 2012).

In addition, the temperature of the interface will have a quick drop, and the rubber is subjected to shear stress at a low calendaring speed. However, this experiment is subjected to an extrusion temperature of 230°C and a calendar temperature of 30°C. In contrast, casted sheet crystallization is simpler as it is only affected by the cooling rate. The cooling rate of the casted sheet is more homogeneous as only involves heat convection on the top surface of gaskets. (Serrat *et al.*, 2012)

Table 4.14: Formulation comparison for mass changes for rolling and casting.

Formulations	Sulphur (phr)	WTP (phr)	DOP (phr)	Mass changes in Rolling (%)	Mass changes in Casting (%)
D10-W90-S1 (C)	1	90	10	38.73	16.24
D10-W90-S2 (A)	2	90	10	36.62	14.02
D15-W80-S2 (C)	2	80	15	37.02	14.42

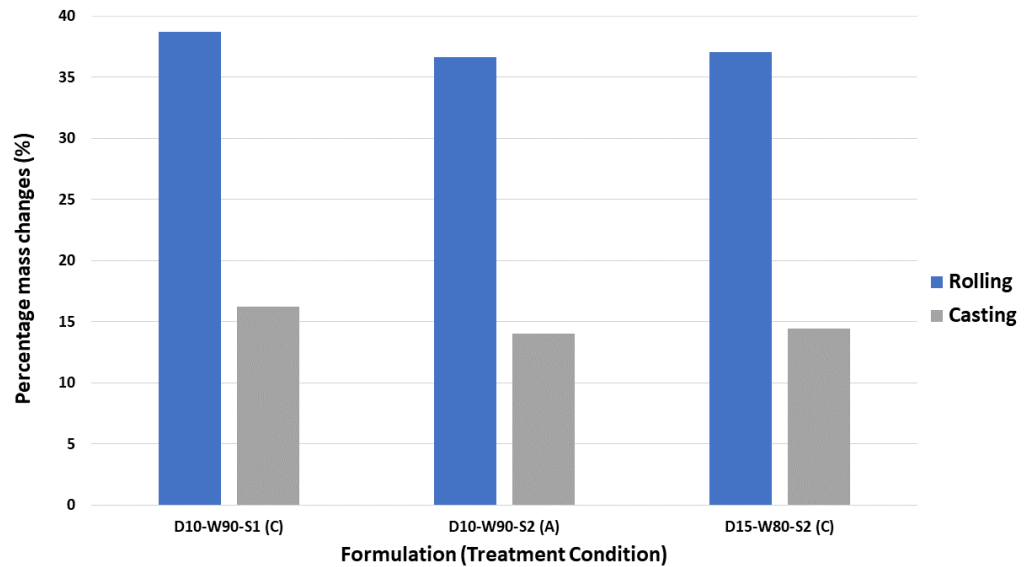


Figure 4.31: Comparison of mass percentage changes in the rolled and cast gasket.

4.4.3 Peeling test

The adhesion property of the rubber can be study through peeling strength. The peeling strength is the ability of the rubber to resist removal by peeling force. Furthermore, the property of adhesive strength can be affected by many factors. Molecular weight is part of the factors that can enhance the peeling strength of the rubber (Yang *et al.*, 2010). The research show that molecular weight increases the peeling strength until certain weight ratio as maximum wettability is observed. At these stages, the rubber tends to be hardened and tough. The adhesive layer has a strong mechanical interlocking so that the mechanism of the layer does not rupture. However, the mechanism failure happens when molecular weight sample is increase due to lower wettability of

adhesive. The higher molecular weight forms excessive entanglement that resist the flow ability of the rubber (Yang *et al.*, 2010).

Moreover, addition of WTP (filler) can affect the strength of adhesive bonds. There are some research shows that corporation of WTP can enhance the adhesive strength. When there is 10wt% increase of WTP filler, the tensile strength of the adhesive bond is recorded to $42.68\text{wt}\% \pm 6.96\%$. However, there are decrease in tensile strength beyond 10wt% concentration of filler is due to maximum volume concentration. Besides, there are increase in strain at strength % up to $12.2 \pm 20.95\%$ when filler concentration increases to 15wt%. The increase in strain show the flexibility of adhesive bonds (Tichý *et al.*, 2018). Table 4.15 shows the comparison of casting and rolling tensile strength (MPa) and hand peeling experience for three formulations. The result show that higher filler loading 90phr has lower peeling strength is due to maximum of wettability of the compounding. The hand peeling experience and ultimate tensile strength (UTS) values for peeling strength are tally.

Apart from that, tear strength values of the NBR/ WTP are increase with the content of plasticizer (DOP). The tearing happen in NBR begins with the crack's propagation from the stress concentration point and passing through the interface of NBR and fillers. However, the present of plasticizer can alter and restrict the cracking propagation along the interface (Rahman *et al.*, 2020). Table 4.15 shows that D15-W80-S2 (C) has the higher tensile strength in adhesive because it has higher DOP loading and the least WTP content.

Table 4.15: UTS (MPa) and hand peeling justification for three formulations in casting and rolling.

Formulations	Hand Peel (Casting)	Hand Peel (Rolling)	UTS, MPa (Casting)	UTS, MPa (Rolling)
D10-W90-S1 (C)	Moderate	Moderate	5.07	5.70
D10-W90-S2 (A)	Easier	Easier	4.66	4.71
D15-W80-S2 (C)	Harder	Harder	8.63	8.87

4.4.4 Scanning electron microscope (SEM)

Moreover, the application of SEM is used to observe and compare the coating properties of NBR mixture under casting and rolling coating technique. The sample are cut into small pieces and cross section of the NBR mixture is evaluated. Figure 35 show the SEM images for casting and rolling gasket. Figure 32 (a-c) is mentioned SEM for casting gasket for formulation D10-W90-S1 (A), D10-W90-S2 (A), and D15-W80-S2 (C) while Figure 36 (d-f) show the images for rolling gasket D10-W90-S1 (A), D10-W90-S2 (A), and D15-W80-S2 (C).

The SEM images taken are used to understand the adhesive properties of different formulations of rubber mixture toward the gasket paper. The formulation D15-W80-S2 has a good adhesion property for NBR/WTP on the surface of gasket paper. The Figure 32 (c) and Figure 32 (f) represent the formulation D15-W80-S2 under rolling and casting. The formulation has small interface gap in between gasket and rubber matrix. The formulation has better

adhesion property due to maximum wettability and higher DOP value. Furthermore, the formulation has the least filler loading as higher filler loading will be causing entanglement and resist the rubber to flow. Besides, Figure 32 (f) has better adhesion strength due to rolling effect. The shear strain from rolling induce diffusion and promote addition copolymerization reaction which because it has better adhesion property.

In addition, sulphur ratio also affecting the adhesion strength of the rubber matrix on the gasket paper. The crosslinking and entanglement generated by sulphur increase the molecular weight of the rubber matrix and reduce the flowability of the whole compounding. Thus, formulation D10-W90-S1 (A)_Casting and Rolling has narrow gap as compared to formulation D10-W90-S2 (A)_Casting and Rolling.

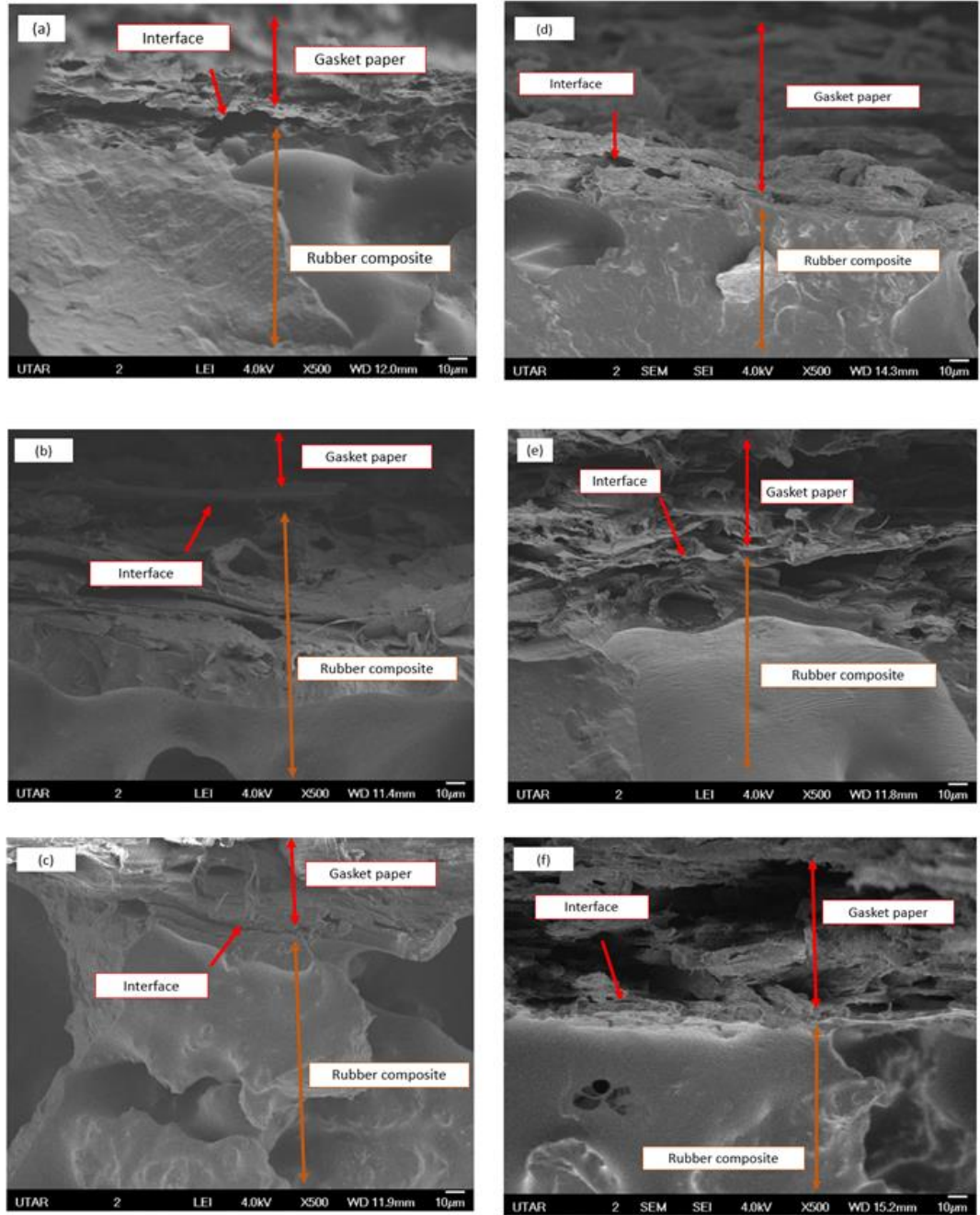


Figure 4.32: The cross-section SEM for rolling and casting gasket under 500X magnification

- | | |
|----------------------------|----------------------------|
| (a) D10-W90-S1 (A)_Casting | (d) D10-W90-S1 (A)_Rolling |
| (b) D10-W90-S2 (A)_Casting | (e) D10-W90-S2 (A)_Rolling |
| (c) D15-W80-S2 (C)_Casting | (f) D15-W80-S2 (C)_Rolling |

CHAPTER 5

CONCLUSION AND RECOMMENDATION

5.1 Conclusion

The feasibility of reinforcement of WTP in NBR matrix was accepted at filler loading of 90phr and the sulphur loading was 2phr, with a 10phr loading of DOP. The filler was initially study under several characterizations such as PSA, TGA, and SEM. The filler particle size was relatively importance to determine the filler distribution. The smaller particulate tends to stick together by fusion of particles and different particles size range might contribute to segregation. The PSA result shown that WTP has single distribution and dominion size of filler was 339.653 μm and the distribution of the particles are in centre. On the other hand, the CB N330 has the single peak, and the graph tends skewed to the left which mean there were finer particles in the distribution. Thus, segregation was easily happened in CB N330 due to board range of filler size. Other than that, TGA show that thermal degradation happens at temperature 260°C and stable at temperature 510°C with 57.70% of mass lost. Furthermore, the SEM images show that CB has higher tendency in agglomerate and formation of segregation due to high aspect ratio. Besides, smooth surface of cryogenic grinding has lower viscosity flow and migration of sulphur into granulate rubber is easier and thus, cross-linking density is higher.

Next, the performance of NBR/ WTP was verified with several mechanical testing. The rubber composite was tested for its oil absorption, mass changes through gel fraction test, thermal aging test, hardness test, TGA and SEM. The thickness of the gasket was specified before the experiments. The 10g of rubber mixture solution was the desire compounding loading to produce a suitable thickness gasket with 0.567mm. The gasket has cured, and dispersion of filler was even distributed. Afterward, the formulation selection was done by using physical observation whereby the gaskets shall have smooth surface and avoid voids on the surface of the gaskets. Thus, there are eight formulations were selected through observation.

The oil absorption required by company was maximum 15% mass changes and 10% thickness changes. The oil absorption is essential for rubber application as rubber will swell and weaken by oil under long term period of immersion. The oil absorption test result show that formulation D10-W90-S1 (C), D10-W90-S2 (A), and D15-W80-S2 (C) have a least oil absorption with the 14.45%, 16.01% and 15.54%. The higher filler loading can form a barrier for oil absorption and sulphur was able to form the cross-linking to retain the structure of the rubber. However, DOP will decrease the cross-linking density of the rubber. Gel fraction shown that D10-W90-S2 (A) has the least solvent extraction continue by D15-W90-S2 (B), and D15-W80-S2 (C). The gel fraction percentage for D10-W90-S2 (A) was 14.022% mass changes. This is due to high filler loading which restrict the rubber chain movement and sulphur provide essential crosslinking so that the rubber become rigid, and extensibility of the rubber was restricted.

The thermal aging test is used to determine the long-term aging effect of NBR/ WTP. The rubber compound was tested with 108°C for 72 hrs and the sample was tested with oil absorption test again under 150°C for 5 hrs. Formulation D10-W90-S2 (A) shown that it has the smallest variance, 16.01% and 16.52% mass changes for before and after aging process. In addition, D10-W90-S2 (A) also gave a smallest mass increasing value among all formulation as more sulphide bonds generate by sulphur strengthen the rubber matrix and filler was able to restrict the mobility of the rubber chain. Furthermore, the addition of WTP under formulation D10-W90-S2 (A) has lowest mass loss at 900°C which equivalent to 78.34%.

Other than that, SEM analysis provided the result that D10-W90-S1 (A) has larger cell size and lower cell density as it has lower foaming temperature, 70°C. The cell will continue to enlarge at lower temperature until viscosity of the rubber increase. Furthermore, filler addition can reduce the cell size and increase the cell density as the viscosity of the rubber mixture increase. In addition, rubber with higher filler loading has even distribution of cell due to more nucleation effect of filler. Moreover, SEM also present that more struts were found at D10-W90-S2 (A) as sulphur loading was to restrict the rubber chain movement and reduce the rubber structural change. Thus, the formulation D10-W90-S2 (A) has the hardest shore A value with 54.6 due to highest loading of sulphur and WTP and least of DOP.

Besides that, this research finding also shown that casting has better mechanical properties than rolling process. The nearly similar thickness gasket with same formulation was compounded using rolling process. The formulation D10-W90-S1 (C), D10-W90-S2 (A), and D15-W80-S2 (C) were made using rolling method and produced average 0.637mm thickness gasket. The oil absorption test result shown that D10-W90-S2 (A) has lowest mass percentage changes in rolling with value 17.13% compared to D10-W90-S1 (C), and D15-W80-S2 (C). The mass percentage for D10-W90-S1 (C), and D15-W80-S2 (C) were 26.32%, and 22.32%.

Furthermore, another justification where rolling has higher mass percentage increase due to shear strain appear during rolling process. Moreover, the sample was repeated with gel fraction. The result shown that D10-W90-S2 (A) has the lowest in rolling and casting with 36.61%, and 14.02% mass changes. The casting gasket has lower mass increase compared to rolling gasket due to deformation of structure when force and shear was applied. In addition, casted gasket has homogeneous cooling rate as convection was only happen on the surface of the gasket. Lastly, the peeling test and SEM revealed that D15-W80-S2 (C) has better adhesion properties as it has lowest molecular weight. The formulation has the least of filler ratio and higher DOP loading for better wettability. As a conclusion, formulation D10-W90-S2 (A) was used as gasket compounding formulation and produced by using casting process. This is because the product produced complied with the standard given by UP Packing Sdn. Bhd with less than 15% mass changes and 10% thickness changes under oil absorption test.

5.2 Recommendation

Study on the curing characteristics of rubber and its viscosity are suggested to be part of study by using Mooney viscometer and Oscillating Disc Rheometer (ODR) for more accurate justification. Mooney viscosity is the measurement for uncured compound stiffness. The measurement is determining from shear rate and torque developed from rotation between compound and rotor which measure in unit Mooney units. The higher the Mooney unit indicate higher viscosity of the compounding. Figure 5.1 shows Mooney graph and the ideal parameter for scorch time, cure time and cure index. The value t_5 refer to scorch time, while t_{35} refer the cure time and cure index is the between ($t_{35} - t_5$).

Besides, Oscillating Disc Rheometer (ODR) is the measurement to study the cure characteristic of the compounds by analyse the cure time and scorch time. However, the rheology measurement is unable to perform after scorch time. Figure 5.2 shows the ODR sample curve and Table 4.16 shows rheometer report reading parameters (Sisanth *et al.*, 2017).

Table 4.16: Rheometer parameters reading method (Sisanth *et al.*, 2017).

ML- Minimum torque, dN.m	MH- Maximum torque, dN.m
t_{S_2} – Time to 2 dN.m rise from ML (scorch time)	t_{90} – Optimum cure time
cure rate index = 100/ (cure time- scorch time)	$t_{90} = ML + 0.90(MH-ML)$

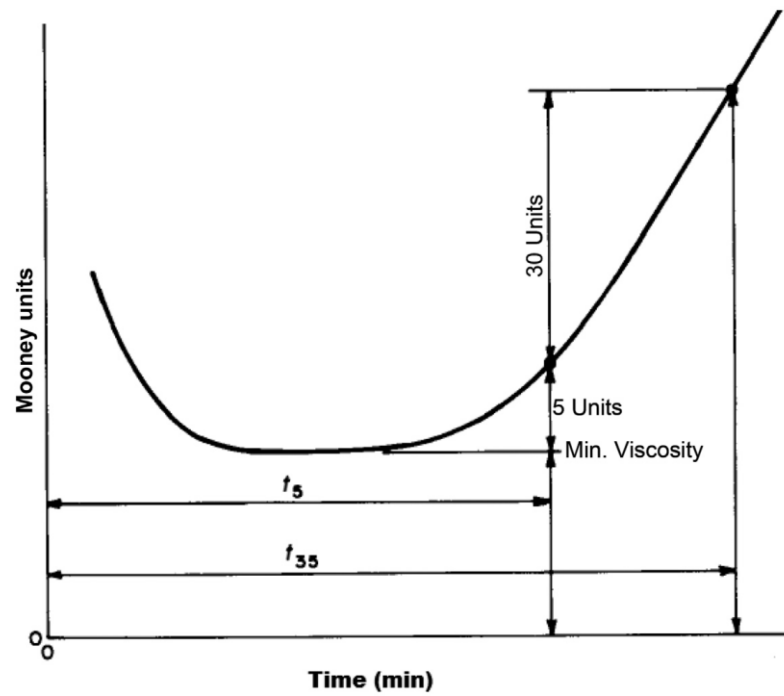


Figure 5.1: Mooney viscosity graph by using large motor (Sisanth *et al.*, 2017).

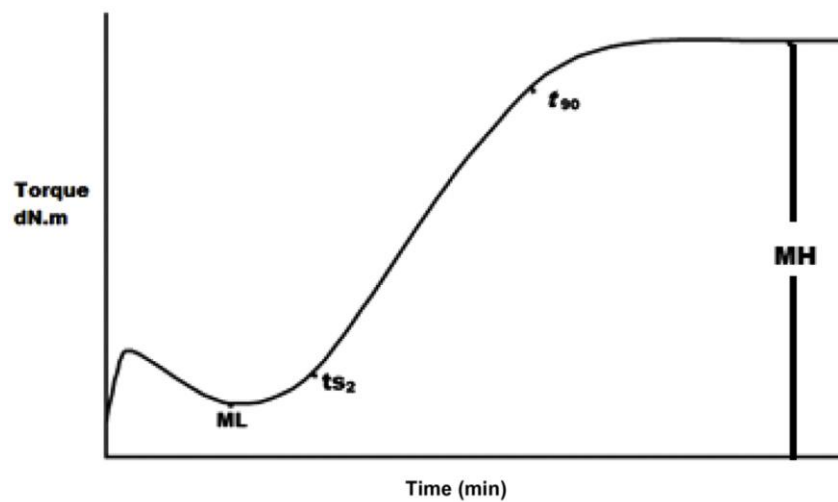


Figure 5.2: ODR cure graph (Sisanth *et al.*, 2017).

Besides, the second recommendation is application of two ovens for different foaming and curing temperatures. The foaming oven shall set at 70°C or 80°C depending on treatment while curing oven shall perform at 130°C. The simultaneous ovens can give an accurate foaming and curing temperature and shorten the rubber curing time in the oven while waiting increase of temperature until 130°C. Due to limitation of oven, the rubber is only able to subject to longer foaming temperature while waiting the temperature rise until curing temperature. Hence, the NBR/ WTP tends to have higher cell growth rate and lower density. Otherwise, single stage of curing is suggested as growing rate of rubber is lower with higher density (Bayat *et al.*, 2020).

Lastly, suggested research for comparison compounding of NBR/CB with the similar formulation can be done with NBR/WTP for the mechanical performance. Hence, the flexibility of material replacement of CB with WTP can have a better comparison.

6.0 REFERENCES

- Abidin, A. N. S. Z. *et al.* (2021) *Overview of Tyre Ecosystem in Malaysia*. Selangor, Malaysia.
- Aibada, N. *et al.* (2017) 'Review on Various Gaskets Based on the Materials, their Characteristics and Applications', *International Journal on Textile Engineering and Processes*, 3(1), pp. 12–18.
- Al-maamori, M. H., Al-Zubaidi, A. A.-A. and Subeh, A. A. (2015) 'Effect of Carbon Black on Mechanical and Physical Properties of Acrylonitrile Butadiene Rubber (NBR) Composite', *Academic Research International*, 6(2), p. 28.
- Ali, M. A. M. *et al.* (2020) 'Thermal and mechanical behavior of SBR/devulcanized waste tire rubber blends using mechano-chemical and microwave methods', *Journal of Polymer Engineering*, 40(10), pp. 815–822. doi: 10.1515/polyeng-2020-0116.
- Alias, R. and Mohd Rafee, A. (2020) 'Characterisation of liquid oil from pyrolysis of waste tyre', *Malaysian Journal of Chemical Engineering and Technology (MJCET)*, 3(1), p. 62. doi: 10.24191/mjcet.v3i1.11244.
- Alneamah, M. and Almaamori, M. (2015) 'Study of Thermal Stability of Nitrile Rubber/Polyimide Compounds', *International Journal of Materials and Chemistry*, 5(1), pp. 1–3. doi: 10.5923/j.ijmc.20150501.01.
- Alshabatat, N. and Abouel-Kasem, A. (2021) 'The Effects of Sulfur Content on the Mechanical Properties of Nitrile Butadiene Rubber with Different Aging Conditions', *Jordan Journal of Mechanical and Industrial Engineering*, 15(4), pp. 387–393.
- American Society for Testing and Materials. ASTM. (2017) 'Rubber Property—Durometer Hardness', *ASTM D 2240*, pp. 1–13. doi: 10.1520/D2240-15.2.
- Asaro, L. *et al.* (2018) 'Recycling of rubber wastes by devulcanization', *Resources, Conservation and Recycling*, 133(February), pp. 250–262. doi: 10.1016/j.resconrec.2018.02.016.
- Asuka Matsushita (2018) *Guidelines on Gasket Selection, Selection Troubles, and Countermeasures*. Available at: <https://www.valqua.co.jp/wp-content/uploads/pdf/technical/34e/vtn034e-06.pdf>.

- Azura, A. R. and Leow, S. L. (2019) 'Effect of carbon black loading on mechanical, conductivity and ageing properties of Natural Rubber composites', *Materials Today: Proceedings*, 17, pp. 1056–1063. doi: 10.1016/j.matpr.2019.06.512.
- Bayat, H. *et al.* (2020) 'An experimental study on one-step and two-step foaming of natural rubber/silica nanocomposites', *Nanotechnology Reviews*, 9(1), pp. 427–435. doi: 10.1515/ntrev-2020-0032.
- Bera, T., Acharya, S. K. and Mishra, P. (2018) 'Synthesis, mechanical and thermal properties of carbon black/epoxy composites', *International Journal of Engineering, Science and Technology*, 10(4), pp. 12–20. doi: 10.4314/ijest.v10i4.2.
- Butt, M. A. (2022) 'Thin-Film Coating Methods: A Successful Marriage of High-Quality and Cost-Effectiveness—A Brief Exploration', *Coatings*, 12(8). doi: 10.3390/coatings12081115.
- Charlene Jones, Mike Shorts, M. P. (2017) *Gasket Handbook 1st Edition*. 1st Editio, *Fluid Sealing Association*. 1st Editio. USA and France: Fluid Sealing Association and European Sealing Association.
- Chen, C. H. *et al.* (2021) 'Effects of dioctyl phthalate on the properties of poly(vinyl chloride)/organically modified montmorillonite nanocomposites', *Polymer Bulletin*, 78(1), pp. 283–294. doi: 10.1007/s00289-020-03109-3.
- Chu, H. *et al.* (2019) 'Analysis of rolling on steel and rubber-covered rollers using viscoelasticity', *Advances in Mechanical Engineering*, 11(11), pp. 1–14. doi: 10.1177/1687814019889800.
- Ciullo, P. A. and Hewitt, N. (1996) *PHYSICAL TESTING OF RUBBER* Most. Noyes Publications. doi: 10.1016/B978-0-8155-1434-3.50005-1.
- Cougo, C. M. dos S. *et al.* (2019) 'Multiscale hybrid composites with carbon-based nanofillers', in *Nanocarbon and its Composites*. Elsevier, pp. 449–470. doi: 10.1016/B978-0-08-102509-3.00014-6.
- Darmawan, A. S. *et al.* (2018) 'Effect of Thickness Reduction on Cold Rolling Process to Microstructure and Brass Hardness', *MATEC Web of Conferences*, 248, pp. 0–4. doi: 10.1051/mateconf/201824801001.
Description of production processes (2012) *Dana Automocion S.A.* Available at: https://glaser.es/img_cpm/004/files/general_principles/environmental_aspects_eng.pdf (Accessed: 23 November 2021).
- Dinsmore, R. P. (2007) 'Rubber Chemistry.', *Industrial & Engineering Chemistry*, 43(4), pp. 795–803. doi: 10.1021/ie50496a014.
- Drobny, J. G. (2014) *Processing Methods Applicable to Thermoplastic Elastomers, Handbook of Thermoplastic Elastomers*. doi: 10.1016/b978-0-323-22136-8.00004-1.

Duy, L. N. P. *et al.* (2022) ‘Dioctyl Phthalate-Modified Graphene Nanoplatelets : An’, pp. 1–11. doi: <https://doi.org/10.3390/polym14132541>.

El-Nemr, K. F. (2011) ‘Effect of different curing systems on the mechanical and physico-chemical properties of acrylonitrile butadiene rubber vulcanizates’, *Materials and Design*, 32(6), pp. 3361–3369. doi: 10.1016/j.matdes.2011.02.010.

El-Nemr, K. F. *et al.* (2020) ‘Innovative γ rays irradiated styrene butadiene rubber/reclaimed waste tire rubber blends: A comparative study using mechano-chemical and microwave devulcanizing methods’, *Journal of Polymer Engineering*, 40(3), pp. 267–277. doi: 10.1515/polyeng-2019-0307.

Fang, S. *et al.* (2020) ‘Notably Improved Dispersion of Carbon Black for High-Performance Natural Rubber Composites via Triazolinedione Click Chemistry’, *Industrial and Engineering Chemistry Research*, 59(48), pp. 21047–21057. doi: 10.1021/acs.iecr.0c04242.

Fazli, A. and Rodrigue, D. (2020a) ‘Recycling waste tires into ground tire rubber (Gtr)/rubber compounds: A review’, *Journal of Composites Science*, 4(3). doi: 10.3390/jcs4030103.

Fazli, A. and Rodrigue, D. (2020b) ‘Recycling Waste Tires into Ground Tire Rubber (GTR)/Rubber Compounds: A Review’, *Journal of Composites Science*, 4(3), p. 103. doi: 10.3390/jcs4030103.

Foroughi-Dahr, M. *et al.* (2017) *Particle Coating in Fluidized Beds, Reference Module in Chemistry, Molecular Sciences and Chemical Engineering*. Elsevier Inc. doi: 10.1016/b978-0-12-409547-2.12206-1.

García-Moreno, I. *et al.* (2019) ‘Effect of thermal ageing on the impact and flexural damage behaviour of carbon fibre-reinforced epoxy laminates’, *Polymers*, 11(1). doi: 10.3390/polym11010080.

Gómez-Hernández, R., PanecatI-Bernal, Y. and Méndez-Rojas, M. Á. (2019) ‘High yield and simple one-step production of carbon black nanoparticles from waste tires’, *Heliyon*, 5(7). doi: 10.1016/j.heliyon.2019.e02139.

Husnan, M. A., Ismail, H. and Shuib, R. K. (2018) ‘The effect of carbon black (CB) loading on curing characteristics and mechanical properties of virgin acrylonitrile butadiene rubber (Nbrv)/recycled acrylonitrile butadiene rubber (Nbr) blends’, *IOP Conference Series: Materials Science and Engineering*, 309(1). doi: 10.1088/1757-899X/309/1/012028.

Indrajati, I. N. and Dewi, I. R. (2017) ‘Performance of maleated castor oil based plasticizer on rubber: Rheology and curing characteristic studies’, *IOP Conference Series: Materials Science and Engineering*, 223(1). doi: 10.1088/1757-899X/223/1/012001.

Jansto, S. G. and Stalheim., D. G. (2020) ‘Hot Rolling Surface Quality Issues’, pp. 405–416. doi: 10.5151/2594-5297-22581.

Jebur, S. K. (2018) ‘Carbon black production, analyzing and characterization’, *Masters Theses.*, p. 22. Available at: https://scholarsmine.mst.edu/masters_theseshttps://scholarsmine.mst.edu/masters_theses/7869.

Joo, B. D. *et al.* (2011) ‘A study on forming characteristics of roll forming process with high strength steel’, *AIP Conference Proceedings*, 1383, pp. 1034–1040. doi: 10.1063/1.3624622.

Kim, D. Y. *et al.* (2020) ‘Correlation between the crosslink characteristics and mechanical properties of natural rubber compound via accelerators and reinforcement’, *Polymers*, 12(9), pp. 1–14. doi: 10.3390/polym12092020.

Li, J. *et al.* (2016) ‘Toward replacement of petroleum oils by modified soybean oils in elastomers’, *Rubber Chemistry and Technology*, 89(4), pp. 608–630. doi: 10.5254/rct.16.84830.

Liang, T. (2017) ‘STRUCTURE AND PROPERTIES OF RUBBERS AND THEIR BLENDS AFFECTED BY ULTRASONICALLY ASSISTED EXTRUSION’, 93(I), pp. 76–79. Available at: https://etd.ohiolink.edu/apexprod/rws_etd/send_file/send?accession=akron1502312081124254&disposition=inline.

Material Safety Data Sheet (Msds) Nitrile Rubber Sheet (2007) *GCP Elastomeric Inc.* Kitchener, ON, Canda. Available at: <https://pdf4pro.com/view/material-safety-data-sheet-msds-nitrile-rubber-53049a.html>.

Mostafa, A. *et al.* (2009) ‘Effect of carbon black loading on the swelling and compression set behavior of SBR and NBR rubber compounds’, *Materials and Design*, 30(5), pp. 1561–1568. doi: 10.1016/j.matdes.2008.07.043.

Munikanan, V. *et al.* (2018) ‘Fine granular of shredded waste tyre for road kerb application as improvised road furniture’, *AIP Conference Proceedings*, 1930, pp. 1–6. doi: 10.1063/1.5022955.

Ng, H. M. *et al.* (2018) ‘Thermogravimetric Analysis of Polymers’, *Encyclopedia of Polymer Science and Technology*, (13), pp. 1–29. doi: 10.1002/0471440264.pst667.

Nuzaimah, M. *et al.* (2018) ‘Recycling of waste rubber as fillers: A review’, *IOP Conference Series: Materials Science and Engineering*, 368(1). doi: 10.1088/1757-899X/368/1/012016.

Pruneda, F. *et al.* (2005) ‘Thermal characterization of nitrile butadiene rubber (NBR)/PVC blends’, *Journal of Thermal Analysis and Calorimetry*, 80(1), pp. 187–190. doi: 10.1007/s10973-005-0634-5.

Rahman, M. M. *et al.* (2020) ‘Influence of bio-based plasticizers on the properties of NBR materials’, *Materials*, 13(9). doi: 10.3390/ma13092095.

Rosato, Dominick V, Rosato, Donald V and Rosato, M. V (2004) *Plastic Product Material and Process Selection Handbook // Calendring*. doi: <https://doi.org/10.1016/B978-185617431-2/50012-8>.

Rostami-Tapeh-esmaeil, E. *et al.* (2021) ‘Chemistry, processing, properties, and applications of rubber foams’, *Polymers*, 13(10), pp. 1–53. doi: 10.3390/polym13101565.

Rothon, R. (2017) ‘Fillers for Polymer Applications’, *Springer*, p. 489. doi: 10.1007/978-3-319-28117-9.

‘Rubber gasket’ (2017) *Sealing Technology*, 2017(3), p. 12. doi: 10.1016/s1350-4789(17)30088-0.

Rubber, N., Finished, T. and Articles, R. (2005) ‘Worldwide Long Term New Rubber Consumption Forecast by Elastomer Statistics, IISRP Worldwide Rubber. Data sheet: Acrylonitrile Butadiene Rubber (NBR)’, (<Http://Www.Iisrp.Com/Webpolymers/07Nbr-18Feb2002.Pdf>). Available at: <http://www.iisrp.com/webpolymers/07nbr-18feb2002.pdf>.

Sanjuan-Navarro, L., Moliner-Martínez, Y. and Campíns-Falcó, P. (2021) ‘Characterization and Quantitation of Carbon Black Nanomaterials in Polymeric and Biological Aqueous Dispersants by Asymmetrical Flow Field Flow Fractionation’, *ACS Omega*, 6(47), pp. 31822–31830. doi: 10.1021/acsomega.1c04527.

Senin, M. S. *et al.* (2016) ‘Analysis of Physical Properties and Mineralogical of Pyrolysis Tires Rubber Ash Compared Natural Sand in Concrete material’, *IOP Conference Series: Materials Science and Engineering*, 160(1). doi: 10.1088/1757-899X/160/1/012053.

Serrat, M. C. *et al.* (2012) ‘Influence of the calendring step on the adhesion properties of coextruded structures’, *International Polymer Processing*, 27(3), pp. 318–327. doi: 10.3139/217.2516.

Shim, E. (2018) *Coating and laminating processes and techniques for textiles, Smart Textile Coatings and Laminates*. Elsevier Ltd. doi: 10.1016/B978-0-08-102428-7.00002-X.

Silva, N. G. S. *et al.* (2020) ‘Evaluation of rubber powder waste as reinforcement of the polyurethane derived from castor oil’, *Waste Management*, 116, pp. 131–139. doi: 10.1016/j.wasman.2020.07.032.

Sisanth, K. S. *et al.* (2017) *General introduction to rubber compounding, Progress in Rubber Nanocomposites*. Elsevier Ltd. doi: 10.1016/B978-0-08-100409-8.00001-2.

Sofi, A. (2018) 'Effect of waste tyre rubber on mechanical and durability properties of concrete – A review', *Ain Shams Engineering Journal*, 9(4), pp. 2691–2700. doi: 10.1016/j.asej.2017.08.007.

Tamási, K. and Kollár, M. S. (2018) 'Effect of different sulfur content in Natural Rubber mixtures on their thermo-mechanical and surface properties', *International Journal of Engineering Research & Science*, 4(2), pp. 28–37.

Tian, C. *et al.* (2021) 'Modeling and simulation for the swelling behavior of unvulcanized rubber during the calendering process', *Applied polymer science*, (December 2020), pp. 1–10. doi: 10.1002/app.50459.

Tichý, M. *et al.* (2018) 'Effect of rubber powder from waste tyre rubbers on mechanical properties of one-component polyurethane putty', *Agronomy Research*, 16(Special Issue 1), pp. 1257–1265. doi: 10.15159/AR.18.098.

Wang, H. *et al.* (2017) 'Effect of Temperature on Foaming Ability and Foam Stability of Typical Surfactants Used for Foaming Agent', *Journal of Surfactants and Detergents*, 20(3), pp. 615–622. doi: 10.1007/s11743-017-1953-9.

Wang, M. *et al.* (2019) 'Comparative pyrolysis behaviors of tire tread and side wall from waste tire and characterization of the resulting chars', *Journal of Environmental Management*, 232(July 2018), pp. 364–371. doi: 10.1016/j.jenvman.2018.10.091.

Wang, W. C. *et al.* (2016) 'Alternative fuel produced from thermal pyrolysis of waste tires and its use in a di diesel engine', *Applied Thermal Engineering*, 93, pp. 330–338. doi: 10.1016/j.applthermaleng.2015.09.056.

Xu, H. *et al.* (2020) 'Plasticization Effect of Bio-Based Plasticizers from Soybean Oil for Tire Tread Rubber', pp. 1–10. doi: 10.3390/polym12030623.

Yang, Z. *et al.* (2010) 'Crystallization behavior of poly(ϵ -caprolactone)/layered double hydroxide nanocomposites', *Journal of Applied Polymer Science*, 116(5), pp. 2658–2667. doi: 10.1002/app.

Yerezhap, D. *et al.* (2021) 'A multifaceted approach for cryogenic waste tire recycling', *Polymers*, 13(15). doi: 10.3390/polym13152494.

Zhang, T. F. *et al.* (2018) 'Size-induced segregation of granular materials during filling a conical hopper', *Powder Technology*, 340, pp. 331–343. doi: 10.1016/j.powtec.2018.09.031.

Zielińska, M. *et al.* (2016) 'Swelling of EPDM rubbers for oil-well applications as influenced by medium composition and temperature Part I. Literature and theoretical background', *Elastomery*, 20(2), pp. 6–17. Available at: <http://yadda.icm.edu.pl/yadda/element/bwmeta1.element.baztech-14da0222-966e-41bb-8e7a-4e6e842cd7a4>.

7.0 LIST OF PUBLICATION

Kah Siong, C., Muniyadi, M. and Munusamy, Y. (2021) 'Optimization of compounding formulation for the development of high-preformance coating material using waste tire powder for gasket application', *IOP Conference Series: Earth and Environmental Science*, 945(1). doi: 10.1088/1755-1315/945/1/012059.